THE PHYSIOLOGICAL ECOLOGY AND NATURAL DISTRIBUTION PATTERNS OF CRYPTOMONAD ALGAE IN COASTAL AQUATIC ECOSYSTEMS

by

TRISHA IRENE BERGMANN

A Dissertation submitted to the

Graduate School-New Brunswick

Rutgers, The State University of New Jersey

in partial fulfillment of the requirements

for the degree of

Doctor of Philosophy

Graduate Program in Oceanography

written under the direction of

Oscar Schofield

and approved by

____

____

____

____

New Brunswick, New Jersey

January, 2004

ABSTRACT OF THE DISSERTATION

The Physiological Ecology and Natural Distribution Patterns of Cryptomonad Algae in Coastal Aquatic Ecosystems

by

TRISHA IRENE BERGMANN

Dissertation Director:

Oscar Schofield

Phytoplankton not only form the base of the oceanic food web, but also act as mediators for a majority of biogeochemical fluxes in aquatic environments. Their functional importance in all natural waters, and especially in coastal areas, is paramount. Consequently much research has concentrated on the physiology, primary production, and distribution of coastal phytoplankton groups. Unfortunately, much of this work has focused on a few major phytoplankton groups while many other taxa of potential significance have been overlooked. One such overlooked group of coastal phytoplankton are the cryptomonads. This thesis clarifies our understanding of the physiological ecology of the Cryptomonads and thus serves as the basis for understanding and forecasting the stability and resilience of coastal ecosystems.

Cryptophytes have an exclusive combination of photosynthetic pigments and, under low light conditions, the ability to mixotrophically exploit available inorganic as well as organic nutrients. This makes them a unique group able to take advantage of several niches in the coastal environment. Specifically, cryptophytes are able to

maximize light absorption and utilization by varying pigments concentrations and PSII:PSI stoichiometry, to use alternative fuel sources such as organic nutrients under low light conditions when photosynthetic rates may not be sufficient to support strictly autotrophic growth, and to use their swimming ability to control their proximity to light and nutrients in the water column. These distinctive strategies allow cryptophytes to rival more customary bloom forming algae under certain conditions. Principally, cryptophytes are most prevalent in areas marked by low light and high concentrations of organic matter. In these areas, their physiological capabilities allow them to potentially out-compete traditional phytoplankton groups. As more coastal areas move towards these types of organically laden, low light environments we should expect to see a proliferation of cryptophyte algae as they exploit their lifestyle to contest other coastal phytoplankton. In order to comprehend the changes this shift in phytoplankton community composition will have on coastal ecosystems, it is essential to understand the current physiological ecology and distribution patterns of cryptophyte algae. This work begins to illuminate the functional importance of cryptophyte algae in coastal areas.

ACKNOWLEDGEMENTS

Many thanks to everyone at IMCS – so many years and so much time spent there, it became a home away from home. Thanks to the crew of the Coastal Ocean Observation Lab, if IMCS was home, they were certainly family. I would especially like to thank Mike Crowley, Josh Kohut, and Jessie Sebbo for all of their help, guidance, support, and friendship. They made the long hours seem shorter and the hard work seem fun.

Thanks to the graduate program in oceanography at Rutgers. There are many members, past and present, who had a significant impact on my life both professionally and personally. Specifically I would like to thank Zoe Finkel, Chris Gregg, Shannon Newby, Matt Oliver, Sasha Tozzi, and Tracy Wiegner. They have been the best peers and friends and I hope to have them as colleagues for many years.

I'd like to thank my committee members – James Pinckney who always managed to find time for me no matter how far away he was, Paul Falkowski who provided both academic guidance and an excellent source of entertainment, Scott Glenn who is the reason I got involved in the crazy world of oceanography in the first place, and Oscar Schofield who has at times played the role of not only mentor and advisor, but confidante, drinking buddy, and friend and without whom I would have neither begun nor finished this dissertation.

And lastly I'd like to thank all of my family and friends who have unconditionally supported through my many long years at Rutgers. It is much easier to attain your goals when you have a strong foundation to reach from - they have always been and continue to be that foundation for me.

TABLE OF CONTENTS

LIST OF TABLES

LIST OF ILLUSTRATIONS

1.0 Introduction

1.1 Coastal phytoplankton community composition

Phytoplankton in aquatic environments play a critical role in biogeochemical cycles and serve as the base of the aquatic food web. This role is especially important in coastal areas where phytoplankton are central to material transformations and primary production rates are very high. Phytoplankton are often categorized into groups based on their primary role in biogeochemical material fluxes and/or primary production. For example, diatoms are considered the principal phytoplankton group contributing to primary production and carbon export in coastal areas; dinoflagellates are often important contributors to biomass in stratified or silica limited areas and are well examined in harmful algal bloom literature; and cyanobacteria are the dominant algal group in offshore continental shelf and oceanic waters (Margalef 1978; Glover *et al.* 1986; Smayda 1989). Consequently, the majority of oceanographic phytoplankton research has largely focused on prolific groups such as diatoms, dinoflagellates, and cyanobacteria. The abundance of these organisms in natural waters and the availability of laboratory strains for research make them obvious choices for both field and laboratory studies. However, phytoplankton community composition in coastal areas is extremely heterogeneous and these well studied groups are often out-competed by alternative phytoplankton groups. Despite this, the importance of these alternative groups to coastal ecosystems and to material transformation rates has yet to be explored. One such under-appreciated phytoplankton group is the Cryptomonads, which are numerically and functionally significant in many aquatic environments.

Cryptophytes are an adaptable group that thrive at depth in oligotrophic waters (Ilmavirta 1988), the Southern Ocean (Fiala et al. 1998), the coastal ocean (Tamigneaux et al. 1995), estuaries (Pinckney et al. 1998), and inland lakes (Klaveness 1988; Higashi and Seki 2000). Despite their abundance, their importance is often under-appreciated and the amount of research conducted on them is small, especially when compared to the more classic phytoplankton groups (Fig. 1.1). The lack of understanding of cryptophyte significance and physiological ecology is particularly unfortunate as in turbid, coastal waters cryptophytes are a quantitatively dominant group and can have a significant impact on biogeochemical transformation rates and food web cycling.

1.2 Cryptophyte morphology

Cryptophytes evolved from a secondary endosymbiotic event involving an ancestral rhodophyte-like eukaryotic cell and a phagotrophic eukaryotic organism (Douglas 1992; Moreira *et al.* 2000). Despite their common ancestry, cryptophytes are distinctly morphologically and physiologically different from other phycobilin containing phytoplankton groups and other secondary endosymbionts.

Cryptophytes are eukaryotic phytoplankton found in both marine and freshwater ecosystems. They are mostly biflagellated and autotrophic, although there are some colorless, heterotrophic species (Davis and Sieburth 1984; Hill and Rowan 1989). The cryptophytes contain two major light harvesting systems – the phycobilin complex which is located in the intra-thylakoid space and a chlorophyll protein complex located in the thylakoid membrane (Gantt *et al.* 1971). The presence of phycobilin pigments in cryptophytes and their integral role in light harvesting for photosynthesis was first discovered in 1959 (Allen *et al.* 1959; Haxo and Fork 1959; ÓhEocha and Raftery 1959). Unlike other phycobilin containing phytoplankton groups, cryptophyte phycobilins are not arranged into phycobilisome protein complexes and their thylakoids are most often in pairs or stacks (Lucas 1970; Maccoll and Guard-Friar 1987; Vesk *et al.* 1992). Phycobilins in cryptophytes are located within the intra-thylakoidal (lumenal) space (Gantt et al. 1971) and are not bound to the thylakoid membrane (Spear-Bernstein and Miller 1989) as is observed in cyanobacteria. Additionally, cryptophytes contain either phycoerythrin or phycocyanin, but never both in the same species, and often have several chromophores associated with their phycobilins (Kobayashi *et al.* 1979). They are the only phytoplankton group to contain this unique arrangement of photosynthetic pigments.

Most phytoplankton with complex plastids as a result of secondary endosymbiosis exhibit limited evidence of the engulfed phototroph [these groups are identified by four plastid surrounding membranes (Wastl and Maier 2000)]. However, cryptophytes are unique in that the cytoplasm and nucleus of the eukaryotic phototrophic endosymbiont endures as the periplastidal space and the nucleomorph respectively (Hansmann, 1988; Gillott and Gibbs, 1990). The nucleomorph contains both DNA and RNA and encodes some plastid genes (McKerracher and Gibbs 1982; Fraunholz *et al.* 1998; Wastl *et al.* 2000). The true functionality of the nucleomorph is an active area of research and sets the cryptophytes apart from other secondary endosymbionts as a unique evolutionary intermediate.

1.3 Cryptophyte distribution in nature

Cryptophytes are eucaryotic flagellates ranging in size from 3 – 50 μm and are found worldwide from inland lakes, to estuaries and coastal areas, to the open ocean. The available information about cryptophytes is minimal as they are typically a background ephemeral phytoplankton group and are difficult to preserve and identify in natural samples (Gieskes and Kraay 1983). Cryptophytes are an opportunistic group and do not follow the traditional paradigms for bloom forming phytoplankton. In general, cryptophytes thrive under dim light conditions and are commonly found at depth (Ilmavirta 1988). In these areas, cryptophytes are considered a permanent presence throughout the year, are often major contributors to total biomass, and are critical to food web dynamics (Klaveness 1988).

Cryptophyte blooms tend to follow perturbations in the system, due either to natural cycles, episodic events, or after the bloom of another phytoplankton group (Dokulil 1988). In many cases, cryptophyte blooms emerge during the decline of the spring diatom bloom as dissolved silica levels reach a concentration limiting to diatom growth (Dokulil and Skolaut 1986). The net result is that diatom and cryptophyte abundances are often inversely correlated, temporally and/or spatially, in many coastal areas (Figs. 1.2 & 1.3). Diatoms and cryptophytes are the only phytoplankton groups that exhibit this tight coupling across a wide range of coastal environments. The only coastal areas where this relationship does not hold are clear, oligotrophic, coastal waters (Fig. 1.3d).

These clear waters are optically deep and high levels of both photosynthetically available radiation (PAR) and ultraviolet radiation (UVR) penetrate into the water column. Cryptophytes are highly sensitive to both PAR and UVR and are not able to produce photoprotective compounds to shield themselves from damaging irradiances (Vernet *et al.* 1994). In response to increased levels of UVR cryptophytes exhibit a decrease in motility and carbohydrate reserves and a bleaching of pigments (Plante and Arts 2000). Phycobilin pigments are readily cleaved by exposure to UVR and are broken down faster than chlorophyll and carotenoid pigments making phycobilin containing groups more susceptible to damage by UV exposure than many other phytoplankton groups (Hader *et al.* 1998). The vulnerability of phycobilin pigments to UV damage may prevent cryptophytes from growing in areas with high, potentially damaging irradiances such as surface waters.

1.4 Physiological strategies of the cryptophytes

The constantly fluctuating conditions in aquatic ecosystems present a dynamic and unstable environment for growth. In natural waters, phytoplankton will often be at an irradiance or nutrient level that is not optimal for growth. Phytoplankton groups have developed mechanisms for dealing with these perturbations in their surroundings and different phytoplankton groups have developed distinctive strategies to take advantage of available niches. Surely cryptophyte algae are no exception and have developed several mechanisms that allow them to adapt to and exploit particular niches in aquatic environments. Specifically, they may be able to adjust cellular concentrations and composition of photosynthetic pigments and photochemical machinery and may use organic nutrients to supplement their growth. These strategies would allow them to continue growth under conditions unfavorable for most photosynthetic organisms and will each be addressed in greater detail in this thesis. The ways in which cryptophyte algae respond to a changing environment needs to be a research focus in order to begin predicting how they will affect population dynamics, food webs, and cycling of nutrients within aquatic systems.

1.5 Objectives of Thesis Research

The overall objective of this thesis is to define the environmental niche for cryptophyte algae. The work is focused specifically on quantifying how light and nutrient distributions impact growth through an analysis of natural and laboratory, freshwater and marine cryptophyte populations. This combined analysis was designed to clarify the fitness and competitive ability of cryptophyte algae under varying environmental factors. I hypothesize that cryptophyte algae have unique adaptation strategies for exploiting coastal aquatic environments and in certain areas this will afford them a competitive advantage over other more prolific phytoplankton groups. This competitive advantage will have a pronounced affect on phytoplankton community composition as well as aquatic food webs and material transformations in coastal waters. Specific questions which were addressed are as follows:

Question 1) *What are some of the defining parameters controlling the temporal and spatial distribution of cryptophytes in natural aquatic environments?* Are cryptophyte distributions defined by their absorption qualities in nature and how does their ability to harvest light at depth differ from other algal groups? Can we use available information to determine a range of 'habitable zones' for cryptophytes?

Question 2) *Are cryptophytes significantly affected by the presence of Ultraviolet Radiation (UVR)?* Will their photosynthetic efficiency and/or growth potential be compromised by exposure to UVR? I hypothesize that cryptophytes are extremely sensitive to UVR and their growth will be significantly impaired by the presence of high amounts of UV light.

Question 3) *How do cryptophytes acclimate to a changing light environment (changes in both light intensity and spectral quality)?* Specifically, do they adjust the concentration and/or ratio of pigments in response to the incoming light field? Are they afforded a competitive advantage in spectrally skewed light environments due to the presence of phycobilin pigments? I hypothesize that cryptophytes will be afforded an advantage in areas of low light availability and areas of spectrally restricted light fields with mostly green and blue-green wavelengths of light. Additionally, I believe cryptophytes will be able to exhibit control over their photosynthetic machinery such that their growth rate and photosynthetic ability is maximized in areas of low light.

Question 4) *Does the uptake of organic matter enhance cryptophyte growth or make them otherwise more competitive against other phytoplankton groups?* Are photoautotrophic cryptophytes capable of heterotrophy and if so how much of an advantage does this provide them over more traditional photoautotrophic algae. I hypothesize that cryptophyte populations grown in the presence of supplemental organic substrates will have higher growth rates than control populations. This increase in growth potential will translate to an increased prevalence of cryptophyte species in areas with high concentrations of organic matter that may supplement growth in low light environments.

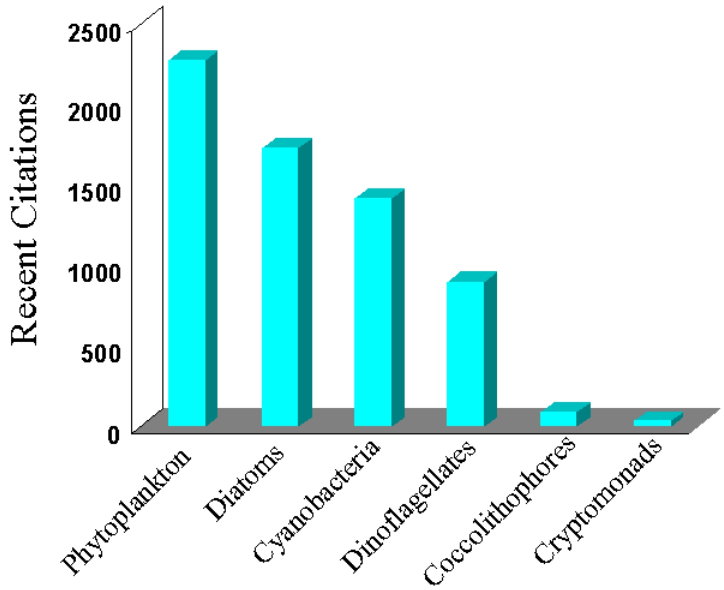

Figure 1.1: Available citations for major phytoplankton taxa (from Web of Science journal search).

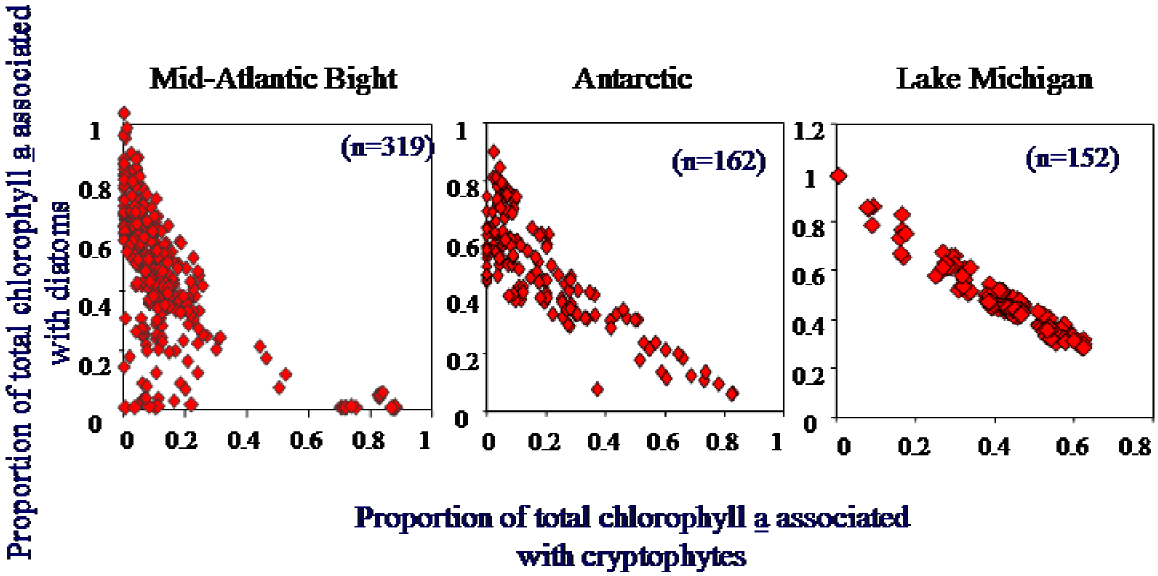

Figure 1.2: Relationship between proportion of total biomass (as chlorophyll *a*) associated with cryptophytes versus the proportion of biomass associated with diatoms in a) the Mid-Atlantic Bight, b) coastal Antarctica, and c) Lake Michigan. Teflon-coated Niskin bottles, lowered to selected depths, were used to collect water for assessment of phytoplankton photopigments. Phytoplankton biomass, as chlorophyll *a*, and phylogenetic group dynamics were calculated using chemotaxonomic pigments measured by High Performance Liquid Chromotography as outlined in (Millie *et al.* 2002). Cryptophytes and diatoms were identified by the presence of the carotenoids alloxanthin and fucoxanthin respectively.

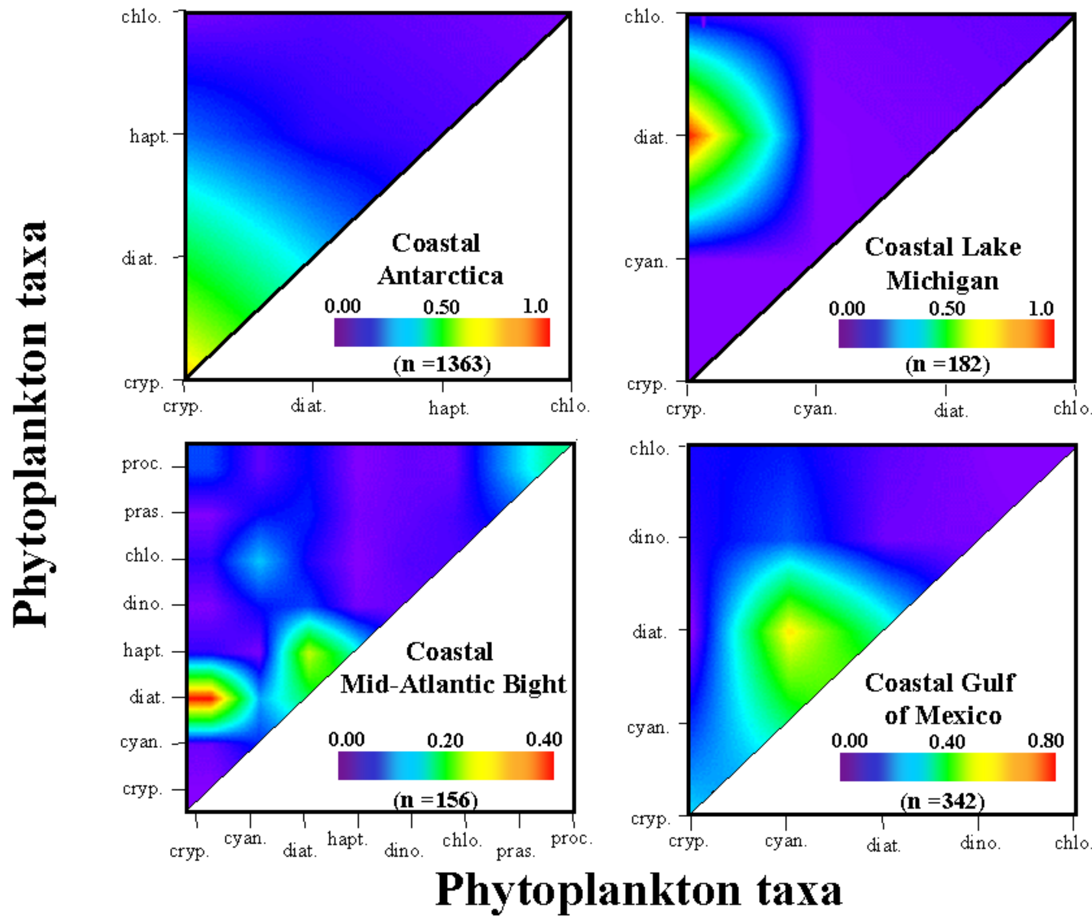

Figure 1.3: Relationship between all major taxa (as R^2 of linear correlation between proportion of total biomass of groups shown) in a) coastal Antarctic, b) coastal Lake Michigan, c) coastal Mid-Atlantic Bight, and d) Coastal Gulf of Mexico. Data were collected as in Fig. 1.2.

2.0 Assessing the relative impact of resuspended sediment and phytoplankton community composition on remote sensing reflectance

Abstract

In order to characterize the impact of turbidity plumes on optical and biological dynamics, a suite of environmental parameters were measured in southern Lake Michigan during the springtime recurrent sediment plume. In-water measurements of inherent optical properties (IOPs) were entered into Hydrolight 4.2 radiative transfer model and the output was compared with measured apparent optical properties (AOPs) across a wide range of optical conditions. Hydrolight output and measured underwater light fields were then used to clarify the effects of the sediment plume on phytoplankton community composition and nearshore remote sensing ocean color algorithms. Our results show that the suspended sediment in the plume did not seriously impact the performance of ocean color algorithms. We evaluated several currently employed chlorophyll algorithms and demonstrated that the main factor compromising the efficacy of these algorithms was the composition of phytoplankton populations. As phycobilin-containing algae became the dominant group, chlorophyll algorithms that use traditional blue/green reflectance ratios were compromised due to the high absorption of green light by phycobilin pigments. This is a notable difficulty in coastal areas, which have highly variable phytoplankton composition and are often dominated by sharp fronts of phycobilin and non-phycobilin containing algae.

2.1 Introduction

The main circulation patterns in Lake Michigan are primarily wind driven. This is an energetic and dynamic environment and it is often seriously affected by short-term episodic events. In the Great Lakes, episodic events are most frequent in the late winter/early spring when high winds and storms are prevalent and thermal stratification is low (Lee and Hawley 1998; Lou *et al.* 2000; Beletsky and Schwab 2001). These events have been hypothesized to play a disproportionately large role in structuring physical and biological systems, but investigating their importance is difficult given the limitations of traditional sampling techniques.

One annual event that occurs in southern Lake Michigan each spring is a recurrent turbidity plume that extends up to 200 km alongshore (Mortimer 1988). Spring in Lake Michigan is marked by frequent, highly energetic storms, turbulent shoreline erosion, and high river runoff. These forces lead to significant resuspension of particles, which are then transported to the southern basin of the lake. The erosive forces in Lake Michigan are episodic in nature and for many biogeochemically important materials this resuspension and transport of sediments in the Southern Basin is greater than external inputs from rivers (Eadie *et al.* 1984; Hawley 1991; Eadie *et al.* 1996). Particles resuspended during the plume event may comprise up to 25% of the total transport of sediment to the southern part of the Lake (Eadie *et al.* 1996; Lou *et al.* 2000). This resuspension and transport of concentrated sediment loads is coincident with the spring phytoplankton bloom (Mortimer 1988). The spring bloom is a crucial time for the ecology of Lake Michigan as it may contribute up to 50% of the total annual primary production in the Lake and is a major source of carbon to higher trophic levels

(Fahnenstiel and Scavia 1987). The physical processes associated with these coastal plumes were believed to be critical in controlling biogeochemical cycling, shaping the light environment, altering available nutrient concentrations, establishing conditions for the spring bloom, and structuring biological communities (Mortimer 1988).

The recurrent turbidity event was first observed in remote sensing data as a highly reflective band nearshore (Mortimer 1988). At that time, Mortimer noted the difficulty in using optical and remote sensing techniques in areas of strong optical gradients and highly variable concentrations of suspended particulate material (SPM), colored dissolved organic matter (CDOM), and chlorophyll such as that observed in coastal areas. Since that time there has been much debate over the utility of such techniques in dynamic coastal environments. Recent efforts have focused on remote sensing techniques in order to increase sampling resolution to ecologically relevant scales for investigation into the effects of short-term episodic events. As part of the Episodic Events – Great Lakes Experiment (EEGLE), we wanted to quantify the effects of the episodic recurrent turbidity plume on optical parameters, phytoplankton dynamics, remote sensing techniques, and the performance of currently employed coastal algorithms.

2.2 Methods

2.2.1 Sampling

Sampling was conducted in the southeastern portion of Lake Michigan (Fig. 2.1) from 24-26 March 1999, 14-15 and 22-24 April 1999, and 18-19 March 2000 onboard the R/V Laurentian. Sampling stations were established both inside and outside of the sediment plume along historic transect lines perpendicular to the coast. Vertical profiles of physical and optical parameters were performed at each station and supplemented with discrete water samples that were taken to the laboratory for more in depth analysis.

2.2.2 Optical Measurements

At each station, hydrographic profiles of the water column were measured with a SeaBird CTD. Optical measurements included surface and vertical profiles of both apparent and inherent optical properties. Inherent optical properties (IOPs) were measured with a dual-path absorption and attenuation meter (AC-9; Wetlabs Inc.). The AC-9 measures both absorption and attenuation at 9 wavelengths of light (412, 440, 488, 510, 532, 555, 630, 676, and 715 nm). The AC-9 was factory calibrated between sampling years and calibrated daily using ultra-clean water from a Barnstead E-Pure water purification system. Absorption data were integrated with concurrently collected CTD data and were temperature (Pegau *et al.* 1997) and scattering [subtraction of a715 from all a channels (Zaneveld and Kitchen 1994)] corrected and binned to 0.25m depth intervals.

Apparent optical properties (AOPs) were collected using a profiling spectral radiometer (Ocean Color Radiometer 200; Satlantic Inc.) and a hyperspectral radiometric buoy (HTSRB; Satlantic Inc.). The OCR-200 measures downwelling irradiance (E_d) and upwelling radiance (L_u) *in-situ* as well as downwelling surface irradiance [$E_d(0^+)$] at 14 wavelengths (305, 324, 339, 380, 406, 412, 443, 490, 510, 555, 619, 665, 670, and 705 nm). The TSRB measures $E_d(0^+)$ and L_u (at 0.7m) at 123 visible wavelengths. All Satlantic sensors were factory calibrated prior to each sampling year. Collected radiometric data were processed using Satlantic's Prosoft software package according to manufacturer protocols. No dark corrections or self shading corrections were applied to these data. Diffuse attenuation coefficient (K_d) values were calculated as

$$K_d = LN\left(\frac{Ed_2}{Ed_1}\right)\frac{1}{\Delta z} \tag{2.1}$$

where E_{d2} is the downwelling irradiance at depth 2, E_{d1} is downwelling irradiance at depth 1, and Δz is the change in depth between these two measurements. Remote sensing reflectance (Rrs) values were calculated using Prosoft as

$$Rrs\left(0^+,\lambda\right) = \frac{L_w\left(0^+,\lambda\right)}{E_d\left(0^+,\lambda\right)} \tag{2.2}$$

where L_w is upwelling radiance propagated up through the surface of the water as

$$L_w\left(0^+,\lambda\right) = 0.54 L_w\left(0^-,\lambda\right) \tag{2.3}$$

Remote sensing reflectance outputs from Prosoft calculations were subsequently used for calculation of chlorophyll *a* concentrations using an array of remote sensing chlorophyll algorithms [Table 1 (O'Reilly *et al.* 1998; O'Reilly *et al.* 2000)].

2.2.3 Discrete Sample Measurements

Teflon-coated Niskin bottles, lowered to selected depths, were used to collect water for assessment of phytoplankton photopigments, photosynthesis-irradiance parameters, and SPM concentrations. Phytoplankton biomass, as chlorophyll *a*, and phylogenetic group dynamics were characterized using chemotaxonomic pigments derived using High Performance Liquid Chromotography as outlined in (Millie *et al.* 2002). Photosynthesis-irradiance parameters were measured as in (Fahnenstiel *et al.* 2000). SPM concentrations were determined gravimetrically after drawing 0.2- to 0.3-L aliquots under low vacuum onto pre-rinsed, tared 47 mm diameter Poretics 0.4-μm polycarbonate filters. The filters were dried in a dessicator to constant weight. When necessary, SPM concentrations were estimated from AC-9 collected data based upon the relationship established between suspended material concentration and attenuation at 650nm (Fig. 2.2).

2.2.4 Solving the Radiative Transfer Equation

In order to evaluate the dynamic response of primary producers to the highly variable *in-situ* light environment, we needed to spectrally characterize the underwater light field under a wide range of conditions. Establishing a solid relationship between the IOPs and AOPs provides confidence that a full set of radiometric parameters can be calculated given *in situ* measurements of the IOPs. A subsection of our data set (n=41 profiles) was input into Hydrolight 4.2 (Sequoia Scientific Inc.) to numerically solve the radiative transfer equation for a realistic radiance distribution. Hydrolight requires four basic input parameters; the IOPs of the water body, wind speed, sky spectral radiance distribution, and water column bottom boundary conditions. In this study we supplied Hydrolight with measured IOPs (a and c) from an AC-9 and measured wind speeds from an anemometer aboard the research vessel. The sky spectral radiance distribution is calculated within Hydrolight via RADTRAN based upon user-supplied date, time of day, location on the globe, and cloud cover at each station. Reflectance of the bottom boundary was set at 20% without spectral dependence for all calculations. In this study, Hydrolight output was obtained solely to determine scalar irradiance values, therefore we wanted to ensure that Hydrolight output closely reflected conditions at the time of sampling. To this end, the backscatter fraction (b_b/b) was optimized at each individual station to minimize the difference between the output and measured values and was input as a Fournier –Fourand (FF) phase function. In the absence of a measured particle phase function, the FF is an acceptable replacement as the exact shape of the phase function is not as critical as the magnitude of the backscatter ratio for calculations of the AOPs (Mobley *et al.* 2002).

To validate our results from Hydrolight, modeled values were compared to concurrently measured AOPs at 41 stations in our sampling area over the course of two years in the spring and summer. These stations encompassed a wide variety of optical and physical environments. K_d and Rrs values were used for the comparisons as they are not extremely sensitive to the geometric distribution of the light field. To correlate K_d, we incorporated 435 data points over spatial and temporal gradients and directly compared the Hydrolight output with measured values (Fig. 2.3a). The correlation was strong with a slope of 0.88 indicating that modeled values were slightly underestimating measured K_d values. Rrs correlations were also strong (average $R^2 = 0.94$) although spectrally dependent (Fig. 2.3b). The slope was very close to 1.0 at lower wavelengths and dropped off towards the red wavelengths (slope range = 0.68 – 1.2). This is not surprising as the magnitude of the Rrs signal is much lower in the red wavelengths of light, therefore part of the error in this part of the spectrum is a signal to noise problem.

Hydrolight output was used to quantify the amount of light available to phytoplankton. Phytoplankton populations are able to use light from all directions for photosynthesis. This light field is represented by the scalar irradiance (E_o). E_o is the integral of the radiance over all angles around a point. This differs from the downwelling irradiance (E_d), which is the traditionally measured irradiance term. E_d accounts only for light propagating in the downward direction and proportionally weights the contribution of radiation at different incidence angles. The E_o output from Hydrolight calculations allowed us to use this E_o term, which we were unable to measure, to examine light utilization by phytoplankton. E_o values were used to calculate the scalar diffuse attenuation coefficient (K_o),

$$K_o = LN\left(\frac{Eo_2}{Eo_1}\right)\frac{1}{\Delta z} \tag{2.5}$$

the scalar optical depth (ζ_o),

$$\zeta_o = K_o z \tag{2.6}$$

and the average cosine,

$$\overline{\mu} = \frac{E_d - E_u}{E_o} \tag{2.7}$$

where E_u is the upwelling irradiance.

2.3 Results

2.3.1 Optical dynamics

The springtime recurrent turbidity plume in Lake Michigan strongly impacted the optical environment in the southern portion of the Lake. The plume can easily be observed in remote sensing reflectance imagery during the spring months (Fig. 2.4a). The spatial extent of the plume can be seen in March 1999, followed by confinement to the coastline in April, and then dissipation in the summer months with thermal stratification (Fig. 2.4). The three major optical zones along a transect line in April 1999 extending 32 km offshore St. Joseph, MI, through the sediment plume area, can readily be observed in collected data. The optical gradients in this area were large over short distances reflecting the interaction of the turbidity plume and outflow from the St. Joseph River. The three distinct water types along this transect line included an onshore river/plume region that extended to roughly 10 km offshore, plume dominated water that extended approximately 10 to 20 km offshore, and offshore stations further than 20 km. Data collected along this transect line in April of 1999 were representative of conditions during the spring of all sampling years for the duration of the sediment plume and were used as a case example during this study.

Nearshore stations were strongly influenced by both the sediment plume and the outflow from the St. Joseph River. Although absorption and scattering were both increased at nearshore stations, spectral changes in the optical signal were controlled by absorption. Concentrations of highly absorbing CDOM and chlorophyll *a* were increased in onshore stations relative to offshore areas. CDOM absorbs light mostly in the blue wavelengths, which was apparent as an increase in the absorption spectra in the blue wavelengths (Fig. 2.5a). These high nearshore CDOM concentrations were probably due to both river outflow and *in-situ* production. Chlorophyll *a* concentrations at onshore stations were relatively high and diatoms dominated the phytoplankton community adding to the high blue light absorption values (Fig. 2.6d-f). The effects of in-water constituents were also apparent in the Rrs spectra. Onshore stations had a proportional decrease in Rrs in the 400-500 nm region relative to stations further offshore due to absorption of light by both CDOM and chlorophyll *a* at these wavelengths. A peak in Rrs due to chlorophyll fluorescence at 676 nm is also evident (Fig. 2.6b, red line). The available light field at the 1% light level was predominately green and red as all of the shorter wavelengths of light were absorbed in the water column (Fig. 2.6c).

Moving offshore into waters impacted less by the river, the effects of the sediment plume became more apparent. Absorption values decreased relative to onshore stations while scattering stayed high resulting in a significant increase in measured b/a ratios (Fig. 2.6a). This high scattering to absorption ratio was used as the primary optical signature of the sediment plume. The proportional decrease in absorption and increase in scattering was reflected in higher Rrs signals as more light was scattered up through the water column (Fig. 2.6b, green line). Chlorophyll values decreased in plume dominated stations and the composition of the phytoplankton community began to change (Fig. 2.6d-f). Further offshore, the optical signature was dominated by phytoplankton absorption. Both absorption and scattering were low relative to onshore waters and Rrs spectra were comparatively low and spectrally flat (Fig. 2.6b, blue line). Available light at the 1% light level was mostly blue-green and the phytoplankton community became dominated by cryptophyte algae in these offshore waters (Fig. 2.6c&e).

The changes in the concentrations of optically active constituents altered the light climate of the different water types. The high blue absorption at onshore stations resulted in the selective removal of blue wavelengths and a red shift of the available light field, while offshore stations had proportionally more blue and green light (Fig. 2.6c). In addition to these spectral changes in light quality, the quantity of available light at depth was decreased in onshore stations. The relationship between scalar optical depth and physical depth was steeper at onshore stations than in plume-dominated and offshore waters (Fig. 2.7a). A deeper optical depth corresponding to the same physical depth indicates that onshore waters were more attenuating than offshore waters. Additionally, the scattering/absorption ratio was higher in plume dominated stations as compared to both onshore and offshore waters, resulting in a change in the diffusivity of the underwater light. The average cosine provides a simple description of the angular radiance distribution of the underwater light field. Average cosine values range from 0 for isotropic light fields to 1 in a collimated beam of light; a lower average cosine value indicates a more diffuse light field. In regions affected by the turbidity plume, the increased scattering resulted in a lower average cosine (Fig. 2.7b). The average cosine was lowest in areas most optically impacted by the plume and highest in clearer, offshore waters.

2.3.2 Biological dynamics

Phytoplankton physiology and community composition were notably impacted by both seasonal changes in the light environment and the optical gradients observed in the spring. The phytoplankton photosynthetic physiology reflected the seasonal variations in the light climate. The irradiance levels corresponding to the photoacclimation parameter (E_k) and the light saturated photosynthetic rate (P^b_{max}) were relatively constant at 77 (±16) μmol photons m^{-2} s^{-1} and 0.61 (±0.28) μg C μg chl^{-1} h^{-1} respectively in both the spring months and during the summer in deeper waters (Fig. 8). E_k values were not dependent on *in-situ* E_o at the time of sample collection in these data. However, summer surface samples, which were collected at a shallower scalar optical depth (samples collected above the thermocline), were dependent on *in-situ* E_o values. As relative E_o at the time of sample collection increased due to the change in season and the shallowing of the mixed layer depth with the onset of stratification, the associated E_k and P^b_{max} values increased. These populations were consistently exposed to higher light levels in surface waters and acclimated to their growth conditions. There was no correlation between SPM concentrations and E_k for any of the samples collected, thus changes in the photoacclimation parameter were not associated with the sediment plume (Fig. 2.8).

The distribution of total chlorophyll and the composition of phytoplankton communities also varied as the optical environment changed during the spring sampling period. Diatoms consistently comprised a higher proportion of chlorophyll *a* onshore and in surface waters, while cryptophytes comprised a higher proportion offshore and in deeper waters (Fig. 2.6d-e). This resulted in a strong inverse relationship between diatom and cryptophyte abundances (Fig. 2.9).

2.4 Discussion

The springtime recurrent turbidity plume observed in southern Lake Michigan established a strong gradient ideal for assessing the utility of optical techniques in coastal waters. The location and extent of the plume could be determined through both remote sensing and *in-situ* sampling techniques (Figs. 2.4 and 2.6). The plume region, delineated by high reflectance values, extended approximately 20 km offshore for much of the EEGLE study. As seen in previous years, the sediment plume began in the early spring and lasted until early summer.

The sharp optical gradients encountered in the sampling area allowed the impact of variable in-water constituents on remote sensing reflectance to be characterized. Remote sensing reflectance offshore of the St. Joseph River showed the characteristic low blue reflectance due to high concentrations of CDOM and chlorophyll *a* that is common in areas offshore of large rivers (Fig. 2.6b). The St Joseph River drains a watershed area of 694,000 acres mainly through agricultural areas of Indiana and is considered a significant source of dissolved organic carbon (Mortimer 1988). Conversely, in offshore waters, reflectance was greatest in the blue wavelengths as absorption by phytoplankton and water dominated light attenuation. The sediment plume was characterized by high blue and green Rrs values due to the reflective materials in Lake Michigan which are eroded from either alongshore bluffs or shallow water glacial deposits; the sediment composition in the southeastern part of the Lake is dominated by these silts and fine sands (Fahnenstiel and Scavia 1987; Eadie *et al.* 1996; Barbiero and Tuchman 2000). This reflective material effectively scatters all of the available light and absorbs very little, resulting in high Rrs values.

It was initially believed that the high sediment concentrations associated with the turbidity plume would significantly affect the magnitude of the underwater light field resulting in light-limited phytoplankton populations leading to a decrease in primary productivity (Millie *et al.* 2002). However, in plume-dominated stations, the incident integrated flux of light was not significantly different than clearer, non-plume offshore waters which had deep mixed layer depths (Fig 2.6c). The increased concentration of particles in the sediment plume resulted in increased scattering (Fig. 2.5) which led to a more diffuse light field (Fig. 2.7b). This scattered light is simply redirected and may still be available for absorption by photosynthetic organisms.

Measured photosynthesis irradiance parameters suggested that phytoplankton populations in plume waters were not significantly more low-light acclimated than phytoplankton in offshore stations (Fig. 2.8). E_k values were fairly uniform throughout the spring bloom and plume events; furthermore the E_k values were not significantly correlated with either suspended particulate material concentrations or light attenuation measurements. Thus there was no observed gradient in phytoplankton photoacclimation between plume and non-plume stations in the spring. However, the significant increase in E_k and P^b_{max} with summer stratification indicated that these populations were capable of photoacclimation; springtime populations were low-light acclimated compared to summer populations. This low-light acclimation reflected the deep mixing of springtime populations.

The actual light field available to a phytoplankton cells is the depth integrated light field as they vertically cycle through the water column (Cullen and Lewis 1988). Under these conditions, cells may photoacclimate to the average light intensity encountered over time. The increase in light attenuation in the plume was balanced offshore where the mixed layer depth was deeper so that phytoplankton populations in these two areas had similar total amounts of light available to them over time. However, the photoacclimation observed in spring populations changed as stratification developed in the summer which is consistent with the historical model for Lake Michigan phytoplankton (Fahnenstiel *et al.* 1989). Summer samples showed a distinct difference in photoacclimation between deep water and surface stations (Fig. 2.8). Surface samples were more acclimated to the incident light field at the time of sample collection whereas photoacclimation parameters for deep water samples collected below the thermocline were independent of the incident light field (Fig. 2.8c&d). Deep water samples collected below the thermocline (thermocline at approximately 20m; Fig. 2.4d) and spring samples were being mixed over a wide vertical range of varying light intensity. The rate of mixing was most likely faster than the rate of photoacclimation and these samples were unable to acclimate to the ever-changing light intensity.

The observed shifts in phytoplankton community composition impacted remote sensing reflectance and thus ocean color algorithms. There was a strong correlation between measured and calculated chlorophyll concentration at most stations (Table 2.2). However, the absorption of green light by cryptophytes selectively removes these wavelengths from the light field. Chlorophyll algorithms utilize Rrs band ratios, which include 550, 555, 560, and 565 nm green light reflectance. These ratios assume case 1 waters where the *in-situ* absorption and water leaving radiance (L_w) signal in the blue wavelengths is dominated by chlorophyll absorption while L_w in the green wavelengths is insensitive to chlorophyll concentrations (Gordon and Morel 1983). However, in Lake Michigan, cryptophyte absorption selectively removed the green light from the reflectance signal. Areas that were not dominated by cryptophytes (those with less than 40% of total chlorophyll contributed by cryptophytes) showed good agreement between measured and satellite estimated chlorophyll concentrations (Fig. 2.10; Table 2.2). In regions with high concentrations of phycobilin containing algae, remotely estimated chlorophyll concentrations were underestimated by an average of 45% for all algorithms tested. Thus contrary to previous beliefs, the sediment plume had little affect on the utility of ocean color remote sensing efforts. The critical parameter impacting the performance of ocean color algorithms in this area was the community composition of phytoplankton.

2.5 Summary and Conclusions

Our results illustrate the minimal effect of the sediment plume on the quantity of available light for phytoplankton populations. There was no significant change in the photosynthetic characteristics between plume and non-plume populations. The phytoplankton plume populations were not significantly low-light acclimated compared to populations in clearer waters offshore. The composition of phytoplankton communities may have been impacted by the spectral quality of light, which was a function of the mixed layer depth and the in-water constituents. In the deep, well-mixed water columns, the average spectral light field was increasingly spectrally skewed which is not uncommon in freshwater systems (Kirk 1994). As the average light distribution becomes restricted, the ability of phytoplankton to absorb light is directly related to their light-harvesting capabilities. In Lake Michigan this may account for the distribution of diatoms nearshore and cryptophytes offshore where phycobilin pigments efficiently absorb the available green light. Surprisingly variability in CDOM and SPM concentrations had no effect on estimating chlorophyll using current satellite algorithms. Changes in the phytoplankton community structure did impact chlorophyll remote sensing algorithms. This suggests that currently employed reflectance algorithms may be compromised in regions of highly variable phytoplankton community composition.

Acknowledgements

Many thanks to: Larry Boihem, Kimberly Kelly, Augie Kutlewski, Mark Moline, Merritt Tuel, Rich Stone, and the Captain and Crew of the R/V Laurentian. Funding provided by NSF (OCE-9727341 and OCE-9727342) and NOAA through the CoOP

Great Lakes Initiative and by ONR's Hyperspectral Coastal Ocean Dynamics Experiment (HyCODE, N0014-99-0196).

Sensor	Equation	R
SeaWiFS/OC2	$C = 10.0^{(0.341-3.001R+2.811R^2-2.041R^3)} - 0.04$	490/555
OCTS/OC4O	$C = 10.0^{(0..405-2.900R+1.690R^2-0.530R^3-1.144R^4)}$	443>490>520/565
MODIS/OC3M	$C = 10.0^{(0.2830-2.753R+1.457R^2-0.659R^3-1.403R^4)}$	443>490/550
CZCS/OC3C	$C = 10.0^{(0.362-4.066R+5.125R^2-2.645R^3-0.597R^4)}$	443>520/550
MERIS/OC4E	$C = 10.0^{(0.368-2.814R+1.456R^2+0.768R^3-1.292R^4)}$	443>490>510/560
SeaWiFS/OC4v4	$C = 10.0^{(0.366-3.067R+1.930R^2+0.649R^3-1.532R^4)}$	443>490>510/555
SeaWiFS/OC2v4	$C = 10.0^{(0.319-2.336R+0.879R^2-0.135R^3)} - 0.071$	490/555

Table 2.1: Algorithms used to calculate chlorophyll *a* from remote sensing reflectance. R is determined as the maximum of the values shown. Sensor algorithms shown are for SeaWiFS (Sea-viewing Wide Field of view Sensor), OCTS (Ocean Color and Temperature Scanner), MODIS (Moderate Resolution Imaging Spectroradiometer, CZCS (Coastal Zone Color Scanner), and MERIS (Medium Resolution Imaging Spectrometer).

sensor/algorithm	slope-all stations	R^2-all stations	slope- non cryptophyte dominated stations	R^2- non cryptophyte dominated stations
SeaWiFS/OC2	0.81	0.66	1.04	0.95
OCTS/OC4O	0.54	0.81	0.6	0.89
MODIS/OC3M	0.6	0.77	0.7	0.89
CZCS/OC3C	0.57	0.76	0.65	0.88
MERIS/OC4E	0.59	0.79	0.62	0.87
SeaWiFS/OC4v4	0.65	0.68	0.73	0.83
SeaWiFS/OC2v4	0.68	0.69	0.78	0.83

Table 2.2: Correlation results for the calculation of chlorophyll from remote sensing reflectance measurements. The slope and R^2 for the linear correlation between measured and calculated chlorophyll is shown (as in Fig. 12) for all stations and for a subset of stations where the phytoplankton community composition is not dominated by cryptophytes (less than 40% of total chlorophyll *a* attributed to cryptophytes). All of the algorithms perform better in areas that were not significantly influenced by cryptophyte absorption.

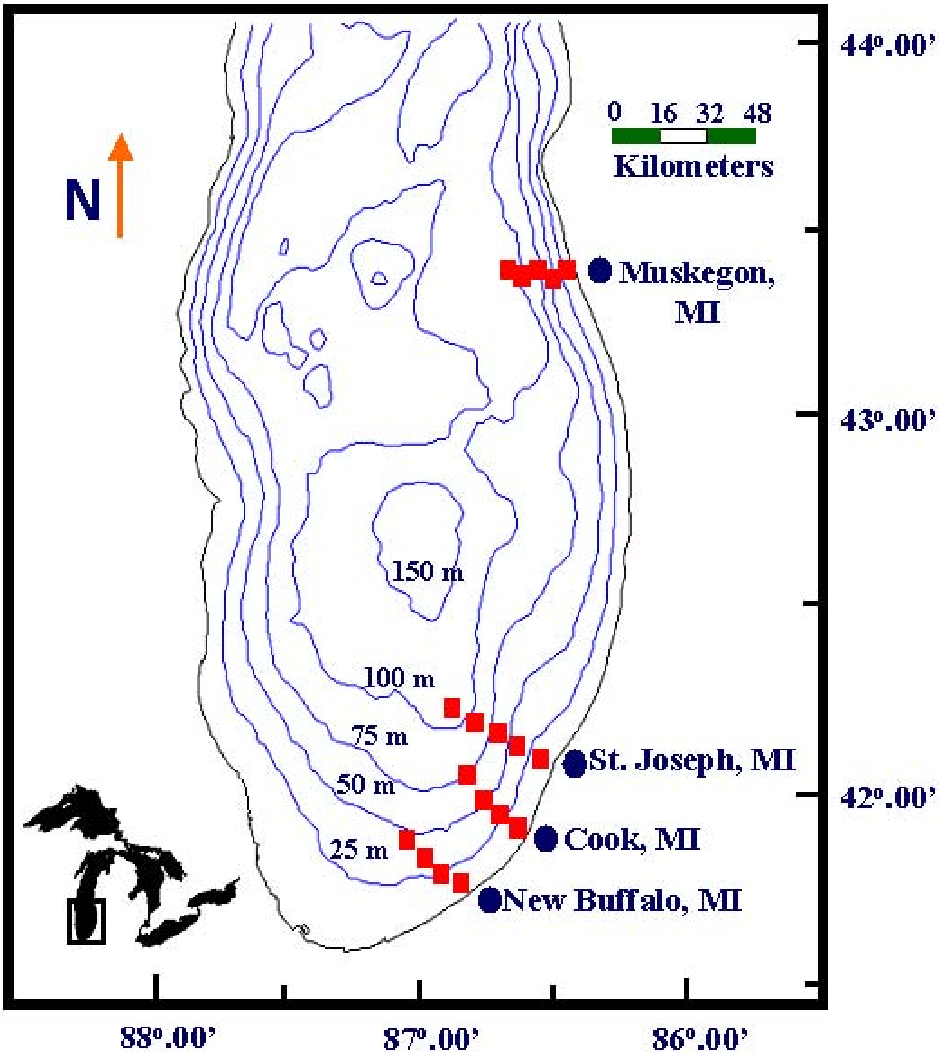

Figure 2.1: Sampling locations in southeastern Lake Michigan occupied in 1998 - 2000.

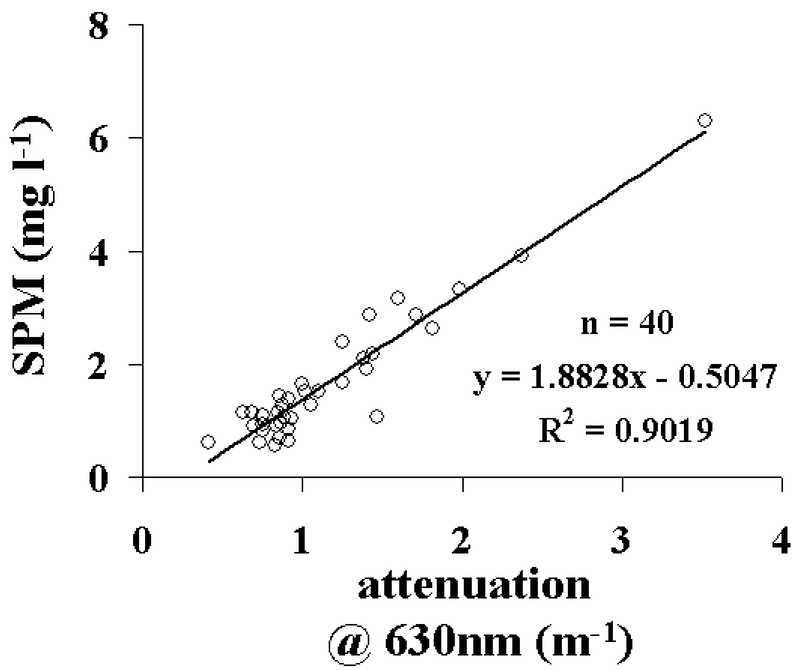

Figure 2.2: Relationship between attenuation at 630nm as measured by an AC-9 and suspended particulate material (SPM).

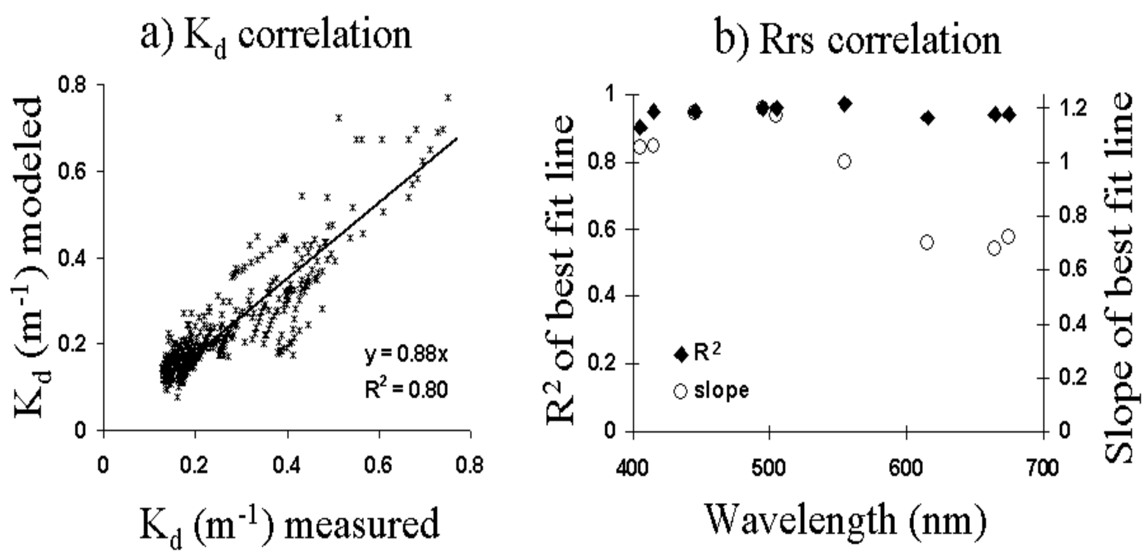

Figure 2.3: Relationship between measured and modeled apparent optical properties. Measured values are from a Satlantic profiling radiometer and modeled values are from Hydrolight output. a) diffuse attenuation coefficient (K_d) for PAR. The solid line is the best fit line with an intercept at the origin. b) remote sensing reflectance (Rrs) - R^2 are represented by closed symbols and the slopes are represented by open symbols.

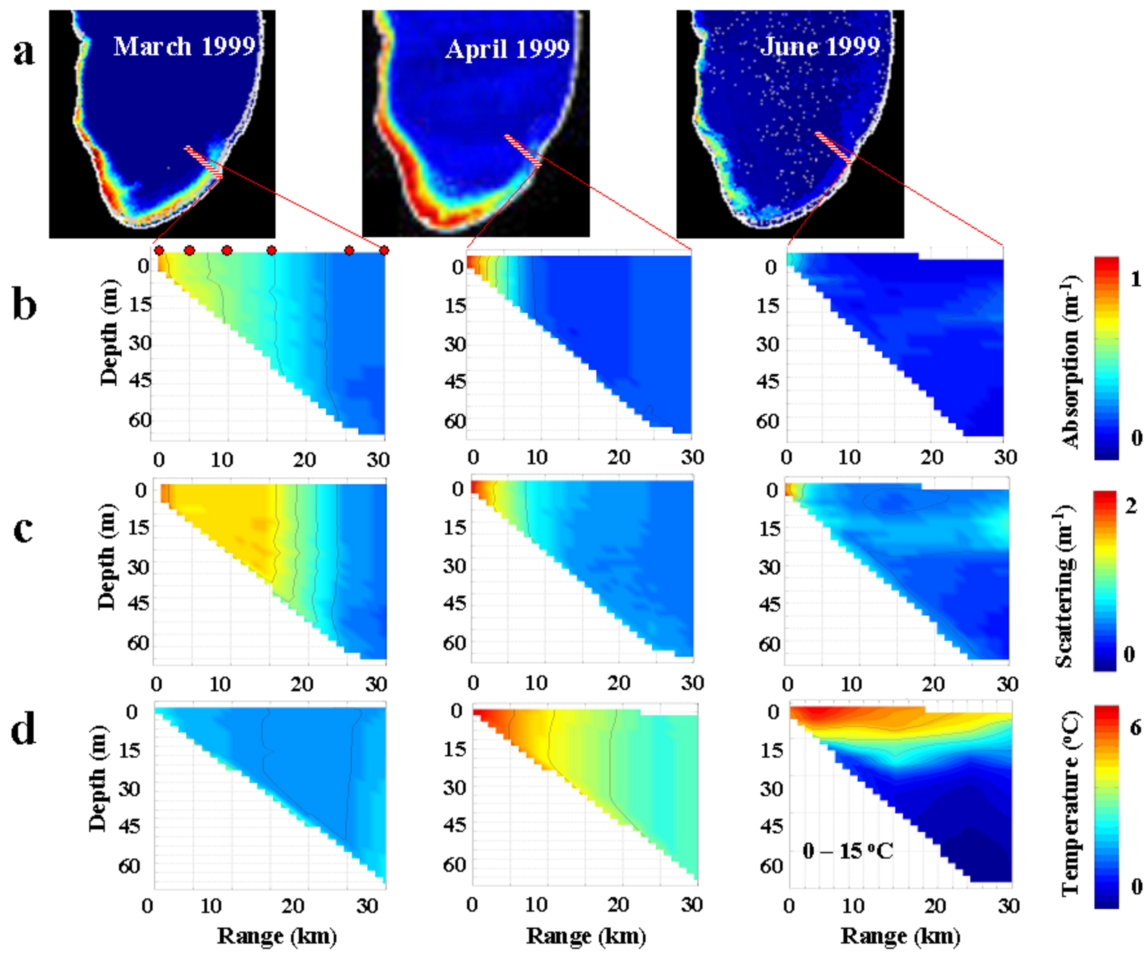

Figure 2.4: The temporal evolution of the southern Lake Michigan recurrent turbidity plume. a) AVHRR remote sensing reflectance and b) absorption, c) scattering, and d) temperature along the transect line shown extending 30km offshore St. Joseph, MI. Red circles on figure b represent station locations of the six sampling stations (stations were located approximately 2, 5, 10, 16, 26, and 30 km from shore). Note the change in scale for the temperature plot associated with June 1999.

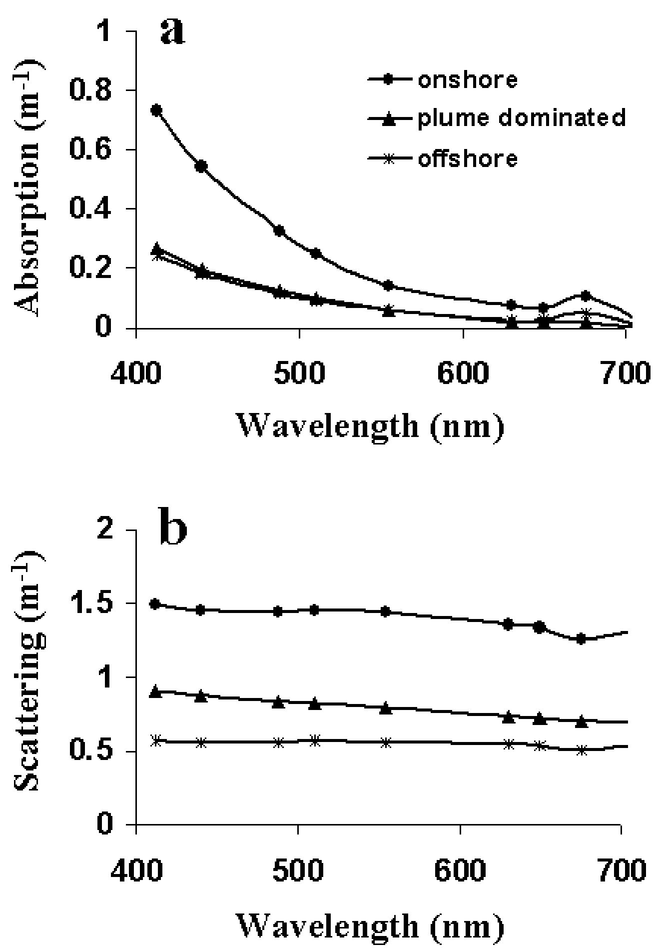

Figure 2.5: Spectral a) absorption and b) scattering coefficients at three stations along an April 1999 cross shelf transect offshore St. Joseph, MI measured with and calculated from an AC-9. Stations are located onshore (circles, 2km offshore), in plume-dominated waters (triangles, 10km offshore), and offshore (stars, 30km offshore).

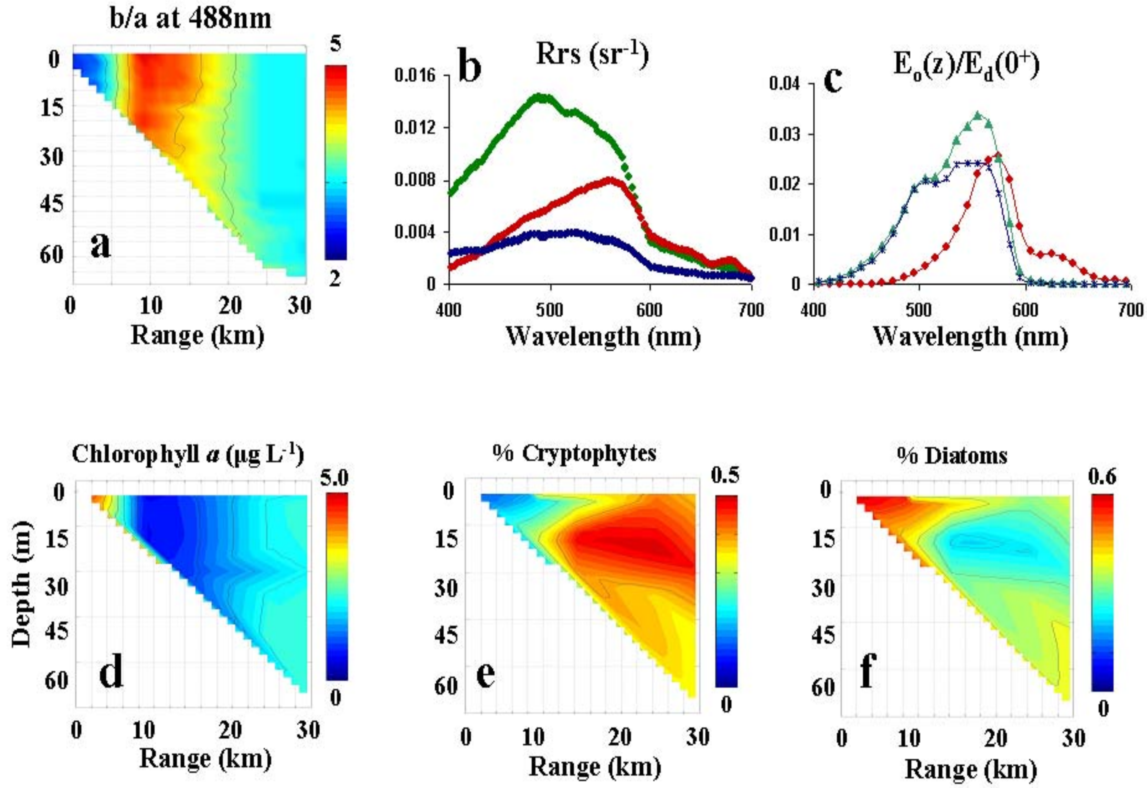

Figure 2.6: Optical and biological properties associated with an April 1999 cross shelf transect offshore St. Joseph, MI - a) scattering/absorption ratio at 488nm, b) remote sensing reflectance at an onshore station (red line, 2km offshore), a plume dominated station (green line, 10km offshore), and an offshore station (blue line, 30km offshore), c) fraction of available light at the 1% light level, as E_o at depth normalized to E_d at the surface (station colors as in c), d) HPLC measured chlorophyll *a* concentrations, e) percent of total chlorophyll *a* associated with cryptophytes, and f) percent of total chlorophyll *a* associated with diatoms. Sampling locations are as in Figure 3.

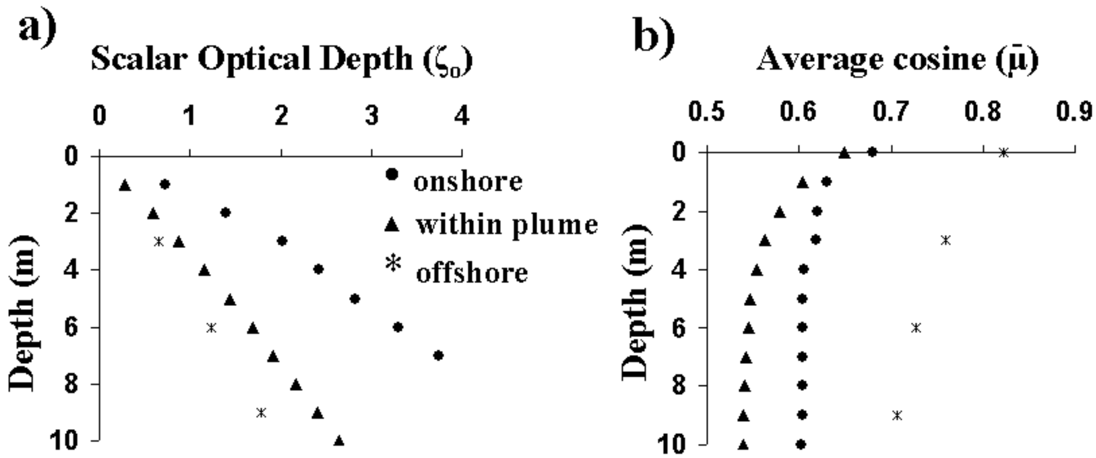

Figure 2.7: Vertical light properties at April 1999 sampling stations onshore (circles, 2km offshore), in plume-dominated waters (triangles, 10km offshore), and offshore (stars, 30km offshore) - a) scalar optical depth (ζ_o) for PAR and b) average cosine (μ) at depth for PAR. A steeper scalar optical depth represents clearer waters. A lower average cosine indicates a more diffuse light field.

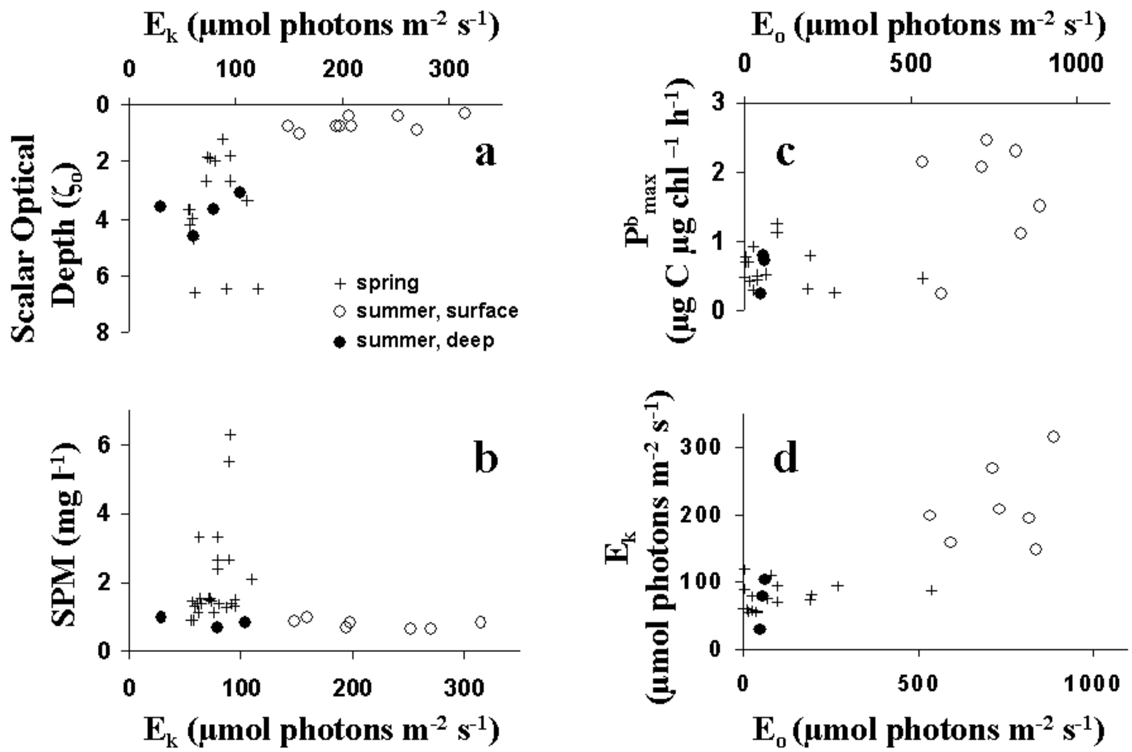

Figure 2.8: Seasonal variability in physiological parameters - a) variability in E_k with scalar optical depth, b) relationship between E_k and suspended particulate material, c) relationship between P^b_{max} and *in-situ* E_o at the time of sample collection, and d) relationship between E_k and *in-situ* E_o at the time of sample collection. During the winter, mixed months E_k and P^b_{max} values were relatively constant at 77 (± 16) µmol photons m^{-2} s^{-1} and 0.61 (± 0.27) µg C µg chl^{-1} h^{-1}respectively and did not depend on available irradiance (E_o) at the sampling depth (plus symbols). During the summer, stratified months E_k and P^b_{max} remained low in bottom waters below the thermocline (closed circles), but were much higher in surface waters (open circles). SPM values were much higher during the spring turbidity event (2.01 ± 1.33 mg l^{-1}) compared to summer time values (0.79 ± 0.12 mg l^{-1}), but there was no significant relationship between measured SPM values and E_k.

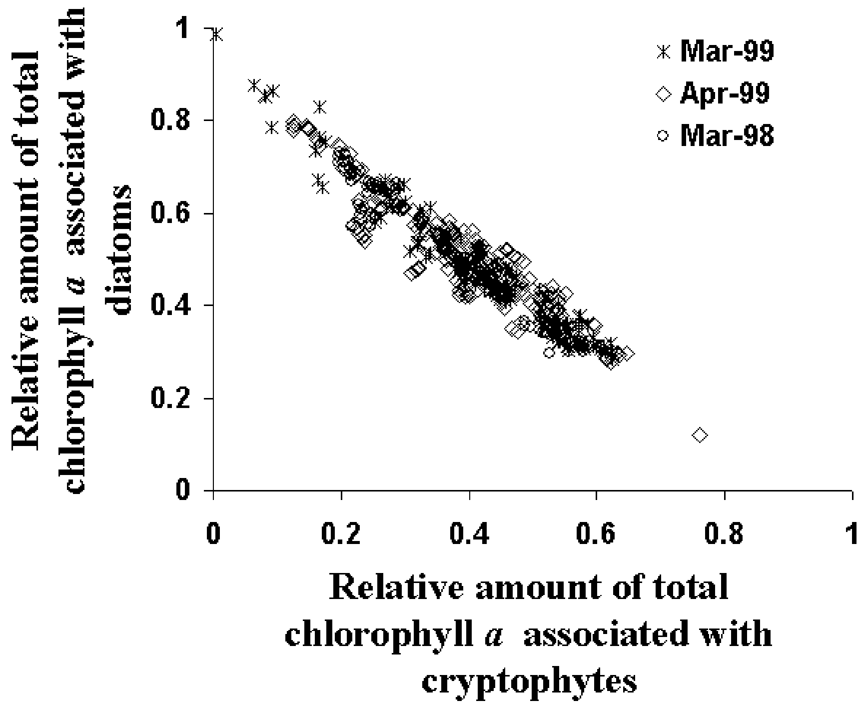

Figure 2.9: Percentage of total chlorophyll *a* associated with cryptophytes vs. percentage of total chlorophyll *a* associated with diatoms from CHEMTAX output for all available data from 1998 and 1999.

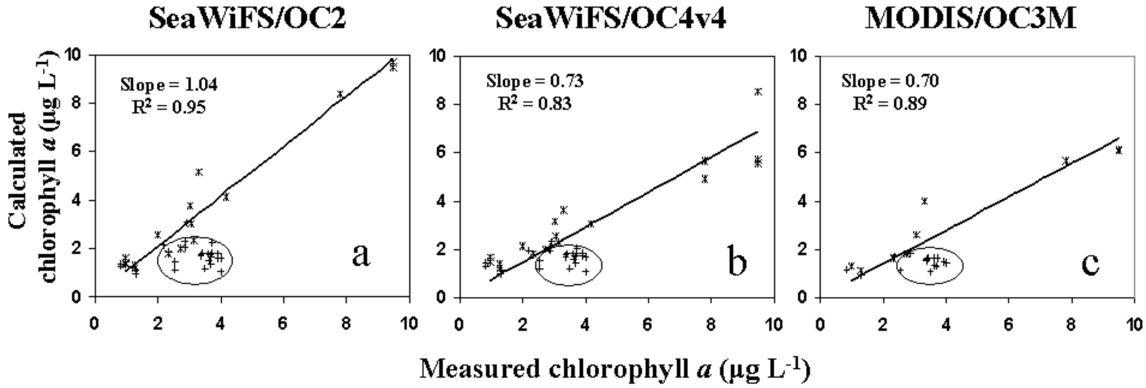

Figure 2.10: Relationship between measured chlorophyll *a* (HPLC) and calculated chlorophyll *a* from three currently used ocean color algorithms - a) SeaWiFS OC2, b) SeaWiFS OC4v4, and c) MODIS OC3M. The relationship is strong until the optical signal is affected by cryptophyte absorption. The circled stations are those where cryptophytes make up 40% or more of the total chlorophyll *a*. The solid line is the best fit line through data not including cryptophyte dominated stations; reported slope and R^2 values are for this best fit line (also see Table 2). To verify the significance of this difference, a series of t-tests were run to compare measured and calculated chlorophyll values for all algorithms tested for the same subset of stations where the phytoplankton community composition is not dominated by cryptophytes and also for the remaining stations which are dominated by cryptophytes. P values for stations dominated by cryptophytes were all <0.0001. These results show that there is a statistically significant difference between measured and calculated chlorophyll concentrations in areas that were dominated by cryptophytes.

3.0 Synergy of light and nutrients on the photosynthetic efficiency of phytoplankton populations from the Neuse River Estuary, North Carolina

Abstract

A series of mesocosm studies were conducted using natural phytoplankton communities isolated from the Neuse River Estuary in the spring of 1998 and 1999 to assess the interactions between nutrient limitation and ultraviolet (UV) radiation on photosynthetic parameters. Treatments consisted of the addition of different forms of nutrients typically found in estuarine environments and the exclusion of ambient UV radiation (wavelengths < 400 nm). The quantum yield of photochemistry (F_v/F_m), phytoplankton community composition, and photosynthesis irradiance parameters were measured repeatedly over the course of 4 days. Spring samples in this area were dominated by a combination of phycobilin containing groups (cyanobacteria or cryptophytes) and diatoms. In spring 1998, during a period of stratification and low runoff, nutrient limitation was observed in the Neuse River. F_v/F_m parameters in all the mesocosm treatments responded to the addition of nitrogen. The form of the nitrogen addition (nitrate, ammonium, or urea) was insignificant and the addition of phosphorous had no observable effect. Conversely, during a period of high mixing in spring 1999, there was no nutrient addition effect on F_v/F_m. During both experiments F_v/F_m exhibited midday light-driven depressions in response to high irradiances with complete recovery at night. UV radiation accounted for a significant fraction of the midday depression seen in F_v/F_m. Samples treated with the D1 protein synthesis inhibitor lincomycin showed that the midday decrease in photochemical efficiency was mostly due to photoinduced

damage to the D1 protein. As an upper limit estimate, 80% of the decrease in F_v/F_m centered around local noon appears to be related to this damage. The decrease in photochemical efficiency seen at high light levels in both UV exposed and UV excluded treatments was not correlated with a decrease in carbon fixation parameters.

3.1 Introduction

Estuarine phytoplankton are subject to many interacting and competing stressors and they must compete for available resources to maximize their photosynthetic rates and growth (Petersen *et al.* 1997). Characterizing the physiological response of phytoplankton to interacting environmental variables is essential to anticipating changes that might occur due to anthropogenic disturbances. This is fundamental to the formation of effective coastal nutrient management practices (Cloern 1996). These human-induced impacts include enhanced nutrient loading (Hobbie and Smith 1975; Paerl *et al.* 1995), modified nutrient ratios (Quian *et al.* 2000), altered flow regimes (Rudek *et al.* 1991), and enhanced ultraviolet radiation (Hader and Worrest 1991). Given this, developing a non-intrusive means to characterize the physiological state of phytoplankton communities and to predict their response to interacting anthropogenic disturbances has long been a goal of environmental scientists. Work over the last two decades by plant scientists and oceanographers (Kolber *et al.* 1988; Schreiber *et al.* 1995) has demonstrated the utility of chlorophyll *a* fluorescence measurements as a sensitive indicator of the physiological state of phytoplankton populations under erratic conditions.

Estuaries are highly variable environments; estuarine populations are exposed to a widely fluctuating light environment and exhibit a broad range of physiological acclimation strategies. These acclimation strategies allow the cells to maximize photosynthetic rates given light levels that range from limiting to photodamaging (Cullen and Lewis 1988; Cullen and MacIntyre 1998). The actual target site for damage due to visible wavelengths is a subject of considerable debate; however, nearly all of the proposed damage sites are primary components of the photosystem complex II (PS II; (Telfer and Barber 1994). During periods of acute light stress, light-saturated photosynthetic rates will be impacted if PSII is damaged (Osmond 1994).

Laboratory studies on higher plants and green algae suggest that UV radiation also inhibits the photosynthetic machinery at PS II (Iwanzik *et al.* 1983; Kulandaivelu and Noorundeen 1983; Renger *et al.* 1989; Jordan 1996). Specifically, UVB radiation appears to degrade the D1/32 kDa protein complex within PSII (Greenberg *et al.* 1989; Richter *et al.* 1990; Melis *et al.* 1992; Jansen *et al.* 1993). Prolonged exposure to UV light will result in damage to the photosynthetic reaction centers and the cell will experience a decrease in the efficiency of photochemistry and ultimately a decrease in productivity (Smith *et al.* 1980; Booth *et al.* 1997). Furthermore, UV exposure may lead to changes in pigment concentration, inhibition of phosphorylation, loss of specific enzyme activity, and decreased carbon and nitrogen assimilation (Worrest *et al.* 1981; Dohler *et al.* 1995; Goes *et al.* 1995; Lohmann *et al.* 1998; Wangberg *et al.* 1998).

Photoinhibition in estuarine phytoplankton may be expected to be minimal due to the increased attenuation of light, especially in the UV wavelengths, associated with high turbidity and colored dissolved organic matter (CDOM) in these systems (Kirk 1994; Arrigo and Brown 1996). However, in the case of UV, there is evidence that there is an enhanced sensitivity to photoinhibition even in turbid environments (Kaczamarska *et al.*

2000; Banaszak and Neale 2001). Even if light-induced damage is minimal, light levels in these systems may still be sufficient to saturate photosynthesis resulting in physiologically induced depressions in F_v/F_m. The significance of any potential damage will be more pronounced in nutrient limited cells due to the impaired synthesis or repair of photosynthetic proteins (Prézelin *et al.* 1986; Lesser *et al.* 1994; Hunt and Mc Neil 1998).

As part of a larger study on the structure and function of phytoplankton communities in the Neuse river, this work focused on characterizing variability in F_v/F_m in natural populations over a range of nutrient and light regimes (Richardson *et al.* 2001). The degree to which Fv/Fm is determined by nutrient limitation, physiological down-regulation and/or light-induced damage, the effects of the interactions between light levels and nutrient concentrations, and the relative importance of UV radiation to total irradiance was examined.

3.2 Methods

3.2.1 Water Collection

Water for mesocosm bioassays was collected from 1 m depth along the southwestern shore (35.08 ^{o}N, 77.00 ^{o}W) of the Neuse River Estuary in June 1998 and May 1999. Water was pumped into a pre-cleaned (flushed with river water) trailer-mounted 4500 liter polyethylene tank using a nondestructive diaphragm pump and transported to the Institute of Marine Sciences (IMS) in Morehead City, NC. Water was transferred within 2 h of collection to translucent (85% PAR transmittance) fiberglass tanks (55 L) arranged in an outdoor, flow-through seawater pond at IMS. The pond was continually flushed with seawater from the adjacent Bogue Sound for temperature control.

3.2.2 Mesocosm Experimental Design

Each tank was randomly assigned one of ten replicated treatment designs consisting of a combination of mixing and nutrient regimes. Tanks were either mixed by gentle bubbling with a slow flow of air or left static. Nutrients, including a control (no additions), +Nitrate (N), +Ammonium (A), +NA, +NAP (Nitrate + Ammonium + Phosphate) in 1998 and +N, +A, +U (Urea), +NAU, +NAP in 1999, were added to the respective treatment tanks in the early morning (0800) of days 0, 1, and 2 and gently mixed thoroughly (see Table 3.1 for concentrations). To assess the importance of UV radiation in the Neuse River, a set of mesocosms were added in 1999 and modified so as to allow penetration of photosynthetically available radiation (PAR) only. Mesocosm tanks were covered with UF3 plexiglass to screen out all UV radiation (referred to as UV excluded samples). These tanks were then mixed by gentle bubbling and had either no nutrients added or were supplemented with + NAP at the same time as the main tanks. Each tank was repeatedly sampled over a four-day period. Measured parameters include phytoplankton pigments, photosystem II quantum yields, and photosynthesis-irradiance parameters. Incident irradiance (PAR only) was measured over the duration of the experiment using a LiCor Li-1000 with a 4π sensor. Irradiance measurements inside the tanks were conducted with a Satlantic OCE 200 spectral radiometer. The OCE-200 measures downwelling irradiance (Ed) and upwelling radiance (Lu) *in-situ* as well as downwelling surface irradiance (Es) at 14 wavelengths (305, 324, 339, 380, 406, 412, 443, 490, 510, 555, 619, 665, 670, and 705 nm). All Satlantic sensors were factory calibrated prior to sampling for quality assurance. Collected radiometric data were processed using Satlantic's Prosoft software package according to manufacturer protocols. No dark corrections were applied to these data.

3.2.3 Photochemical Quantum Yield

Chlorophyll fluorescence data for each sample was collected six times per day using a Pulse Amplitude Modulation Fluorometer (PAM; Heinz-Walz, Germany). Samples were dark adapted for five minutes to allow for relaxation of nonphotochemical quenching and then minimal fluorescence (F_o) was measured. A 600 ms flash from a Schlott saturation flash lamp (Schlott Inc., Germany) was administered to measure maximum fluorescence (F_m). Increasing flash intensity or duration did not result in higher fluorescence values indicating that PSII was saturated. These values were then used to calculate the maximum quantum yield for charge separation at PSII as

$$F_v / F_m = \frac{\left(F_m - F_o\right)}{F_m} \tag{3.1}$$

where F_v/F_m is the maximum quantum yield of photochemistry at photosystem II, F_o is the minimum fluorescence measured after a short (5 minute) dark period, F_m is the maximum fluorescence measured after a saturating flash of light, and F_v is the variable fluorescence calculated as $F_m – F_o$. F_o is a measure of fluorescence at photosystem II when all the reaction centers are open and can accept incoming electrons for photosynthesis whereas F_m is measured when the reaction centers are closed and the plastoquinone pool is reduced.

On day 2 of the 1999 experiment a subset of samples were incubated with lincomycin which specifically blocks the synthesis of only the D1 protein in photosystem II. Water was drawn from the control and nutrient enhanced (both UV exposed and UV excluded) tanks before sunrise and lincomycin was added to a final concentration of 150μg ml^{-1}. The lincomycin spiked samples were then enclosed in polyethylene Whirl-Pak (NASCO) bags, returned to the tank from which they were collected, and sampled over the course of the day with the same frequency as control samples.

3.2.4 Phytoplankton Photopigments

Phytoplankton community composition was characterized using high-performance liquid chromatographic (HPLC) derived pigment data. The major phylogenetic groups of interest in the Neuse River were chlorophytes (with corresponding diagnostic pigment chlorophyll *b*), cyanobacteria (zeaxanthin), diatoms (fucoxanthin), dinoflagellates (peridinin), and cryptomonads (alloxanthin) (Pinckney *et al.* 1997; Pinckney *et al.* 1998). Aliquots (0.2 to 1.0 L) of water were filtered under a gentle vacuum (<50 kPa) onto 4.7 cm dia. glass fiber filters (Whatman GF/F), immediately frozen, and stored at –80 ^oC. Frozen filters were placed in 100% acetone (3 mL), sonicated, and extracted at –20 ^oC for 12 - 20 h. Filtered extracts were injected into a Spectra-Physics HPLC equipped with a single monomeric (Rainin Microsorb-MV, 0.46 x 10 cm, 3 μm) and two polymeric (Vydac 201TP, 0.46 x 25 cm, 5 μm) reverse-phase C_{18} columns in series. This column configuration was devised to enhance the separation of structurally similar photopigments and degradation products. A nonlinear binary gradient was used for pigment separations (for details, see (Pinckney *et al.* 1996).

Solvent A consisted of 80% methanol:20% ammonium acetate (0.5 M adjusted to pH 7.2) and Solvent B was 80% methanol:20% acetone. Absorption spectra and chromatograms (440 nm) were acquired using a Shimadzu SPB-M10av photodiode array detector. Pigment peaks were identified by comparison of retention times and absorption spectra with pure crystalline standards, including chlorophylls *a*, *b,* β-carotene (Sigma Chemical Company), fucoxanthin, and zeaxanthin (Hoffman-LaRoche and Company). Other pigments were identified by comparison to extracts from phytoplankton cultures and quantified using published extinction coefficients (Jeffrey *et al.* 1999).

The concentrations of algal photopigments were analyzed using CHEMTAX (Chemical Taxonomy), a matrix factorization program, to determine best-fit pigment ratios for the five major algal groups present in the Neuse River (Pinckney *et al.* 1998). This program uses steepest descent algorithms to determine the best fit based on an initial estimate of pigment ratios for algal classes. Both the absolute and relative contributions of algal groups to the total biomass can be calculated. The absolute contribution of any algal group is the concentration of chl *a* (in $\mu g\ L^{-1}$) that is contributed by that group. Relative contributions are calculated as the proportion of total chl *a* that is accounted for by the group, such that the sum of contributions of all groups equals 1. Evaluations of the CHEMTAX method have shown it to be generally insensitive to values chosen for the initial pigment ratio matrix (Mackey *et al.* 1996; Schluter *et al.* 2000). Full discussions, validation, and sensitivity analyses of CHEMTAX are provided in Mackey et al. (1996) and Wright et al. (Wright *et al.* 1996).

3.2.5 Photosynthesis vs. Irradiance

The relationship between photosynthesis and irradiance (P-E) was determined using the small volume ^{14}C incubation method of Lewis and Smith (Lewis and Smith 1983). Ten ml of estuary water taken from the surface or bottom of the water column was spiked with ^{14}C-bicarbonate (Amersham, Inc.) to a final concentration of 29600 Bq ml^{-1}. Triplicate samples for T_o counts (containing 500 μl of sodium borate-buffered formalin in 10 ml of sample) were collected to correct for any uptake of ^{14}C label that occurred during the distribution process. Samples collected for total counts (T_c) were prepared by adding 500 μl of phenethylamine (PEA) into a 20 ml scintillation vial and then adding 10 ml of Ecolume scintillation cocktail. During incubation, a range of irradiances was provided from the side by a Cool-Lux 75 W projector lamp directed through a heat filter of circulating water. Incubations were performed for 45 min, after which 500 μl of formalin was added to each vial to terminate the experiment. Samples were then acidified directly with 1 ml of 50% HCl and were placed on a shaker table overnight to allow for purging of unincorporated label. After purging, an additional 10 ml of scintillation cocktail was added to each vial. Vials were allowed to sit overnight, then counts per minute were enumerated with a Beckman model LS 5000TD liquid scintillation counter. Counts per minute were converted to disintegrations per minute using quench curves constructed from a calibrated ^{14}C-toluene standard. Dissolved inorganic carbon in estuary water was determined by using a LiCor model LI6252 CO_2 analyzer.

Quantum scalar irradiance (μmoles photons m^{-2} s^{-1}) in each position of the photosynthetron was measured using a Biospherical Instruments Model QSL-100 irradiance meter with a QSL-101 4 π sensor. For each measurement, the sensor was inserted into a 20 ml glass scintillation vial that contained 10 ml of estuary water. Temperature was kept constant during the incubations with a circulating water bath. The temperature was set to the ambient temperature at the time of collection.

Results were modeled using the equation of Platt et al.(Platt *et al.* 1980):

$$P^B = P_s^B\left(1 - e^{\left(-\alpha E/P_s^B\right)}\right)\left(e^{\left(-\beta E/P_s^B\right)}\right) \tag{3.2}$$

where P^B is the rate of photosynthesis normalized to chlorophyll (μgC μg Chl^{-1} h^{-1}), $P^B{}_s$ is the maximum rate of photosynthesis in the absence of photoinhibition (μgC μg Chl^{-1} h^{-1}), E is irradiance (μmol photons m^{-2} s^{-1}), α is the initial slope of the P-E curve ((μgC μg Chl^{-1} h^{-1}(μmole photons m^{-2} $s^{-1})^{-1}$), and β is a parameter that characterizes photoinhibition (μgC μg Chl^{-1} h^{-1}(μmole photons m^{-2} $s^{-1})^{-1}$). Curves were fit to P-E data using a least-squares non-linear curve fitting routine in Kaleidagraph. Values for $P^B{}_{max,}$ the realized maximum rate of photosynthesis, and E_k, the conventional index of light saturation, were calculated by the method of Platt et al. (1980) from values of $P^B{}_s$, α, and β determined from curve fits. Measurements of total chl *a* for P-E experiments were done fluorometrically using a Turner Designs model TD-70 fluorometer after grinding and extraction of triplicate samples in ice-cold 90% acetone for at least 24h in the dark at –10°C.

3.3 Results

The maximum quantum yield of photochemistry (F_v/F_m) varied over hourly and daily time scales and between years. However, the diurnal trends in F_v/F_m were consistent between sampling years, treatment conditions, and phytoplankton community composition. The diurnal variability in F_v/F_m was highly dependent on incident irradiance (Fig. 3.1). There was an inverse relationship between quantum yield and irradiance with minimum F_v/F_m values corresponding to local noon (maximum incoming PAR between 1500-2000 μmol photons m^{-2} s^{-1}) and complete recovery at night.

The 1998 experiment was marked by low overall F_v/F_m values (initial value of 0.102). All samples exhibited daily decreases in F_v/F_m values coincident with local noon (Fig. 3.1a). The diel variation resulted in a 54% change (average for all samples) in F_v/F_m over the course of the day. The decreases in F_v/F_m were more dependent on lower F_m values rather than an increase in F_o. A night-time recovery phase was observed for all treatment conditions, however the recovery phase was more rapid for samples which were provided nutrients (see Fig. 3.1a). All nutrient additions resulted in a significant increase in F_v/F_m (Fig 3.2a); however there was no significant impact associated with phosphorus (one way anova, $p<0.05$).

Similar diurnal trends were observed in 1999 as in 1998 with an inverse relationship between quantum yield and irradiance. Likewise, changes in F_v/F_m were dependent on F_m rather than F_o values. In 1999, F_v/F_m values were higher at the start of the sampling period (initial value of 0.204) than in the 1998 experiment and also increased within the mesocosms during the experiment (Fig. 3.1b). This increase was seen in both the control and all of the nutrient treatments. In contrast to 1998, there was no observable increase in F_v/F_m in response to any of the nutrient additions in 1999 (Fig. 3.2b).

Disparities in F_v/F_m values between sampling years may be due to a shift in phytoplankton community composition. The 1998 sampling period was marked by an abundance of cyanobacteria (Table 3.2). In 1999, the mesocosms began dominated by cryptophytes which were quickly replaced by diatoms. This succession is probably due to both competitive and grazing pressures within the mesocosms, which is not unusual for the Neuse River Estuary. The summer months in this area are typically dominated by diatoms with sporadic cryptophyte blooms throughout the year (Pinckney *et al.* 1998)

UF3 covers on select tanks in 1999 altered both the quality and quantity of the surface light field in the tanks (Fig. 3.3). UV exposed samples were subject to an average 64 μmol photons m^{-2} s^{-1} of UVB wavelengths (305-400 nm). UV excluded samples were subject to an average 6.4 μmol photons m^{-2} s^{-1} of UVB light. Diurnal trends in F_v/F_m are the same for UV exposed and UV excluded tanks, however exclusion of UVB alleviates a significant fraction of the midday depression in F_v/F_m (Fig. 3.1b, Fig. 3.4). UV exposed samples had an average 57% decrease in F_v/F_m values from morning to noon (similar to results from 1998) while UV excluded samples had only a 42% average change.

The exclusion of UV light did not produce a concomitant decrease in photosynthesis-irradiance parameters (Fig. 3.5). There was no significant change in P_{max}, α, or E_k between UV exposed and UV excluded samples (paired t-test, $p<0.01$; Fig. 3.5a). Additionally, there was no change in total chlorophyll *a* concentrations between UV exposed and UV excluded samples in either the control or nutrient enhanced samples (Fig. 3.5b).

The addition of lincomycin greatly diminished the ability of all samples to recover from a proportion of the midday depression observed in F_v/F_m values by blocking the synthesis of the D1 protein. Lincomycin treated samples recovered approximately 10% of their initial photochemical quantum yield as measured by F_v/F_m (Fig. 3.4). F_v/F_m

values began at 0.527 ± 0.013 (average for all data shown) at 0600 of our sampling day. Control samples (no lincomycin added) increased slightly to 0.547 ± 0.032 while lincomycin treated samples decreased significantly to 0.065 ± .010 at 2110 (Fig. 3.4).

3.4 Discussion

Phytoplankton from the Neuse River have been shown to exhibit symptoms of nitrogen limitation (Rudek *et al.* 1991; Boyer *et al.* 1994; Mallin 1994). Nutrient limitation was demonstrated in the F_v/F_m data, but only during periods of prolonged stratification after nutrients had been depleted from the water column. The Neuse River tends to undergo periods of intense stratification due to freshwater runoff and low turbulent mixing, as in 1998 (Paerl *et al.* 1995; Robbins and Bales 1995). The marked decrease in vertical mixing allows surface depletion of nutrients resulting in a state of nutrient limitation. During these times phytoplankton populations respond by a shift in community composition (Pinckney *et al.* 1998) and will exhibit increases in photochemical quantum yields with nutrient additions as seen during the 1998 experiment (Fig. 3.2). The 1998 data reflect the stratified and nutrient limited state of the water column at the time of water collection. Nitrate and phosphate levels were one half and one third lower than in 1999 (Table 3.3). The increases in F_v/F_m in 1998 suggest nitrogen limitation in the Neuse River as additions of phosphate did not change F_v/F_m values. In 1999, there was no significant response in F_v/F_m with the addition of nutrients. However, nutrient additions did result in an increase in overall biomass (Fig. 3.5) indicating that these samples were somewhat limited in nutrients.

The diurnal variability seen in F_v/F_m is dependent upon the incoming irradiance; midday depressions reflect the light saturation of the photosynthetic reaction centers and subsequent oxidation of the plastoquinone pool (Falkowski and Raven 1997). Historically, midday decreases in F_v/F_m have been linked to the inactivation of the photosystem II reaction centers. Despite protective mechanisms, high light will still damage some PSII reaction centers which can then lead to a reduction in carbon fixation (Renger *et al.* 1989; Jordan 1996). In our experiment, midday light levels (up to 1200 µmol photons m^{-2} s^{-1} at the tank surface at noon) were always higher than E_k (average E_k value 300 µmol photons m^{-2} s^{-1}; see Figs. 3.1 & 3.5). At these irradiance levels the system is light saturated and F_v/F_m values decrease as light intensities approach E_k. The decreases in F_v/F_m were due mainly to decreases in F_m. A decrease in F_m is most often interpreted as a non-functional form of the primary electron acceptor, Quinone a (Q_a) as incoming light energy is irreversibly passed to Q_a resulting in a stable charge separation (Styring and Jegerschold 1994). This is a slow reaction with very little chance for a back reaction resulting in florescence, thus decreasing total fluorescence (F_m).

The observed photoinhibition in this experiment reflects damage from both UV radiation (Smith *et al.* 1980; Goes *et al.* 1995) and visible light (Prézelin *et al.* 1986). Approximately 12-15% of the midday drop in Fv/Fm in 1999 was associated with UVB radiation. This significant UV inhibition was not entirely expected given the high loads of CDOM that are traditionally found in rivers such as the Neuse River, which strongly absorb at UV wavelengths (Kirk 1994). This supports the idea that UV radiation can be a significant factor for surface or well mixed populations even in highly turbid waters (Cullen and Lewis 1988). These environments are particularly inhibiting for cryptophyte algae which are very sensitive to UV radiation (Vernet *et al.* 1994) and were the dominant phytoplankton group in our samples (Table 3.2).

Phytoplankton have several physiological strategies allowing them to thrive in super saturating light environments. At high levels of incoming irradiance, photosynthetic algae are not able to utilize all of the incoming light energy for photosynthesis; the rate of electron transport through PSII is no longer dependent on light absorption (Falkowski *et al.* 1994). This was the case in our experiment as evidenced by the decrease in F_v/F_m. However, this decrease in photochemical efficiency seen at high light levels was not reflected in the carbon fixation potential ($P^B{}_{max}$). Since light-saturated carbon fixation remains unaffected by super saturation at PSII this indicates that there has been an increase in the turnover rate of electrons through PSII as

$$P^B{}_{max} = n\left(1/\tau_{PSII}\right) \tag{3.3}$$

where $1/\tau_{PSII}$ = electron turnover through PS II reaction centers and n is the number of photosynthetic units (Kolber *et al.* 1988; Behrenfeld *et al.* 1998). Under these conditions, as F_v/F_m decreases with no concomitant change in P_{max}, the instantaneous rate of photosynthesis is limited by the dark reactions as electron turnover through PSII ($1/\tau$) has increased to keep up with the demand for electrons through the light reactions. These results support the findings of Behrenfeld et al. (1998) who hypothesized that decreases in productivity are not necessarily proportional to photoinhibition.

The lack of photoinhibition at supersaturating light levels has also been attributed to increased turnover of the D1 protein (Aro *et al.* 1993; Rintamaki *et al.* 1994; Park *et al.* 1995). As light exposure increases, the PSII reaction center proteins are damaged and must be synthesized and replaced in order to restore photosynthetic operation (Aro *et al.*

1993). The actual amount of measurable (net) damage is a balance between damage and synthesis and repair rates. The protein synthesis inhibitor lincomycin specifically blocks the synthesis of the D1 protein (Osmond 1994). The difference between lincomycin treated and non-lincomycin treated samples provides an upper limit estimate of the light induced loss of the D1 protein. Our results show that preventing D1 turnover by blocking its synthesis almost completely eliminates the pool of PSII capable of recovery from light induced inhibition. The disparity in recovery rates between lincomycin treated and non-treated samples implies that a significant fraction of the decline in the photochemical efficiency at high light levels reflects damage to the D1 protein and illustrates how the balance between damage, synthesis and repair is critical to maintaining photosynthetic functionality of the cell.

In this study, an increased availability of nutrients afforded a more rapid recovery in photochemical efficiency, but did not protect against photoinduced impairment and downregulation of PSII. Nitrogen starved cultures have been shown to be more susceptible to photoinhibition both by excess PAR and UV radiation as compared to nutrient replete cells (Prézelin *et al.* 1986; Kolber *et al.* 1988; Lesser *et al.* 1994; Hunt and Mc Neil 1998). This may be due to changes in D1 protein concentration or turnover (Kolber *et al.* 1988; Renger *et al.* 1989), changes in rubisco functioning (Jordan 1996; Yin and Johnson 2000), or decreased ability to uptake N (Lohmann *et al.* 1998). The variations in UV sensitivity for natural phytoplankton assemblages under nutrient limited conditions have yet to be fully explored. Our results demonstrate that nitrogen limited phytoplankton do not appear more susceptible to photoinduced impairment. Alternatively their repair/recovery processes are adversely affected. Thus, nutrient limited samples cannot recover from photoinduced damage as quickly as nutrient replete samples. Over time, this will emerge as a decrease in photosynthetic ability leading to a decrease in carbon fixation.

Acknowledgements

We gratefully acknowledge the technical assistance of Larry Boihem, Karin Howe, Malia Go, Pam Wyrick, Ben Peierls, Nathan Hall, and Lois Kelly. Special thanks to David Millie (USDA-ARS) and Gary Kirkpatrick (Mote Marine Lab). This work was funded by the USDA-ARS NRI program (NRI 96-351010-3122), a USDA Agricultural Research Service Cooperative Agreement (ARS 58-6435-6-028) and the EPA Competitive Grants program (#R825243).

Nutrient Additions (μM)	**1998**	**1999**
Nitrate	10	10
ammonium	10	10
NO_3 + NH_4	5+5	n/a
urea	n/a	10
NO_3 + NH_4 + urea	n/a	3.3+3.3+3. 3
NO_3 + NH_4 + PO_4	3+3+5	3+3+2

Table 3.1: Nutrient treatments for the 1998 and 1999 experiments. Nutrient concentrations represent amount added to collected water samples. All concentrations are μmol N or μmol P. Nitrate = N, ammonium = A, urea = U, phosphate = P. n/a = not applicable, not all nutrient treatments were used each sampling year.

1998	Chlorophytes	Cryptophytes	Cyanophytes	Diatoms	Dinoflagellates	Total Chl *a*
Day 0	3.12	0.00	**68.24**	28.64	0.01	12.39
Day 1	3.68	0.00	**68.54**	27.78	0.01	9.74
Day 3	3.94	1.56	**64.04**	30.45	0.01	5.84
1999						
Day 0	12.63	**51.00**	10.00	26.36	0.01	12.81
Day 1	16.35	32.86	9.09	**41.68**	0.01	22.93
Day 3	19.56	16.08	6.51	**57.85**	0.00	40.48

Table 3.2: The phytoplankton community composition over the course of the experiment for both 1998 and 1999 as determined from HPLC measurements. The dominant group is in boldface. There were not any significant alterations in phytoplankton community structure in response to nutrient or light treatments. Total chlorophyll *a* concentrations are $\mu g\ L^{-1}$. Note that values are an average for all treatments.

Neuse River Conditions	**1998**	**1999**
Temperature (^{o}C)	24	20
Salinity (ppt)	2	3
pH	8.5	7
C:N	7	7
NOx (ug N L^{-1})	4	12
NH_4 (ug N L^{-1})	13	12
PO_4 (ug P L^{-1})	3.5	7
Chl a (ug L^{-1})	20	15
K_d (m^{-1})	2.3	1.85

Table 3.3: Conditions in the Neuse River prior to mesocosm water collection. NO_x and PO_4 levels were significantly higher in 1999, due to a storm mixing event, than in 1998. These data were collected during routine water quality monitoring in the Neuse River.

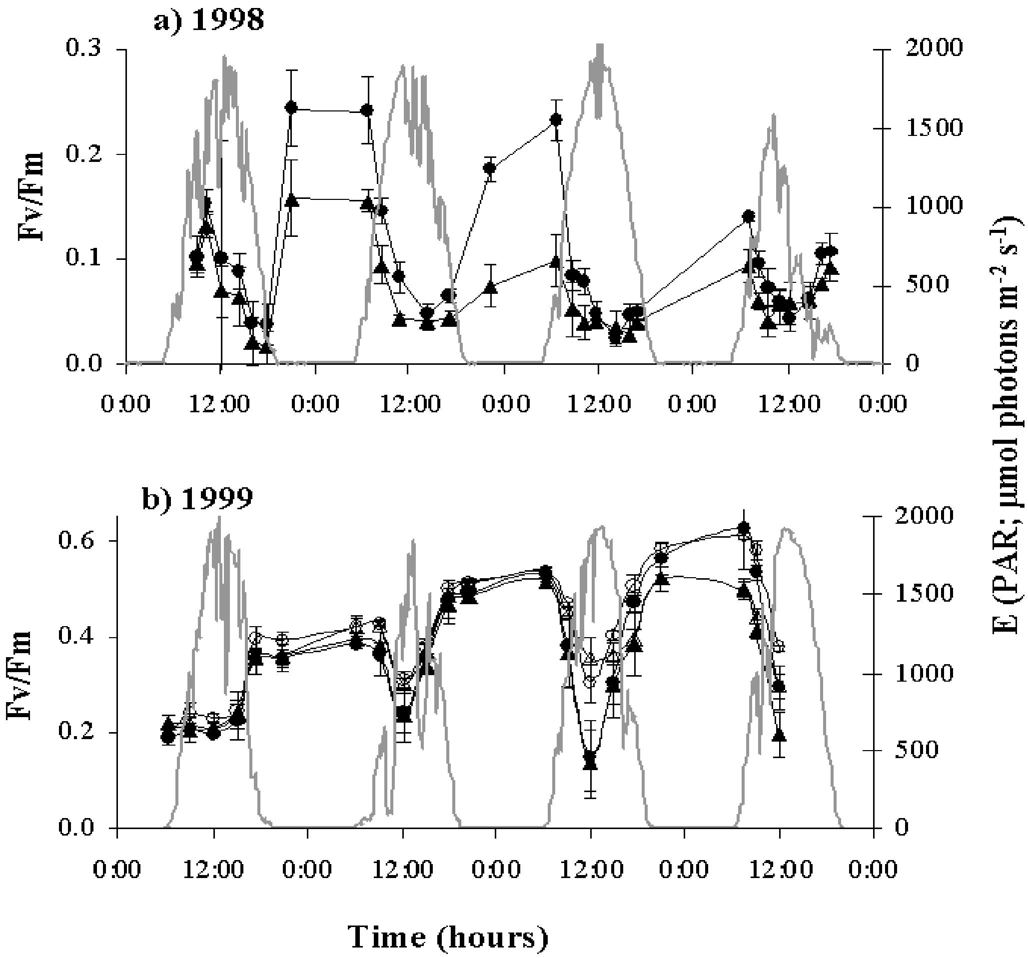

Figure 3.1: The diurnal pattern in F_v/F_m values for both A) 1998 and B) 1999 (note the change in scale for F_v/F_m values). Light treatments were added in 1999. ▲ control, UV exposed; ● NAP addition, UV exposed; Δ control, UV excluded; ○ NAP addition, UV excluded. Each point represents the average of triplicate measurements and error bars represent standard deviation from the mean. Superimposed is the amount of available light (PAR).

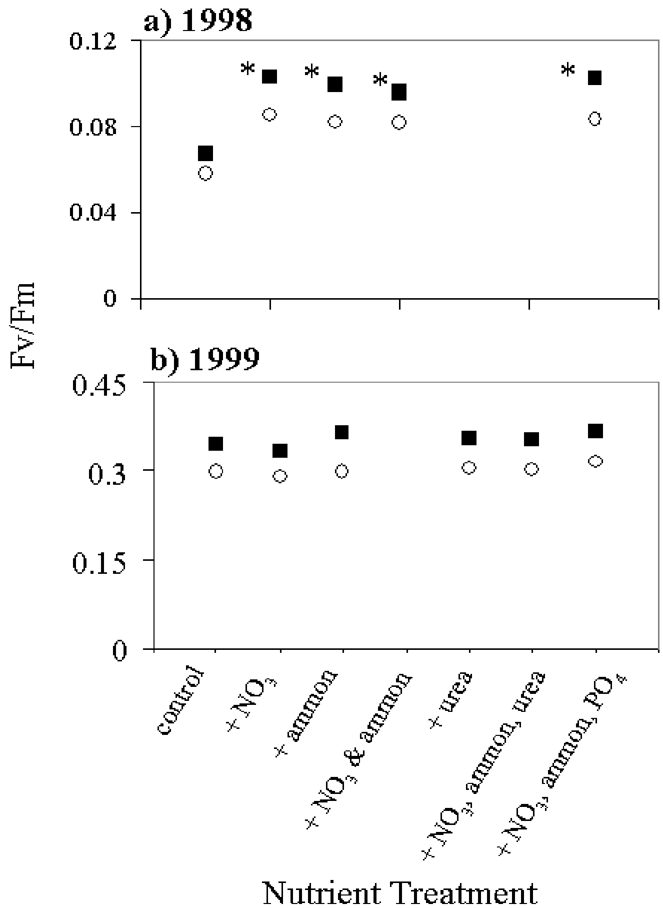

Figure 3.2: Four day average change in F_v/F_m values for the different nutrient treatments in a) 1998 and b) 1999 for both mixed (■) and static (○) incubations. Stars represent nutrient addition treatments that are significantly different from the control ($p< 0.05$). None of the nutrient addition treatments were significantly different from the control in 1999.

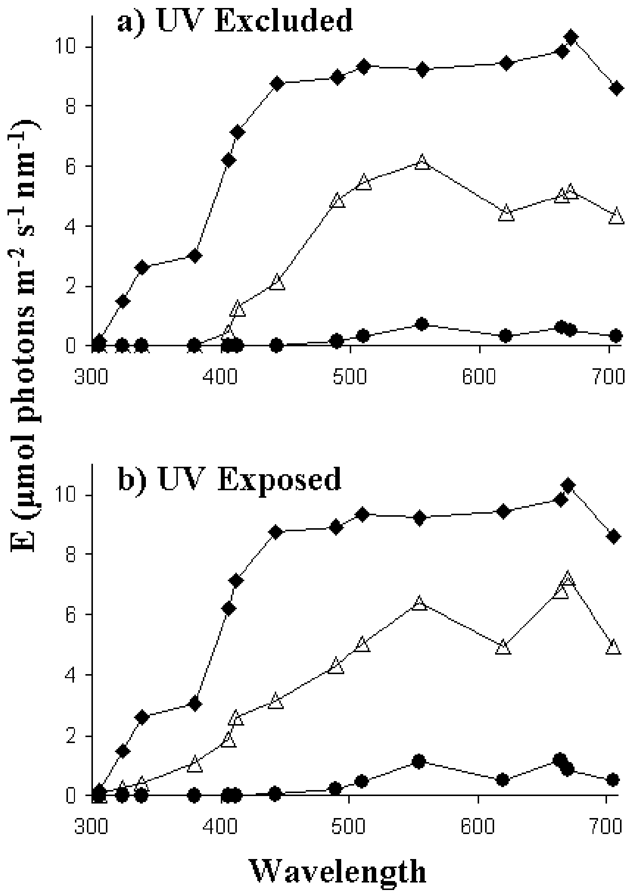

Figure 3.3: Average spectral irradiance in the mesocosm tanks. Irradiance measurements were taken just above the surface (♦), just below the surface (Δ), and at the bottom of the tanks (●) in A) tanks with UV exclusion and B) tanks receiving incident light. UV radiation propagated 0.65m into tanks receiving incident sunlight (to the 1% light level). UV excluded tanks received PAR only while UV exposed samples received 64 µmol photons m^{-2} day^{-1} of UV radiation.

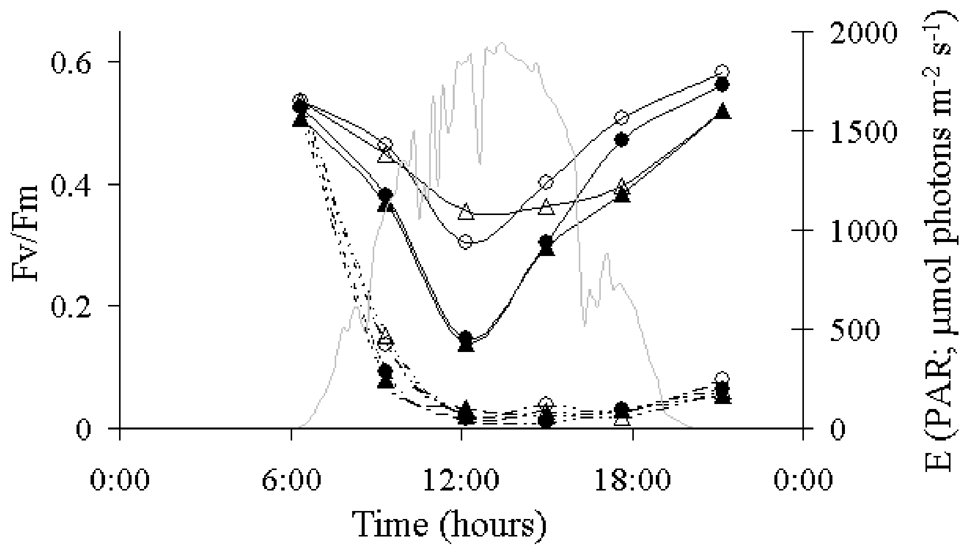

Figure 3.4: The diurnal pattern in F_v/F_m values for day 2 of the 1999 experiment for both control samples (solid line) and a subsample that has been treated with the inhibitor lincomycin (dotted line). Symbols are as in Figure 1. Error bars have been omitted for clarity; see Fig. 1 for error associated with control samples. Each point represents the average of triplicate measurements. Superimposed is the amount of available light (PAR).

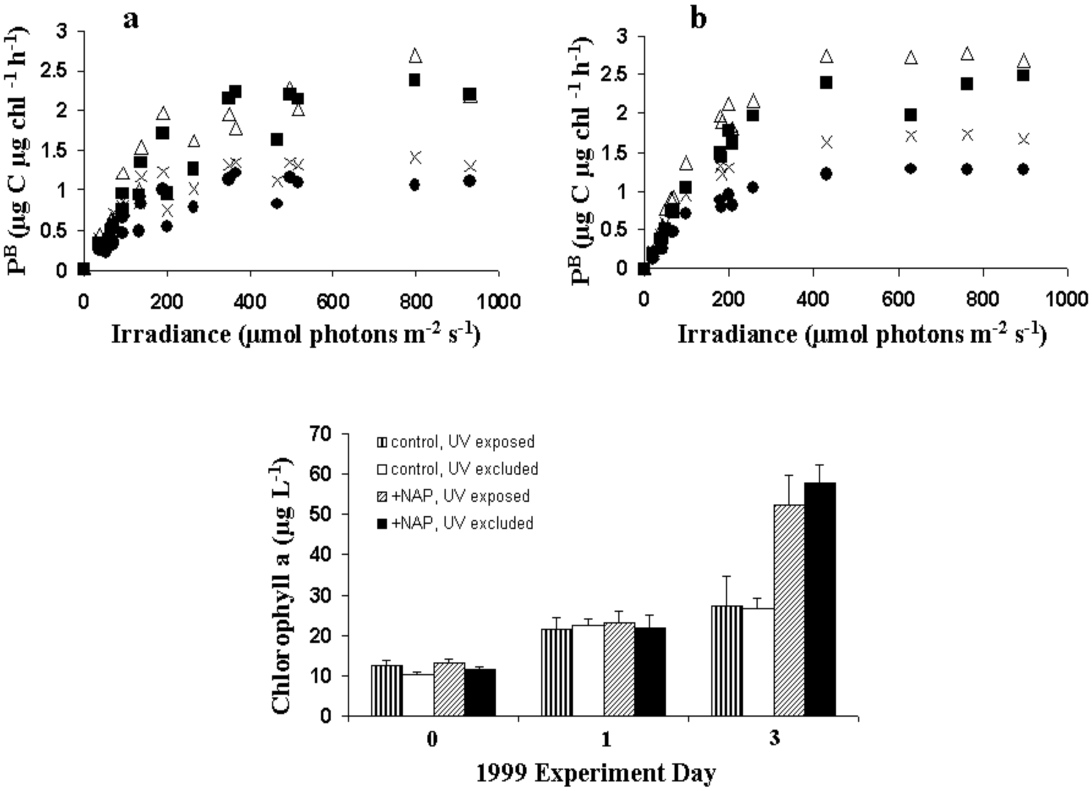

Figure 3.5: Top: Photosynthesis – Irradiance curves over the course of one day of the 1999 experiment for a) UV exposed and b) UV excluded samples. Measurements were conducted at 0600 (●), 1200 (■), 1500 (Δ), and 1730 (X). There is no significant difference in PE curve parameters between UV exposed and UV excluded samples (paired t-test, $p<0.01$). Bottom: Total HPLC derived chlorophyll *a* concentrations over the course of the 1999 experiment; control, UV exposed (vertical bars); control, UV excluded (white); +NAP, UV exposed (diagonal bars); +NAP, UV excluded (black). The exclusion of UV radiation did not effect chlorophyll *a* concentrations in either the control or nutrient addition treatments.

4.0 Cryptomonads Survival Strategies at Low Light

4.1 Introduction

4.1.1 Photoacclimation to low light

Phytoplankton have developed a suite of strategies to maintain their growth potential in a range of irradiances and nutrient concentrations (Falkowski 1980; Richardson *et al.* 1983). The exponential extinction and sharp spectral changes of the light field at depth in aquatic habitats makes for a dynamic light environment. Algal groups which are highly adapted to living in the range of available irradiances will be strongly favored. Much work has focused on the many light harvesting and photoacclimation strategies of diatoms, dinoflagellates, cyanobacteria, and green algae. Additionally, the morphology and functionality of phycobiliproteins has been well documented (Gantt 1977; Glazer 1981; MacColl 1982; Maccoll and Guard-Friar 1987; Sidler 1994). Little effort has focused on the specific strategies of cryptophyte algae under varying light conditions.

Cryptophytes are the only phytoplankton group to contain both chlorophylls *a* and *c* in addition to phycobilins and carotenoids (alloxanthin; Fig. 4.1). This unique pigment system allows cryptophytes to absorb a wide range of wavelengths and is optimized for the blue and green wavelengths of light found at depth in natural waters. This is advantageous in coastal and estuarine ecosystems where high concentrations of colored dissolved organic matter (CDOM) significantly reduce available irradiance and skew the light field at depth to the green wavelengths of light [(Kirk 1994; Cauwet 2002) Fig. 4.2]. Under these conditions, cryptophytes may have an advantage over other phytoplankton groups as their absorption potential is well suited to utilizing dim, green light. The diminished quantity and spectral quality of the light field in turbid areas and in deep water alters the competitive ability of phytoplankton groups. In these areas, cryptophytes have much higher potential absorption efficiencies than other prevalent coastal phytoplankton groups and are able to outcompete more traditional bloom forming algae (Bergmann *et al.* 2003). This work focuses on cryptophyte photoacclimation under light limited conditions which are often found in turbid, organically laden coastal waters.

Phycobilin containing phytoplankton have evolved several strategies to maximize cellular absorption in order to increase their photosynthetic potential under low light conditions. For example, phycobilin containing algae have the ability to respond to the incoming light field by altering the composition of chromophores associated with their phycobilins (Tandeau de Marsac 1977), the concentrations of intracellular pigments (Faust and Gantt 1973; Mackey *et al.* 1998), the distribution of excitation energy between photosystem I (PSI) and photosystem II [PSII (Bonaventura and Myers 1969; Murata 1969)], or the stoichiometry of PSII:PSI (Falkowski *et al.* 1981; Dubinsky *et al.* 1986; Fujita *et al.* 1987).

All photosynthetic phytoplankton have the ability to increase intracellular concentrations of photosynthetic pigments in response to low growth irradiances (Richardson *et al.* 1983; Falkowski and LaRoche 1991). In phycobilin containing algae, maximizing the intracellular phycobilin concentration increases overall cellular absorption but can also alter photosynthetic efficiency (Fujita et al. 1994). Efficient carbon fixation in any photoautotrophic organism is dependent upon the coordinated excitation of two different photosystems (Hill and Bendall 1960; Duysens and Amesz 1962). Any light field that preferentially excites one photosystem more than the other will decrease photosynthetic efficiency. At low light, phycobilin containing algae can adjust this disequilibrium by increasing the light transfer to or increasing the concentration of the understimulated photosystem (Fujita *et al.* 1994; Grossman *et al.* 1994; Campbell 1996). Light absorbed by phycobilins in cryptophytes is primarily used to drive photochemical reactions at PSII (Haxo and Fork 1959) while chl *a* preferentially excites PSI (Lichtlé *et al.* 1980). High phycobilin absorption will cause an overstimulation of PSII and the phytoplankton will compensate by decreasing the PSII:PSI ratio in order to maintain the balance between photosystems and keep photosynthetic quantum efficiency high (Melis 1991). The ability of phycobilin containing organisms to modify their chromophoric composition and alter the stoichiometry of their photosystems makes them highly adaptable to changes in available irradiance. A considerable amount of work has focused on these strategies in cyanobacteria (Bryant 1994), however very little research has examined if these strategies exist in cryptophytes and if so what impact they have on photosynthesis and growth potential.

4.1.2 Mixotrophy

Mixotrophy occurs in species with hetrotrophic capabilities that have maintained functional chloroplasts. There are many species of heterotrophic algae which do not require light for growth; these groups are capable of utilizing preformed organic compounds as a nutrient and/or energy source (Danforth 1962). While previous research has focused on strictly heterotrophic plankton groups (Danforth 1962; Lloyd and Cantor 1979; Hobbie and Williams 1984; Tuchman 1996; Sanders *et al.* 2000), only few studies have examined the importance of mixotrophy in coastal phytoplankton. Mixotrophy can be a critical survival strategy for algal populations growing in sub-saturating light. It has been suggested that some phytoplankton groups which are generally considered autotrophic may be able to resort to heterotrophy under severe light limitation (Tuchman 1996). Cryptophytes may be one such group with mixotrophic potential under light limiting conditions.

In inland lakes, estuaries, and many coastal zones where cryptophytes thrive, significant amounts of dissolved organic nutrients are available (Cauwet 2002). These organic compounds are strongly absorbing and although they may serve as an energy source for some plankton, they also serve to reduce the amount of available light. The ability to use these organic compounds as an energy source to supplement photosynthetic growth under low light conditions may provide a competitive advantage over strictly autotrophic phytoplankton groups and effectively expand the depth of the cryptophyte euphotic zone. Organic molecules may be an especially important nutrient source for cryptophytes as this group has high nutrient requirements (Someer, 1983) and slow nutrient uptake rates (Cloern 1977; Plante and Arts 2000). Given this, although cryptophytes are not phagotrophic (Salonen and Jokinen 1988; Gervais 1997a), several studies have shown photoautotrophic species of cryptophytes have enhanced growth in the presence of organic nutrients (Faust and Gantt 1973; Lewitus *et al.* 1991). Under limiting irradiances too low to support strictly photoautotrophic growth, cryptophytes have been shown to sustain limited growth by the uptake of organic compounds (Lewitus *et al.* 1991; Gervais 1997a). Cryptophyte cultures incubated in the laboratory with ecologically relevant concentrations of organic nutrients will continue growth for a short time in complete darkness (Gervais 1997a) and have enhanced rates of growth and respiration when cultured in the light (Antia *et al.* 1969).

In addition to the mixotrophic potential exhibited by many cryptophytes, cultures grown in the lab may also produce high levels of starch reserves resulting in large, dense cells (Morgan and Kalff 1975; Lichtlé 1979; Lewitus and Caron 1990; Sciandra *et al.* 2000). These starch reserves are then respired as fuel under times of light limitation such as at night (Gasol *et al.* 1993) and during the winter months (Marshall and Laybourn-Parry 2002). Furthermore, cryptophyte cultures grown for several generations in complete darkness will continue to produce phycobilin pigments (Antia *et al.* 1969) perhaps solely as a nutrient store (Ojala 1993b); under times of macronutrient limitation, cryptophytes will use their phycobilins as a nutrient storeroom (Rhiel *et al.* 1985; Lewitus and Caron 1990). Although mixotrophic potential has been documented in several species of cryptophytes, few studies have examined the implication of this beneficial strategy in competing with more prevalent coastal phytoplankton groups. If the mixotrophic contribution to cryptophyte growth is significant, it may impact the ecological range of this phytoplankton group.

4.1.3 Motility

Cryptophytes are biflagellated organisms and are strong swimmers that can cross ecologically significant density gradients (Jones 1988). On the cellular level, motility is beneficial if organisms can cross light or nutrient gradients (Sommer 1988) and in nature, the vertical migration observed in cryptophytes leads to increases in their growth rates (Ojala *et al.* 1996). In most natural waters cryptophytes undergo diel vertical migration in response to changes in both light and nutrient levels (Burns and Rosa 1980; Smolander and Arvola 1988). Cryptophytes contain a photoreceptor that is highly sensitive to green light (Erata *et al.* 1995) which allows them to respond very quickly to changes in underwater irradiance (Watanabe and Furuya 1978) and migrate in response to light fields to effectively control their place in the vertical light gradient thereby maintaining optimal placement in the water column. For example, in inland lakes cryptophytes will migrate to the surface during the day in brown lakes with high light attenuation and deeper in the water column during the day in clear water lakes where surface light levels would be potentially damaging (Arvola *et al.* 1991).

This observed vertical movement is a function of both available light and nutrient concentrations. Under nutrient replete conditions, cryptophytes will move into areas of higher light while avoiding saturating irradiances when nutrient limited (Arvola *et al.* 1991). Also, cryptophytes are more motile at low irradiances (Brown and Richardson 1968) presumably to look for areas with more favorable light and/or nutrient concentrations. For example, cryptomonas species exhibit positive chemotaxis towards amino acids (Lee *et al.* 1999) and may be able to use these amino acids as a nitrogen source (Wheeler *et al.* 1974).

In most cases, cryptophytes will swim to avoid surface waters midday and at night (Olli 1999). This midday response is to avoid damaging light intensities as cryptophytes prefer dimly lit environments and can be significantly damaged by high irradiances. At night, cryptophytes swim deeper in the water column to utilize available nutrients below the chemocline or to avoid predators (Smolander and Arvola 1988). The ability to control their placement in the water column is a significant advantage for cryptophyte algae especially in areas of stratification and low nutrient concentrations.

The ability to adjust their photosynthetic machinery, to supplement their nutritional needs, and to control their location in the water column may allow cryptophytes to compete with more traditional bloom forming algae in coastal areas. The mechanisms and benefits of cryptophyte motility have been well documented in both natural environments and laboratory experimentation (Jones 1988; Smolander and Arvola 1988; Arvola *et al.* 1991). In this study, we examine the effects of both photoacclimation strategies and mixotrophic ability on photosynthetic efficiency and growth for both cryptophytes and diatoms and speculate about their potential for success in coastal waters.

4.2 Methods

4.2.1 Laboratory Methods

Cultures of *Cryptomonas erosa* were isolated from Lake Michigan and cultured in modified MBL media. *Cyclotella meneghiniana* (CCAP # 1070/5) was cultured in DM media. Cultures were unialgal, but not axenic. *C.* erosa cultures were grown at a range of temperatures at both high (80 µmol photons m^{-2} s^{-1}) and low (15 µmol photons m^{-2} s^{-1}) light under a 12:12 light dark regime and sampled to assess optimum growth conditions. Each experiment was performed with at least three replicates for each treatment condition per species. After six days of incubation, growth of the population was measured as total cells ml^{-1} by repeated counts with a hemacytometer. Each subsample was counted a minimum of six times. Chlorophyll fluorescence data for each sample was measured using a Fast Repetition Rate Fluorometer [FRR-F (Kolber *et al.* 1998)]. Samples were dark adapted for five minutes before sampling.

After these preliminary observations, further experiments were all conducted at 20°C and measurements concentrated on intermediate and lower irradiance levels (less than 180 µmol photons m^{-2} s^{-1}). *C. erosa* and *C. meneghiniana* cultures were incubated in 250 ml flasks as semi-continuous cultures for 8-10 days at a range of irradiances (2.5, 3.5, 8, 22, 45, 97, and 180 µmol photons m^{-2} s^{-1}) with and without addition of 100 µM glucose. Irradiance measurements inside the flasks were conducted with a HobiLabs Hydrorad hyperspectral radiometer. The Hydrorad measures irradiance (E) every 0.3nm. All Hydrorad sensors were factory calibrated prior to sampling for quality assurance and each measurement was the average of 4 scans taken in each flask. Irradiance values were then interpolated for continuous data and binned to every 2 nm. For PAR values, measurements were integrated over the visible spectrum (400-700 nm). Over the course of the experiment, light levels were monitored by repeated measurements every 5-8 days. Cultures were sampled every two days; aliquots were removed and cultures were replenished with fresh inorganic media either supplemented with 100 µM glucose or Milli-Q water (control). Aliquots were tested for growth rates and F_v/F_m. F_v/F_m measurements have been used as an indicator of cell health and nutrient limitation in phytoplankton and higher plants (Kolber *et al.* 1988; Schreiber *et al.* 1995). F_v/F_m values remained constant over the course of the experiment indicating that samples were not nutrient limited (data not shown).

At the end of the experiment cultures were counted for growth rates and sampled for F_v/F_m, chlorophyll concentration, spectral absorption, and spectral fluorescence parameters. Chlorophyll concentrations were assessed by filtering a known volume under low pressure onto Whatman GF/F filters. Filters were quick frozen in liquid nitrogen and stored at $-80^{o}C$ until extraction (usually about 1 week). Chlorophyll was extracted in either 100% acetone (for *C. erosa*) or 90% acetone (for *C. meneghiniana*) overnight. Absorption values were measured with a Hewlett Packard 8451A spectrophotometer and chlorophyll *a* and *c* concentrations were calculated as per (Jeffrey and Humphrey 1975). Spectral absorption measurements were conducted on an Aminco DW-2a split beam spectrophotometer using sterile media as a blank. Spectral fluorescence data were collected both at room temperature and at 77K with an SLM Aminco Bowman series 2 luminescence spectrometer. 77K samples were collected and quick frozen in liquid nitrogen. The cuvette chamber of the spectrometer was cooled and maintained at liquid nitrogen temperatures for the duration of the measurements. Respiration measurements were taken on the last day of the experiment. Cultures were concentrated, counted, and placed on a silver platinum oxygen electrode. Oxygen evolution was recorded over time, the rate of oxygen evolution was calculated, and normalized to either cell number (μmol O_2 cell^{-1} hr^{-1}) or intracellular chlorophyll concentration (μmol O_2 chl^{-1} hr^{-1}). CHN measurements were conducted by filtering a known sample volume onto precombusted 25mm GF/F filters under low vacuum pressure. Filters were then dried and analyzed for carbon and nitrogen content using a Carlo Erba Instruments Eager 200.

4.2.2 Field Methods

Teflon-coated Niskin bottles, lowered to selected depths, were used to collect water for assessment of phytoplankton photopigments and microphotometry assays. Phytoplankton biomass, as chlorophyll *a*, and phylogenetic group dynamics were characterized using chemotaxonomic pigments derived using High Performance Liquid Chromotography as outlined in (Millie *et al.* 2002).

For microphotometry analysis, raw water samples were filtered under low vacuum (<50 mm Hg) onto 1.0 μm Nuclepore filters with GF/A backing filters. When the last 1-2 ml of water was still in the filtering funnel, vacuum pressure was released, and the filter, along with a few drops of water, was transferred to a gelatin slide. It is critical not to filter all of the water, as delicate cells are likely to rupture if some water is not retained on the filter. The back of the filter was gently swiped with a damp cotton swab and then removed from the gelatin slide. One to two drops of a 30% glycerol solution was placed on the transferred samples along with a coverslip. The slide was then immediately frozen by placing it on an aluminum block that had been previously immersed in liquid nitrogen. The frozen slides were placed in a slide box and kept frozen (-20^{o} C) until analysis.

The absorption efficiency factor, Q_a , can be measured on individual cells using a microphotometric technique (Itturriaga and Siegel 1989; Stephens 1995). This absorption efficiency factor is defined as the ratio of light absorbed by a cell to the light impinging on the cell's geometrical cross section. Microphotometric measurement of Q_a requires direct measurement of spectral transmittance of a cell or particle relative to a blank

$$Q_a(\lambda) = \frac{I_b(\lambda) - I_s(\lambda)}{I_b(\lambda)} \quad (4.1)$$

where $I_s(\lambda)$ = the radiant flux or transmittance for the sample, and $I_b(\lambda)$ = the radiant flux or transmittance for the blank. The raw data were smoothed by averaging over five wavelength bins. To correct for any light that might have been lost by scattering, which in our system was likely minimal (Itturriaga and Siegel 1989), the mean Q_a value at 750-760 nm was subtracted from all other measurements.

A Leica DMR HC microscope system equipped with an optic coupler was used for microphotometric measurements. An Ocean Optics, Inc. collimating lens (74-VIS) was used to couple light from the microscope head to a 400 um patch silica optical fiber which was interfaced with an Ocean Optics, Inc. miniature spectrometer (S2000) interfaced with a 500 KHz ADC board. The optical configuration provided an effective resolution of approximately 2 nm at FWHM (full width half maximum). The CCD array of the spectrometer consisted of a 2048-element linear detector extending over a wavelength range of 350-1000 nm. Ten scans were averaged for each measurement, and the sampling rate was such that the total scan time was approximately 10 seconds.

4.3 Photoacclimation Strategies

4.3.1 Photoacclimation to available light

Preliminary experiments were conducted to find the optimum growth conditions for *C. erosa*. Growth rates (represented as total biomass) were higher at high light and intermediate temperatures (Fig. 4.3 and Table 4.1). However, cryptophytes are considered a shade adapted group as they are typically found in dim light conditions and have a lower optimum growth irradiance than other groups of phytoplankton (Morgan and Kalff 1979; Klaveness 1988). In general, algae with more accessory pigments have lower optimum growth irradiances and phycobilin containing groups are the most dim light adapted phytoplankton group (Brown and Richardson 1968). Research with natural populations has shown that cryptophytes respond to low light by increasing both chloroplast area and intrathylakoidal width indicating that they are capable of increasing both the number and size of the photosynthetic unit (Thinh 1983). Further, deep water cryptophyte populations are capable of extreme low light acclimation and have much lower E_k and P_{max} parameters compared with populations found closer to the surface (Gasol *et al.* 1993). Further experiments focused on photoacclimation under low light conditions.

After 8-10 days of growth under different treatment conditions (Table 4.2), each culture was examined to determine the ability to adapt to varying irradiance levels. 77K fluorescence spectra show the primary energy transfer from chl *c* and phycoerythrin to PSII and from chl *a* to PSI in *C. erosa* (Fig. 4.4). In cryptophytes, the phycobilins (here phycoerythrin) are the primary light harvester for photochemistry at PSII while chl *a* is primarily responsible for funneling absorbed energy to PSI.

Under low light conditions the transfer of energy absorbed by phycoerythrin to PSII is more efficient than at high light (Fig. 4.5). Energy transfer between the chromophores and from the phycobilin complex to PSII is extremely efficient in cryptophytes (Kobayashi *et al.* 1979; Wedemayer *et al.* 1991). This efficiency of energy transfer allows them to maintain photosynthetic potential at lower light levels than many other phytoplankton groups as much of the absorbed light is channeled to PSII. However, the act of photosynthetic carbon fixation is dependent upon the coordinated transfer of electrons through two photosystems and the primary light harvesting pigments are different for the two photosystems. Thus different wavelengths of light can unevenly stimulate the photosystems so that one is preferentially excited; this will lead to an unbalanced system and a decrease in the photosynthetic efficiency. Phytoplankton and higher plants have adapted mechanisms to adjust the functionality of the two photosystems in order to maintain photosynthesis at its maximum potential and increase the quantum efficiency of carbon fixation (Chow *et al.* 1990). Similarly, cryptophytes can shift the stoichiometry of PSII:PSI in response to their growth irradiance. Cultures grown in low light conditions produce more PSI thereby decreasing the PSII:PSI ratio (Fig. 4.6 top).

In cyanobacteria, high light conditions mimic an increase in PSI light (blue and far-red light) while low light conditions overstimulate PSII leading to an increase in PSI synthesis (Fujita *et al.* 1994; Samson and Bruce 1995). In nature, phytoplankton populations found at depth will experience both low intensities of light and a spectral skewing of the light field limited to the green and blue-green wavelengths. This will lead to a marked overstimulation of PSII in phycobilin containing organisms and to a decrease in the photosynthetic activity at limiting light levels. Under these conditions, PSI synthesis will increase due to the overstimulation of PSII and the need for extra ATP to supplement the energy requirements of the cell. In this study, *C. erosa* populations increased PSI synthesis in response to low light conditions.

In contrast, diatoms have more PSII than PSI and under low light conditions responded by increasing PSII:PSI (Fig. 4.6 bottom). Diatoms grown at low light increase concentrations of PSII in concert with increases of cellular chlorophyll (Falkowski *et al.*

1981). This increase in pigment concentration is a well known photoacclimation strategy under sub-saturating light intensities. However, it only affords an advantage to a point as with an increase in pigment concentration, each molecule of pigment becomes less efficient at absorbing available light (Duysens 1956). Conversely, the ability of cryptophytes to alter the stoichiometry of PSII:PSI in response to both light intensity and spectral irradiance is an efficient photoacclimation mechanism to balance electron flow through the two photosystems and maintain optimal levels of carbon fixation at very low light levels.

4.3.2 Implications of photoacclimation for natural populations

Photosynthetic organisms in natural waters have to contend with a highly variable light environment. It has been proposed that phytoplankton populations are capable of adjusting the structure of community composition in response to both the quality (Engelmann 1883; Kirk 1994) and quantity (Berthold 1882) of available light. As a case study, field populations of cryptophytes and diatoms were examined in southern Lake Michigan during a spring turbidity plume which strongly affected both the quality and intensity of available light (Bergmann *et al.* 2003). Total light availability was decreased in plume dominated stations due to the high attenuation properties of the water column. Similarly, phytoplankton populations in the well mixed offshore stations had less total light available to them due to the deep mixing depth (up to 120m). In well mixed areas, phytoplankton will acclimate to the average light intensity encountered over time, i.e. the depth integrated light field as they vertically cycle through the water column (Cullen and

Lewis 1988). The increase in light attenuation in the plume and the deep mixed layer depth in offshore stations resulted in similar total amounts of available light.

Although the intensity of light in both plume dominated and offshore stations in spring was similar when averaged over the depth of the water column, the average light field for a deep water station was spectrally different than a shallower station. Deep water stations had a distinct spectral shift in available light with green light dominating at depth. This greening of the water altered the competitive ability of the two main phytoplankton classes encountered in Lake Michigan. The observed shift in the phytoplankton community from diatoms onshore to cryptophytes offshore was controlled in part by the spectral shift in the available light field (Fig. 4.7) and led to a strong inverse correlation between these two groups (Fig. 4.8).

Although the absorption efficiencies for a representative diatom (*Melosira islandica*) and cryptophyte (*Rhodomonas lens*) were equal when integrated under PAR, they were distinctly spectrally different (Fig. 4.9). *M. islandica* and *R. lens* are prevalent species in Lake Michigan that significantly contribute to total phytoplankton biomass (Holland 1969; Danforth and Ginsburg 1980; Makarewicz *et al.* 1994). The primary photosynthetic pigments for diatoms are chlorophyll and fucoxanthin, which absorb maximally in the blue and red wavelengths of light while the cryptophytes primarily utilize phycobilin pigments, which have an absorption maximum in the green wavelengths. The growth potential for photosynthetic organisms is dependent upon their ability to absorb the spectra of light that is available.

The incoming irradiance at the sea surface is spectrally flat (Fig. 4.10 top, shaded area. Potential absorption for *M. islandica* and *R. lens* was calculated based upon their measured absorption efficiencies and the available irradiance at both the surface (Fig. 4.10 top) and for the average light field throughout the mixed layer depth at an offshore station (Fig. 4.10 bottom). In surface waters with a spectrally unrestricted light field (white light) potential absorption efficiencies for *M. islandica* and *R. lens* were approximately equal when integrated under the visible light curve (Fig. 4.10 top). Under these conditions, all phytoplankton groups are at their maximum potential for light absorption.

Assuming that the isothermal water columns were completely vertically mixed during the spring months, an average light field was computed based upon the spectral light availability in the mixed layer depth. This average light field is spectrally skewed as the blue and red wavelengths of light are selectively removed leaving mostly green light (Fig. 4.10 bottom). Although the potential absorption for both species was equal at the surface, the cryptophytes had a higher potential for absorption in the average mixed layer depth light field. The chlorophyll and fucoxanthin pigments of the diatom were less effective than the cryptophyte's phycobilin pigments as the light field became more restricted to the green wavelengths of light. Additionally, cryptophytes often have multiple accessory chromobilins associated with their phycobilin pigments that extends their range of absorption (Kobayashi *et al.* 1979; Wedemayer *et al.* 1991). They can alter the concentration of these photosynthetic pigments in response to both the intensity and the spectral quality of the available light field (Kamiya and Miyachi 1984) thus allowing them to maintain higher levels of cellular absorption as the quality of the light field changes. Given the spectral quality of light at depth in the lake, the cryptophytes were better suited to utilize the available irradiance. This spectral selection for cryptophytes may explain the offshore distribution observed in phytoplankton populations. This is consistent with the idea that absorption of green light by phycobilins in cyanobacteria may allow them to be superior competitors at depth in spectrally skewed light fields (Huisman *et al.* 1999).

4.4 Mixotrophic Potential

C. erosa and *C. meneghiniana* cultures grown under a range of irradiances both with and without the addition of glucose showed a striking difference between these two groups. Growth rates for *C. meneghiniana* were unaffected by the addition of glucose, while *C. erosa* growth was significantly enhanced by glucose supplementation (Fig. 4.11 and Table 4.2). The addition of organic nutrients also affected the carbon:chlorophyll ratio such that low light samples with added glucose had higher C:Chl ratios than samples grown on inorganic nutrients alone (Table 4.3). C:Chl ratios for *C. meneghiniana* were not significantly different for samples grown with and without glucose (data not shown). This observed increase in C:Chl ratios for *C. erosa* samples supplemented with glucose reflects an increase in intracellular carbon without the advantage afforded by a concomitant increase in cellular pigment concentrations. The difference between +glucose and control *C. erosa* cultures indicates that *C. erosa* carbon fixation and growth was benefited by the presence of an organic carbon source. Laboratory studies with cryptophytes have demonstrated their potential for mixotrophy when grown in the presence of organic substrates (Antia *et al.* 1969; Lewitus *et al.* 1991; Gervais 1997a). Cryptophytes have the ability to supplement their photosynthetic growth at low light levels when available irradiances may not be sufficient to support growth.

Additionally, both *C. erosa* treatments were able to sustain growth at lower irradiances than *C. meneghiniana* (Fig. 4.11). The +glucose *C. erosa* treatment continued to grow at a faster proportional rate than *C. meneghiniana* up to approximately 40 µmol photons m^{-2} s^{-1}. At higher growth irradiances all cultures were growing close to their maximum; the addition of glucose had no effect at these light levels.

Photosynthetic growth as a function of the growth irradiance can be estimated (Laws and Bannister 1980; Kiefer and Mitchell 1983; Falkowski *et al.* 1985). At a given irradiance

$$\mu = E \times \frac{Chl}{C} \times a^* \times \phi_p \qquad (4.2)$$

where µ is growth rate (day^{-1}), E is available irradiance (µmol photons m^{-2} day^{-1}), Chl:C is the cellular chlorophyll *a* to carbon ratio (mg mg^{-1}), a* is the chlorophyll specific absorption coefficient (m^2 mg chl a^{-1}), and Φ_p is the quantum yield of carbon fixation (mg C µmol $photons^{-1}$). In this study each of the above parameters were measured with the exception of the quantum yield of carbon fixation which was assumed to be variable between 0.0015 mg C µmol $photons^{-1}$ (0.125 mol C mol $photons^{-1}$) at low light and 0.00015 mg C µmol $photons^{-1}$ (0.0125 mol C mol $photons^{-1}$) at high light. Under nutrient replete conditions Φ_p is primarily determined by variations in available irradiance. Chosen values approach the theoretical maximum under low light conditions and vary inversely with irradiance as cryptophytes are less efficient carbon fixers at high light.

Calculating growth rates using equation 4.2 leads to an underestimation of growth for samples grown at low light and an overestimation of growth for high light samples (Table 4.4). Growth rate calculations for low light samples showed the most error for those treatments that received supplemental glucose. Low light, + glucose treatments had significantly higher growth rates than would be expected based upon the available irradiance. The enhanced growth afforded by the ability to uptake organic nutrients was not accounted for by equation 4.2. Conversely, at high light, equation 4.2 overestimated actual growth rates, especially for the + glucose treatments, due to a decrease in measured growth rates caused by competition for available resources by bacteria. Cultures used in this study were not axenic and therefore the addition of organic nutrients to the growth media led to an abundance of bacteria in the growth chamber. Over time, phytoplankton populations were adversely affected by competition with the rapidly growing bacteria for both organic and inorganic nutrients.

Equation 4.2 may also be used to back-calculate Φ_p (Table 4.5). These calculated values for Φ_p showed that low light, +glucose samples had a higher quantum yield for growth than control samples. The addition of organic nutrients allowed these cultures to fix more carbon per photons absorbed as compared to cultures grown with only inorganic nutrients at the same light level. Under light saturating conditions, the addition of organic nutrients had little effect on Φ_p. The increased quantum yield for growth observed at low light in response to supplemental organics may have a significant effect in natural waters with sub-saturating irradiances and high levels of organic material.

Additionally, respiration rates were higher in + glucose treated samples (Table 4.5). Respiration rates were concurrently measured with growth rates and may explain some of the variability seen between measured and calculated growth rates. All samples had increased respiration when supplemented with organic nutrients (Table 4.6); however *C. erosa* samples most significantly affected were low light, + glucose samples corroborating that the addition of organic nutrients increases respiration more than photosynthesis at low irradiances (Lewitus and Kana 1995). This increase in respiration can be directly linked to respiration of the available organic carbon allowing cells to increase energy stores and growth potential without a concomitant increase in photosynthesis and carbon fixation.

Coastal aquatic habitats are often turbid areas laden with organic material. The combination of river runoff and *in-situ* production leads to elevated concentrations of dissolved organics (Cauwet 2002). These high concentrations of strongly absorbing dissolved organics act as an energy source for mixotrophic phytoplankton and serve to reduce the amount of available light in the water column. Coastal waters are characterized by high concentrations of dissolved organic matter and low light levels where available light is confined to the blue-green and green wavelengths. Cryptophytes are successful in these areas because they have developed three main strategies for maintaining growth in these low light settings; these include 1) maximizing light absorption and utilization by altering pigment concentration, pigment ratios, and PSII:PSI stoichiometry, 2) using alternative external and internal fuel sources to supplement cellular energy requirements at low light when photosynthetic rates are not sufficient to fuel growth, and 3) strong swimming allows them to control their proximity to light and nutrient sources. The ability to utilize organic nutrients as an energy source under sub-saturating light levels and to acclimate to available irradiances allows cryptophyte algae to outcompete more traditional bloom forming phytoplankton under some conditions. In optically shallow, organically laden water columns, the window of cryptophyte dominance will be greatest.

4.5 Implications for future change in coastal zones

The coastal ocean plays a pivotal role in marine systems. Coastal zones provide a link between terrestrial and oceanic nutrient cycling, are extremely active areas for primary production, and are an important link in global biogeochemistry. These areas are delicately balanced and are strongly affected by anthropogenic alterations and climatic changes to the ecosystem (Zimmerman and Canuel 2000). For example, eutrophication of coastal areas due to river runoff and atmospheric deposition of nutrients alters the supply and distribution of nutrients and increases primary production and phytoplankton and bacteria turnover in affected areas (Meybeck 1982; Cornell *et al.* 1995; Ortner and Dagg 1995). This increase in primary productivity of the water column affects the transfer of material to higher trophic levels and the deposition, burial, and degradation of organic matter (Deuser *et al.* 1981; Asper *et al.* 1992). The anthropogenic addition of highly concentrated nutrients into coastal waters will have long ranging effects on nutrient cycling and carbon sequestration as well as reverberating through the marine food web. In addition to obviously increasing the availability of organic nutrients in coastal areas, this will also increase water column turbidity leading to decreased light levels at depth.

Climatic change has far reaching effects in estuaries (Sullivan *et al.* 2001), coastal areas (Paerl 1998), and inland lakes (Schindler *et al.* 1990; Ducrotoy 1999). These changes will alter marine community composition, biogeochemical cycles, and food web structure (Roemmich and McGowan 1995) especially in coastal areas which are very biologically diverse (Gray 2001). Oceanic warming trends will alter biological community composition, especially of primary producers, and will lead to the preferential extinction of predators (Petchey *et al.* 1999). Increased temperatures will also intensify erosion, river runoff, and flooding of dry lands and wetlands leading to increased organic matter concentrations and light attenuation in affected coastal waters (Titus *et al.* 1991; Gornitz 1995; Gregory and Oerlemans 1998; Oppenheimer 1998; Pethick 2001). These coastal areas will be marked by a significant change in the quantity and quality of available light as the introduction of high levels of suspended matter and organics leads to an increase in total light attenuation, especially in the UV region, and a spectral skewing to predominantly green and blue-green wavelengths of available light at depth. Additionally, the increased concentration of organic material will enhance the competitive potential for phytoplankton groups capable of using these newly available resources for growth.

As coastal ecosystems are disrupted by climatic and anthropogenic alterations, these impacted areas are the principal locations where shifts in community composition will be most apparent. I hypothesize an increase in the prevalence of cryptophyte algae which are uniquely suited for growth in these organically laden, dim light, coastal waters.

Light Level	Temperature (^oC)	Biomass (cells ml^{-1} X 10,000)	Biomass standard deviation	F_v/F_m	F_v/F_m standard deviation
Low	23.4	10.77	1.00	0.66	0.01
Low	20.1	13.94	2.09	0.67	0.01
Low	16.8	14.11	1.09	0.68	0.02
Low	13.5	16.83	1.11	0.66	0.00
Low	10.2	15.17	0.92	0.67	0.01
Low	6.9	13.59	0.59	0.65	0.00
High	23.4	15.18	1.95	0.62	0.03
High	20.1	19.48	1.61	0.64	0.00
High	16.8	20.09	1.00	0.63	0.00
High	13.5	20.90	0.81	0.63	0.01
High	10.2	16.87	2.18	0.63	0.00
High	6.9	17.02	0.73	0.62	0.00

Table 4.1 Biomass and F_v/F_m results for preliminary experiments with *C. erosa*.

C. erosa	Nutrient Treatment	Irradiance (μmol photons m^{-2} s^{-1})	Irradiance standard deviation	Growth Rate (day^{-1})	Growth Rate standard deviation
	control	2.35	0.06	-0.10	0.07
	control	3.51	0.25	-0.05	0.06
	control	8.18	0.50	0.12	0.05
	control	22.51	0.16	0.26	0.06
	control	44.15	1.81	0.36	0.05
	control	96.88	1.14	0.62	0.23
	control	180.15	0.80	0.76	0.09
	plus glucose	2.37	0.26	-0.01	0.10
	plus glucose	3.63	0.58	0.31	0.10
	plus glucose	8.64	0.60	0.42	0.08
	plus glucose	22.18	0.32	0.44	0.07
	plus glucose	42.55	4.61	0.54	0.13
	plus glucose	95.01	2.37	0.58	0.12
	plus glucose	181.93	2.80	0.69	0.17
C. meneghiniana	**Nutrient Treatment**	**Irradiance (μmol photons m^{-2} s^{-1})**	**Irradiance standard deviation**	**Growth Rate (day^{-1})**	**Growth Rate standard deviation**
	control	3.51	0.25	-0.01	0.06
	control	8.18	0.50	-0.02	0.06
	control	22.51	0.16	0.12	0.05
	control	44.15	1.81	0.20	0.03
	control	96.88	1.14	0.26	0.08
	control	180.15	0.80	0.29	0.10
	plus glucose	3.63	0.58	-0.04	0.01
	plus glucose	8.64	0.60	-0.02	0.06
	plus glucose	22.18	0.32	0.11	0.02
	plus glucose	42.55	4.61	0.24	0.07
	plus glucose	95.01	2.37	0.30	0.02
	plus glucose	181.93	2.80	0.32	0.02

Table 4.2 Irradiance levels and growth rates for *C. erosa* and *C. meneghiniana* grown both with and without the addition of 100 μmol glucose.

	C (ng cell^{-1})		N (ng cell^{-1})		C:Chl	
C. erosa **LL Control**	0.074	±0.007	0.018	±2.838	32.81	±0.73
C. erosa **LL + glucose**	0.081	±0.002	0.019	±0.001	38.01	±2.73
C. erosa **HL Control**	0.071	±0.005	0.016	±0.001	32.73	±1.89
C. erosa **HL + glucose**	0.077	±0.003	0.018	±0.001	32.19	±1.08
C. erosa **control**	0.075	±0.006	0.016	±0.001	40.24	±5.48
C. erosa **+ glucose**	0.066	±0.007	0.014	±0.002	36.05	±5.57
C. meneghiniana **control**	0.235	±0.020	0.013	±0.001	184.45	±15.42
C. meneghiniana **+ glucose**	0.253	±0.013	0.014	±0.001	184.94	±17.32

Table 4.3 Carbon, nitrogen, and C:Chl ratios for top: *C. erosa* samples grown at low light (12 μmol photons m^{-2} s^{-1}) and high light (90 μmol photons m^{-2} s^{-1}) and bottom: *C. erosa* and *C. meneghiniana* samples grown at medium light (45 μmol photons m^{-2} s^{-1}) both with and without the addition of 100 μM glucose. C per cell and C:Chl ratios are highest for low light samples grown with the addition of organic nutrients. At medium and high light levels C:Chl ratios are not significantly different for samples with added organic nutrients.

Sample Treatment	growth rate (measured; day $^{-1}$)	E (µmol photons m^{-2} s^{-1})	a* (m^2 mg chl a^{-1})	Chl:C	Φ (mg C µmol phot $^{-1}$)	growth rate (estimated; day^{-1})
LL, Control	0.57	12.36	0.019	0.0305	0.0015	0.477
LL, + Glucose	0.61	12.36	0.021	0.0266	0.0015	0.481
HL, control	0.50	89.75	0.035	0.0306	0.00015	0.659
HL, + Glucose	0.46	89.75	0.038	0.0300	0.00015	0.677

Table 4.4 Measured and calculated growth rates, growth irradiance, chlorophyll specific absorption coefficient (a*), and Chl:C ratio for *C. erosa* samples grown at low light (12 µmol photons m^{-2} s^{-1}) and high light (90 µmol photons m^{-2} s^{-1}) both with and without the addition of 100 µM glucose. The quantum yield of carbon fixation was estimated and held constant for low light and high light samples.

Sample Treatment	growth rate (measured; day $^{-1}$)	E (µmol photons m^{-2} s^{-1})	a* (m^2 mg chl a^{-1})	Chl:C	Calc Φ (mg C µmol phot $^{-1}$)	
LL, Control	0.57	12.36	0.017	0.0305	0.0015	±0.0001
LL, + Glucose	0.61	12.36	0.021	0.0266	0.0019	±0.0002
HL, control	0.50	89.75	0.035	0.0306	0.00013	±0.000026
HL, + Glucose	0.46	89.75	0.038	0.0300	0.00012	±0.000016

Table 4.5 Measured growth rate, growth irradiance, chlorophyll specific absorption coefficient (a*), and Chl:C ratio, for *C. erosa* samples grown at low light (12 µmol photons m^{-2} s^{-1}) and high light (90 µmol photons m^{-2} s^{-1}) both with and without the addition of 100 µM glucose. The quantum yield of carbon fixation (Φ) has been back-calculated using equation 4.2. The slightly higher Φ for low light, +glucose samples indicates that these cultures are capable of fixing more carbon per photons absorbed due to the additions of organic nutrients to supplement their photosynthetic growth. Note that calculated values for Φ_p were not used to calculate growth rates in Table 4.4.

species	treatment	R (µmol O_2 chl^{-1} hr^{-1})	R (µmol O_2 cell^{-1} hr^{-1})
C. erosa	LL, control	0.035	7.32E-08
C. erosa	LL, +glucose	0.042	9.88E-08
C. erosa	HL, control	0.021	4.65E-08
C. erosa	HL, +glucose	0.025	5.64E-08

species	treatment	R (µmol O_2 chl^{-1} hr^{-1})	R (µmol O_2 cell^{-1} hr^{-1})
C. erosa	control	0.051	9.45E-08
C. erosa	glucose	0.054	9.88E-08
C. meneghiniana	control	0.070	1.19E-07
C. meneghiniana	glucose	0.089	1.29E-07

Table 4.6 Respiration measurements for top: *C. erosa* samples grown at low light (12 µmol photons m^{-2} s^{-1}) and high light (90 µmol photons m^{-2} s^{-1}) both with and without the addition of 100 µM glucose and bottom: *C. erosa* and *C. meneghiniana* samples at medium light (45 µmol photons m^{-2} s^{-1}) both with and without the addition of 100 µM glucose. The increase in respiration was most significant for *C. erosa* samples grown at low light with the addition of glucose. At low light *C. erosa* was supplementing photosynthetic growth with energy from available organic nutrients.

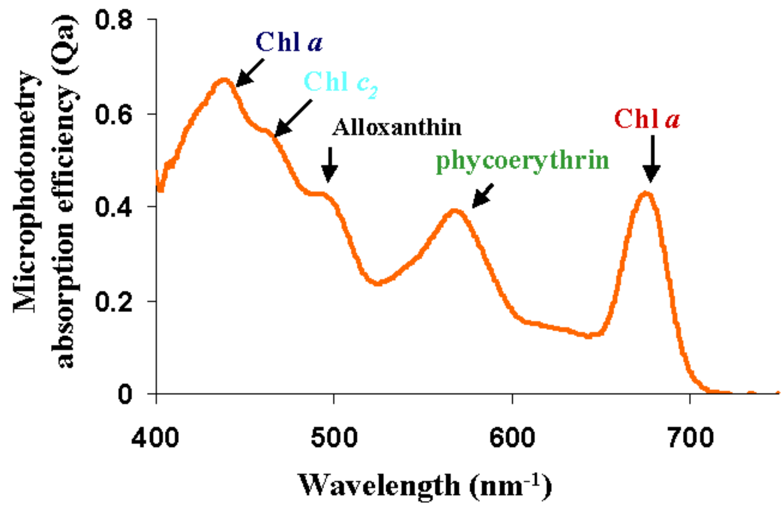

Figure 4.1 Cryptophyte absorption spectra. Cryptophytes are the only phytoplankton group to contain both chlorophyll *a* and c_2 as well as carotenoids and phycobilins.

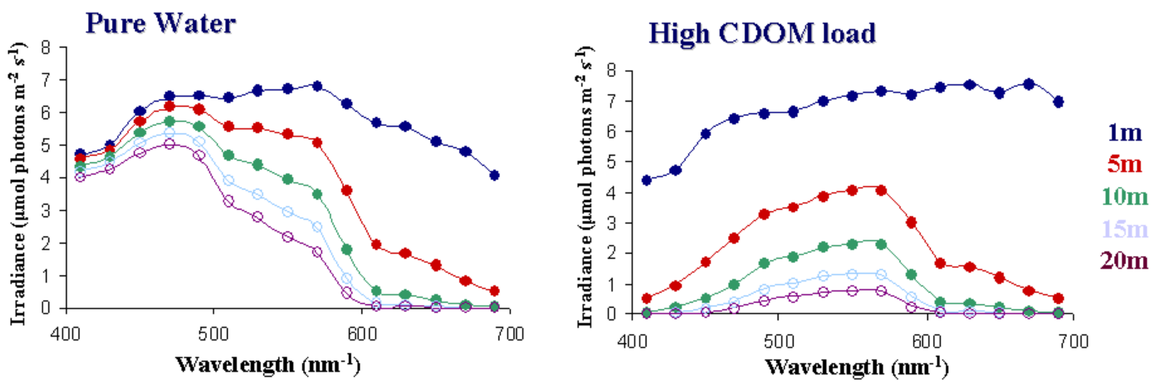

Figure 4.2: Spectral distribution of available light in a) a water column comprised of pure water alone and b) a water column with high concentrations of dissolved organic matter. Irradiance values are output from Hydrolight 4.2 radiative transfer model.

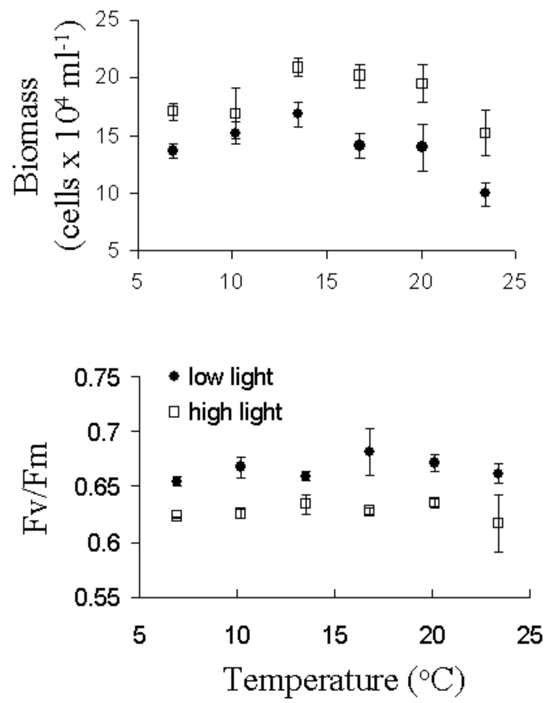

Figure 4.3: Biomass (top) and F_v/F_m (bottom) for *C. erosa* at a range of temperatures. Cultures were grown at a series of light and temperature treatments and sampled for biomass (cell counts with a hemacytometer) and F_v/F_m (Fast Repetition Rate Fluorometer). Growth was fastest at high light levels and intermediate temperatures. Photochemical efficiency was consistently higher at low light and was independent of temperature.

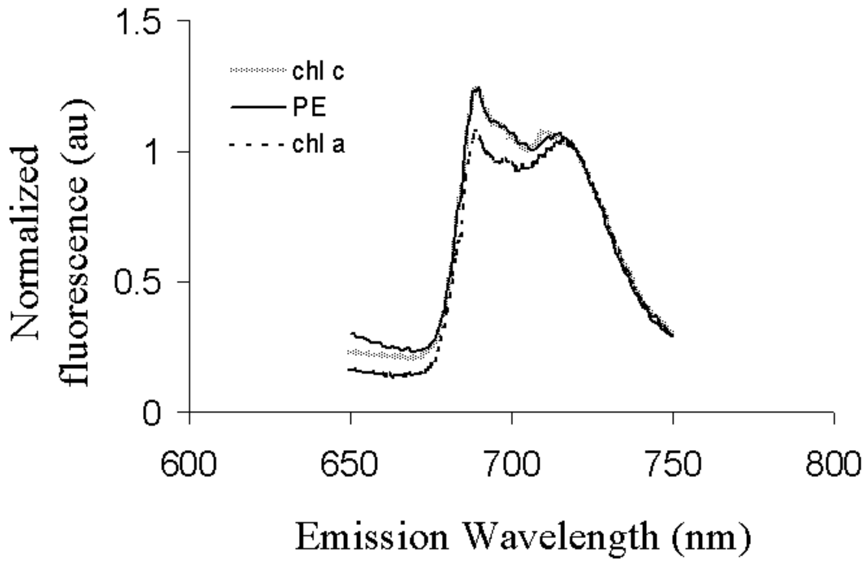

Figure 4.4: 77K fluorescence emission spectra for *C. erosa*. Cultures were excited at chl *a* (435nm), chl *c* (462nm), and phycoerythrin (566nm). All fluorescence curves were normalized to 720nm. Emission at 690nm corresponds to PSII and at 720nm to PSI. Phycoerythrin and chl *c* are the primary light harvesters for PSII while chl *a* is the primary light harvester for PSI.

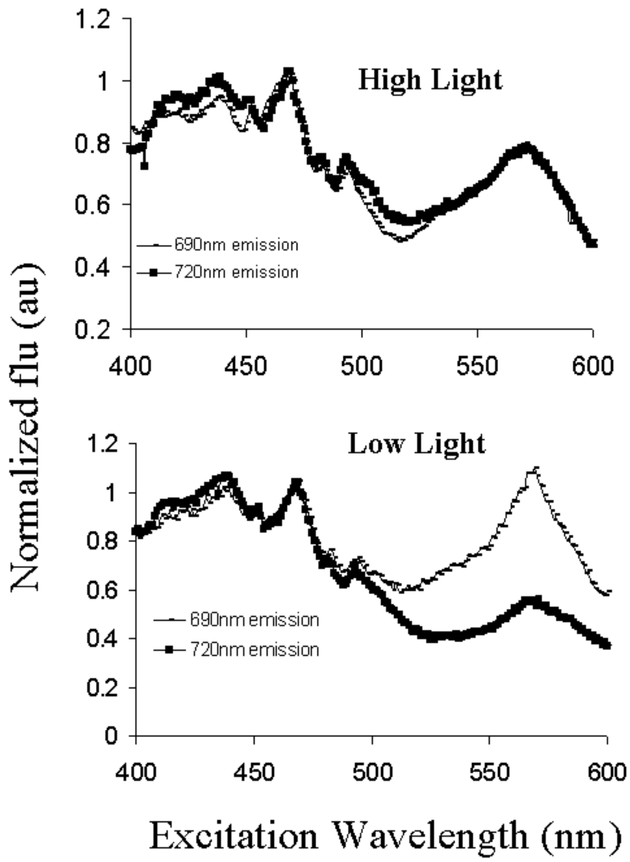

Figure 4.5: 77K fluorescence excitation spectra for *C. erosa* cultures grown in high light (top) and low light (bottom). Fluorescence emission is at 690nm (solid line) or 720nm (squares) and data have been normalized to 435nm. Cultures grown at low light show much higher fluorescence from PSII than PSI when excited at phycoerythrin compared to high light grown cultures indicating more efficient transfer from PE to PSII under low light conditions.

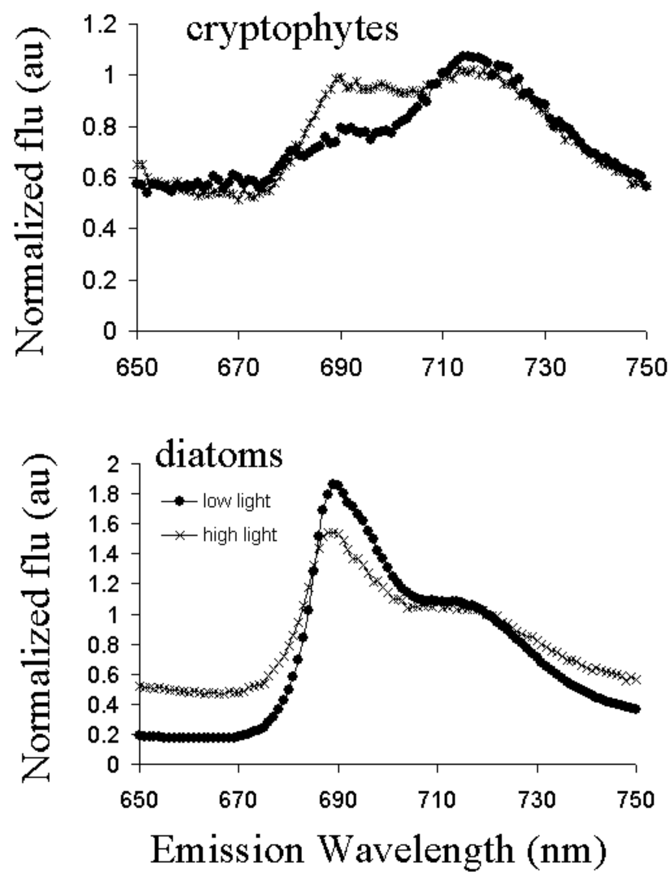

Figure 4.6: 77K fluorescence emission (excitation at 435nm) for *C. erosa* (top) and *C. meneghiniana* (bottom) cultures grown at low light (closed symbols) or high light (open symbols). At low light, *C. erosa* responds by decreasing the stoichiometry between PSII:PSI, while *C. meneghiniana* increases this ratio. Under low light conditions, light is preferentially absorbed by the phycobilins and transferred to PSII and cultures are light limited. PSI synthesis is stimulated by both high levels of PSII absorption and by the need for extra ATP under these conditions.

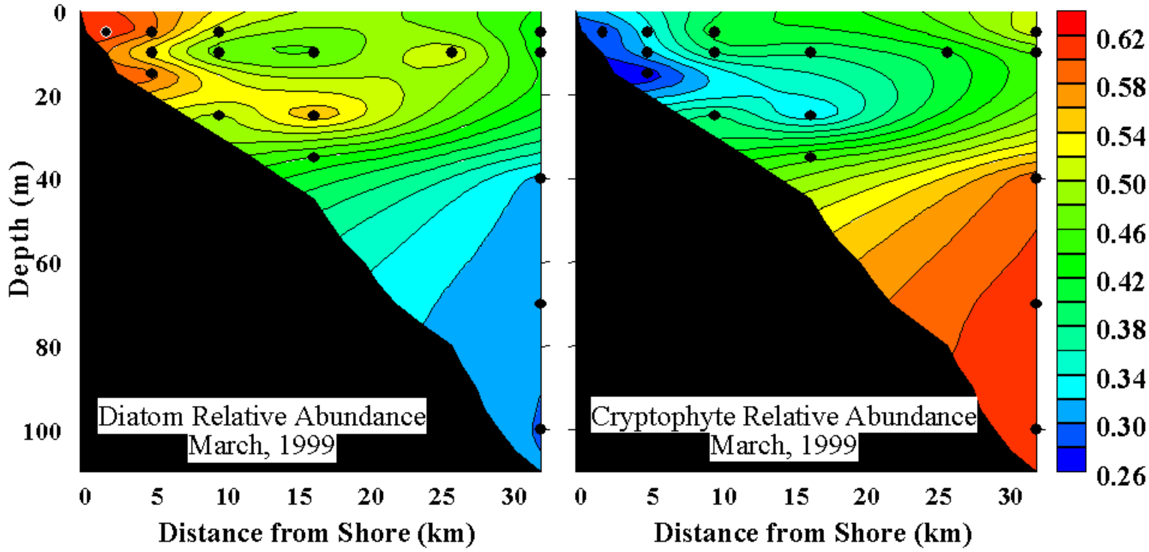

Figure 4.7 Cross shelf transects of the distributions of diatoms (left) and cryptophytes (right) in southern Lake Michigan

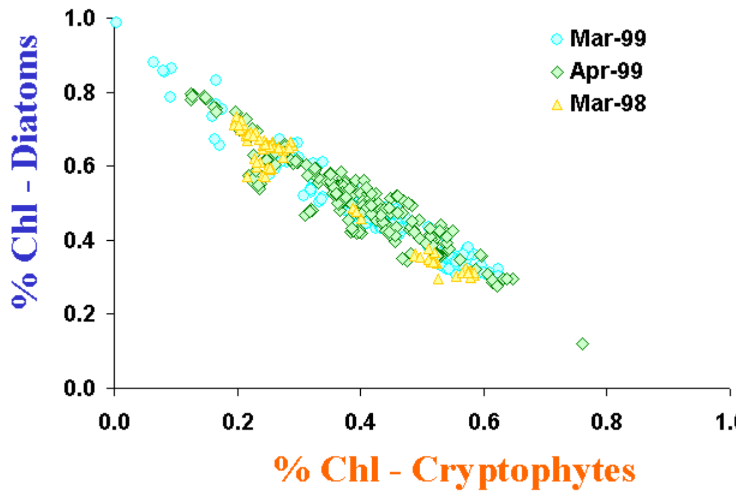

Figure 4.8 Proportion of chlorophyll *a* associated with cryptophytes Vs. Proportion of chlorophyll *a* associated with diatoms in coastal Lake Michigan.

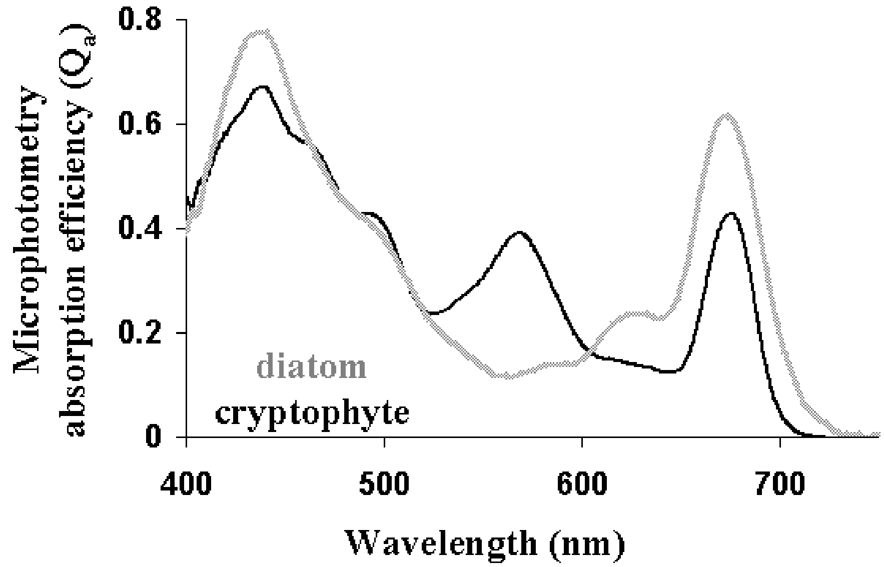

Figure 4.9: Microphotometry absorption efficiency (Q_a) for a representative diatom (*Melosira islandica*, gray line) and cryptophyte (*Rhodomonas minuta*, black line) collected offshore St. Joseph, MI. Total integrated potential absorption is equal for the two species.

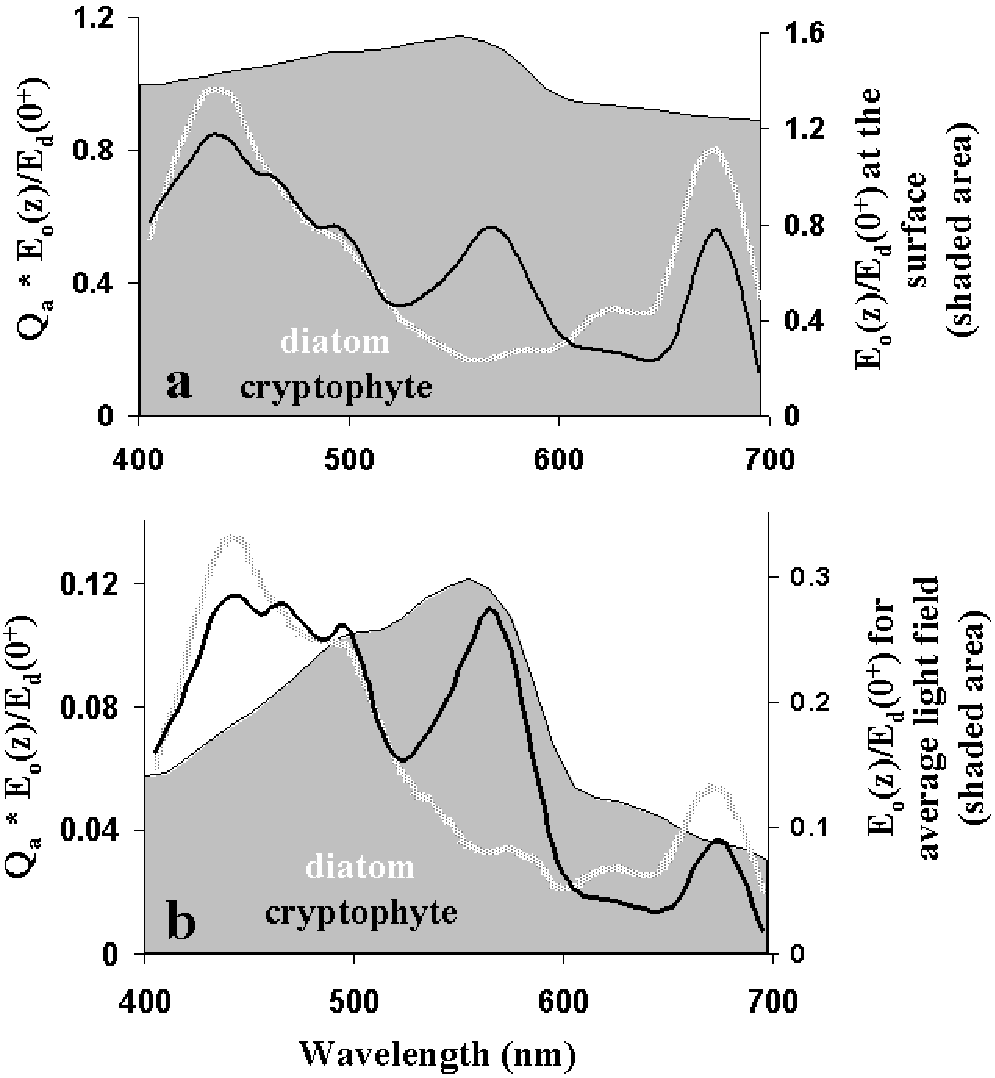

Figure 4.10: Product of the absorption efficiency (Qa) for a representative diatom (gray line) and cryptophyte (black line) and the scalar irradiance (E_o), normalized to the downwelling irradiance at the surface - a) scalar irradiance at the surface $E_o(0^-)$ and b) scalar irradiance for the average light field experienced by a phytoplankton cell over the mixed layer depth assuming total mixing of the water column. Superimposed is the available light field shaded in gray.

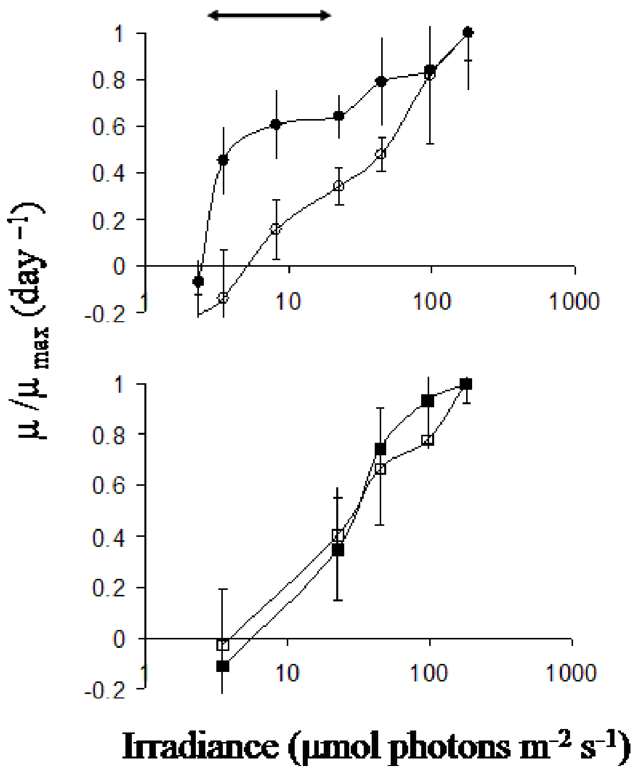

Figure 4.11: Growth rates for *C. erosa* (top) and *C. meneghiniana* (bottom). Cultures were incubated in 250ml flasks at 20°C at a range of irradiance values under a 12:12 light:dark cycle either with (+ glucose) or without (control) the addition of 100 μM glucose. At low light levels the growth of *C. erosa* is enhanced by the addition of glucose. Samples under the arrow show a statistically significant difference between control and +glucose treatments (light levels = 3.5, 8.5, 22, and 43 μmol photons m^{-2} s^{-1}) for *C. erosa*. None of the samples were significantly different between the control and +glucose treatments for *C. meneghiniana*. All growth rates have been normalized to the maximum growth rate for each species.

References

Allen, M., E. Dougherty and J. McLaughlin (1959). Chromoprotein pigments of some cryptomonad flagellates. *Nature* **184**: 1047.

Antia, N., J. Cheng and F. Taylor (1969). The heterotrophic growth of a marine photosynthetic cryptomonad (*Chroomonas salina*). *Proc. Intl. Seaweed Symp.* **6**: 17-29.

Aro, E., S. McCaffery and J. Anderson (1993). Photoinhibition and D1 protein degradation in peas acclimated to different growth irradiances. *Plant Phys.* **103**: 835-843.

Aro, E., I. Virgin and B. Andersson (1993). Photoinhibition of photosystem II. Inactivation, protein damage, and turnover. *Biochim. Biophys. Acta* **1143**: 113-134.

Arrigo, K. and C. Brown (1996). Impact of chromophoric dissolved organic matter on UV inhibition of primary productivity in the sea. *Mar. Ecol. Prog. Ser.* **140**: 207-216.

Arvola, L., A. Ojala, F. Barbosa and S. Heaney (1991). Migration behaviour of three cryptophytes in relation to environmental gradients: an experimental approach.

Asper, V., W. Deuser, G. Knauer and S. Lohrenz (1992). Rapid coupling of sinking particle fluxes between surface and deep ocean waters. *Nature* **357**: 670-672.

Banaszak, A. and P. Neale (2001). Ultraviolet radiation sensitivity of photosynthesis in phytoplankton from an estuarine environment. *Limnol. Oceanogr.* **46**(3): 592-603.

Barbiero, R. and M. Tuchman (2000). Results from the Great Lakes National Program Office's Biological Open Water Surveillance Program of the Laurentian Great Lakes for 1998. Chicago, IL, US EPA Great Lakes Program.

Behrenfeld, M., O. Prasil, Z. Kolber , M. Babin and P. Falkowski (1998). Compensatory changes in Photosystem II electron turnover rates protect photosynthesis from photoinhibition. *Photosynthesis Research* **58**: 259-268.

Beletsky, D. and D. Schwab (2001). Modeling circulation and thermal structure in Lake Michigan: Annual cycle and interannual variability. *JGR* **106**(C9): 19745-19771.

Bergmann, T., G. Fahnenstiel, S. Lohrenz, D. Millie and O. Schofield (2003). The Impacts of a Recurrent Resuspension Event and Variable Phytoplankton Community Composition on Remote Sensing Reflectance. *J. Geophys. Res.*

Berthold, G. (1882). Uber die verteilung der algen im golf von neapel nebst einem verzeichnis der bisher daselbst beobachten arten. *Mitt. Zool. Sta. Neopol.* **3**: 393-536.

Bonaventura, C. and J. Myers (1969). Fluorescence and oxygen evolution from *Chlorella pyrenoidosa*. *BBA* **189**: 366-383.

Booth, C., J. Morrow, T. Coohill, J. Cullen, H. Frederick, D. Hader, O. Holm-Hansen, W. Jeffrey, D. Mitchell, P. Neale, I. Sobolev, J. van der Leun and R. Worrest (1997). Impacts of solar UVR on aquatic microorganisms. *Photochem. Photobio.* **65**(2): 252-269.

Boyer, J., D. Stanley and R. Christian (1994). Dynamics of NH4 and NO3 uptake in the water column of the Neuse River Estuary, NC. *Estuaries* **17**(2): 361-371.

Brown, T. and F. Richardson (1968). The effect of growth environment on the physiology of algae: light intensity. *J . Phyc.* **4**: 38-54.

Bryant, D. (1994). <u>The Molecular Biology of Cyanobacteria</u>. Netherlands, Kluwer Academic Publishers.

Burns, N. and F. Rosa (1980). In situ measurement of the settling velocity of organic carbon particles and 10 species of phytoplankton. *Limnol. Oceanogr.* **25**(5): 855-864.

Campbell, D. (1996). Complementary chromatic adaptation alters photosynthetic strategies in the Cyanobacterium *Calothrix*. *Microbio.* **142**: 1255-1263.

Cauwet, G. (2002). DOM in the coastal zone. <u>Biogeochemistry of Marine Dissolved Organic Matter</u>. D. Hansell and C. Carlson, Elsevier Science**:** 579-609.

Chow, W., A. Melis and J. Anderson (1990). Adjustments of photosystem stoichiometry in chloroplasts improve the quantum efficiency of photosynthesis. *Proc. Natl. Acad. Sci.* **87**: 7502-7506.

Cloern, J. (1977). Effects of light intensity and temperature on *Cryptomonas ovata* (Cryptophyceae) growth and nutrient uptake rates. *J . Phyc.* **13**: 389-395.

Cloern, J. (1996). Phytoplankton bloom dynamics in coastal ecosystems; a review with some general lessons from sustained investigation of San Francisco Bay, California. *Reviews of Geophysics* **34**: 127-168.

Cornell, S., A. Rendell and T. Jickells (1995). Atmospheric inputs of dissolved organic nitrogen to the oceans. *Nature* **376**: 243-246.

Cullen, J. and M. Lewis (1988). The kinetics of algal photoadaptation in the context of vertical mixing. *J. Plankton Res.* **10**: 1039-1063.

Cullen, J. and J. MacIntyre (1998). Behavior, physiology and the niche of depth-regulating phytoplankton. The Physiological Ecology of Harmful Algal Blooms. D. Anderson, A. Cembella and G. Hallegraff. Heidelberg, Springer-Verlag, Heidelberg.

Danforth, W. (1962). Substrate assimilation and heterotrophy. Physiology and Biochemistry of Algae. R. Lewin. New York**:** 99-123.

Danforth, W. and W. Ginsburg (1980). Recent changes in the phytoplankton of Lake Michigan near Chicago. *J. Great Lakes Res.* **6**(4): 307-314.

Davis, P. and J. Sieburth (1984). Estuarine and oceanic microflagellate predation of actively growing bacteria: Estimation by frequency of dividing-divided bacteria. *Mar. Ecol. Prog. Ser.* **19**: 237-246.

Deuser, W., E. Ross and R. Anderson (1981). Seasonality in the supply of sediment to the deep Sargasso sea and implications for the rapid transfer of matter to the deep ocean. *Deep-Sea Research* **28**: 495-505.

Dohler, G., E. Hagmeier and C. David (1995). Effects of solar and artificial UV radiation on pigments and assimilation of 15 N ammonium and 15N nitrate by microalgae. *Journal of Photochemistry and Photobiology B: Biology* **30**: 179-187.

Dokulil, M. (1988). Seasonal and spatial distribution of cryptophycean species in the deep, stratifying, alpine lake Mondsee and their role in the food web. *Hydrobiologia* **161**: 185-201.

Dokulil, M. and C. Skolaut (1986). Succession of phytoplankton in a deep stratifying lake: Mondsee, Australia. *Hydrobiologia* **138**: 9-24.

Douglas, S. (1992). Probable Evolution History of Cryptomonad Algae. <u>Origins of Plastids</u>. R. Lewin. New Tork and London, CHapman and Hall**:** 265.

Dubinsky, Z., P. Falkowski and K. Wyman (1986). Light harvesting and utilization in phytoplankton. *Plant and Cell Physiol.* **27**: 1335-1349.

Ducrotoy, J. (1999). Indication of change in the marine flora of the North Sea in the 1990s. *Mar. Poll. Bull.* **38**(8): 646-654.

Duysens, L. (1956). The flattening of the absorption spectrum of suspensions as compared to that of solutions. *Biochim. Biophys. Acta* **19**: 1-12.

Duysens, L. and J. Amesz (1962). Function and identification of two photochemical systems in photosynthesis. *Biochim. Biophys. Acta* **64**: 243-260.

Eadie, B., R. Chambers, W. Gardner and G. Bell (1984). Sediment trap studies in Lake Michigan: Resuspension and chemical fluxes in the southern basin. *J. Great Lakes Res.* **10**(3): 307-321.

Eadie, B., D. Schwab, R. Assel, N. Hawley, N. Lansing, G. Miller, N. Morehead, J. Robbins, P. Van Hoof, G. Leshkevich, T. Johengen, P. Lavrentyev and R. Holland (1996). Development of recurrent coastal plume in Lake Michigan observed for first time. *EOS* **77**(35): 337-338.

Engelmann, T. (1883). Farbe und assimilation. *Bot. Zeit.* **41**: 1-13.

Erata, M., M. Kubota, T. Takahashi, I. Inouye and M. Watanbe (1995). Ultrastructure and phototactic spectra of two genera of cryptophyte flagellate algae, Cryptomonas and Chroomonas. *Protoplasma* **188**(3-4).

Fahnenstiel, G., J. Chandler, H. Carrick and D. Scavia (1989). Photosynthetic characteristics of phytoplankton communities in Lakes Huron and Michigan: P-I parameters and end-products. *J. Great Lakes Res.* **15**(3): 394-407.

Fahnenstiel, G. and D. Scavia (1987). Dynamics of Lake Michigan phytoplankton: The Deep Chlorophyll Layer. *J. Great Lakes Res.* **13**(3): 285-295.

Fahnenstiel, G., R. Stone, M. McCormick, C. Schelske and S. Lohrenz (2000). Spring isothermal mixing in the Great Lakes: evidence of nutrient limitation and nutrient-light interactions in a suboptimal light environment. *Can. J. Fish. Aquat. Sci.* **57**: 1901-1910.

Falkowski, P. (1980). Light-shade adaptation in marine phytoplankton. Primary Productivity in the Sea. P. Falkowski. New York, Plenum Press**:** 99-119.

Falkowski, P., Z. Dubinsky and K. Wyman (1985). Growth-irradiance relationships in phytoplankton. *Limnol. Oceanogr.* **30**(2): 311-321.

Falkowski, P., R. Greene and Z. Kolber (1994). Light utilization and photoinhibition of photosynthesis in marine phytoplankton. Photoinhibition of Photosynthesis: from molecular mechnisms to the field. N. Baker and J. Bowyer. Oxford, UK, BIOS Scientific Publishers Limited.

Falkowski, P. and J. LaRoche (1991). Acclimation to spectral irradiance in algae. *J. Phycol.* **27**: 8-14.

Falkowski, P., T. Owens, A. Ley and D. Mauzerall (1981). Effects of growth irradiance levels on the ratio of reaction centers in two species of marine phytoplankton. *Plant Phys.* **68**: 969-973.

Falkowski, P. and J. Raven (1997). Aquatic Photosynthesis, Blackwell Science.

Faust, M. and E. Gantt (1973). Effect of light intensity and glycerol on the growth, pigment composition, and ultrastructure of *Chroomonas* sp. *J . Phyc.* **9**: 489-495.

Fiala, M., M. Semeneh and L. Oriol (1998). Size-fractionated phytoplankton biomass and species composition in the Indian sector of the Southern Ocean during austral summer. *J. Mar. Sys.* **17**: 179-194.

Fraunholz, M., J. Wastl, S. Zauner, S. Rensing, M. Scherzinger and U. Maier (1998). The evolution of cryptophytes**:** 163.

Fujita, Y., A. Murakami and K. Aizawa (1994). Short-term and long-term adaptation of the photosynthetic apparatus: Homeostatic properties of thylakoids. The Molecular Biology of Cyanobacteria. D. Bryant. Netherlands, Kluwer Academic Publishers**:** 677-692.

Fujita, Y., A. Murakami and K. Ohki (1987). Regulation of Photosystem Composition in the Cyanobacterial Photosynthetic System: the Regulation Occurs in response to the redox state of the electron pool located between the two photosystems. *Plant and Cell Physiol.* **28**(2): 283-292.

Gantt, E. (1977). Yearly Review: Recent contributions in phycobiliproteins and phycobilisomes. *Photochem. Photobio.* **26**: 685-689.

Gantt, E., M. Edwards and L. Provasoli (1971). Chloroplast structure of the Cryptophyceae - Evidence for phycobiliproteins within intrathylakoidal spaces. *J. Cell Biol.* **48**: 280-290.

Gasol, J., J. García-Cantizano, R. Massana, R. Guerrero and C. Pedrós-Alió (1993). Physiological ecology of a metalimnetic *Cryptomonas* population: relationships to light, sulfide, and nutrients. *J. Plankton Res.* **15**(3): 255-275.

Gervais, F. (1997a). Light-dependent growth, dark survival, and glucose uptake by cryptophytes isolated from a freshwater chemocline. *J. Phycol.* **33**: 18-25.

Gieskes, W. and G. Kraay (1983). Dominance of Cryptophyceae during the phytoplankton spring bloom in the central North Sea detected by HPLC analysis of pigments. *Marine Biology* **75**: 179-185.

Glazer, A. (1981). Photosynthetic Accessory Proteins with Bilin Prosthetic Groups. The Biochemistry of Plants. M. Hatch and N. Boardman, Academic Press. **8**.

Glover, H., M. Keller and R. Guillard (1986). Light quality and oceanic ultraphytoplankters. *Nature* **319**: 142-143.

Goes, J., N. Handa, S. Taguchi and T. Hama (1995). Changes in the patterns of biosynthesis and composition of amino acids in a marine phytoplankter exposed to UV-B radiation: Nitrogen limitation implicated. *Photochem. Photobio.* **62**(4): 703-710.

Gordon, H. and A. Morel (1983). Remote assessment of ocean color for interpretation of satellite visible imagery. New York, Spriner-Verlag.

Gornitz, V. (1995). Monitoring sea level changes. *Climatic Change* **31**: 515-544.

Gray, J. (2001). Marine diversity: the paradigms in patterns of species richness examined. *Sci. Mar.* **65(Suppl. 2)**: 41-56.

Greenberg, B., V. Gaba, O. Canaani, S. Malkin, A. Mattoo and M. Edelman (1989). Separate photosensitizers mediate degradation of the 32-kDa photosystem II reaction center protein in the visible and UV spectral regions. *Proc. Natl. Acad. Sci.* **86**: 6617-6620.

Gregory, J. and J. Oerlemans (1998). Simulated future sea-level rise due to glacier melt based on regionally and seasonally resolved temperature changes. *Nature* **391**: 474-476.

Grossman, A., M. Schaefer, G. Chiang and J. Collier (1994). The response of cyanobacteria to environmental conditions: light and nutrients. The Molecular Biology of Cyanobacteria. D. Bryant. Netherlands, Kluwer Academic Publishers**:** 641-675.

Hader, D., H. Kumar, R. Smith and R. Worrest (1998). Effects on aquatic ecosystems. *Journal of Photochemistry and Photobiology B: Biology* **46**: 53-68.

Hader, D. and R. Worrest (1991). Effects of enhanced solar ultraviolet radiation on aquatic ecosystems. *Photochem. Photobio.* **53**(5): 717-725.

Hawley, N. (1991). Preliminary observations of sediment erosion from a bottom resting flume. *J. Great Lakes Res.* **17**(3): 361-367.

Haxo, F. and D. Fork (1959). Photosynthetically active accessory pigments of cryptomonads. *Nature* **184**: 1051.

Higashi, Y. and H. Seki (2000). Ecological adaptation and acclimatization of natural freshwater phytoplankters with a nutrient gradient. *Env. Poll.* **109**: 311-320.

Hill, D. and K. Rowan (1989). The biliproteins of the Cryptophyceae. *Phycologia* **28**(4): 455-463.

Hill, R. and F. Bendall (1960). Function of the two cytochrome components in chloroplasts, a working hypothesis. *Nature* **186**: 136-137.

Hobbie, J. and N. Smith (1975). Nutrients in the Neuse River Estuary, NC. Raleigh, N.C, UNC Sea Grant Program, North Carolina State University.

Hobbie, J. and P. Williams (1984). <u>Heterotrophic Activity in the Sea</u>. New York, Plenum Press.

Holland, R. (1969). Seasonal fluctuations of Lake Michigan diatoms. *Limnol. Oceanogr.* **14**: 423-436.

Huisman, J., P. van Oostveen and F. Weissing (1999). Species dynamics in phytoplankton blooms: Incomplete mixing and competition for light. *Amer Nat* **154**(1): 46-68.

Hunt, JE and D. Mc Neil (1998). Nitrogen status affects UV-B sensitivity of cucumber. *Aust. J. Plant Physiol.* **25**: 79-86.

Ilmavirta, V. (1988). Phytoflagellates and their ecology in Finnish brown water lakes. *Hydrobiologia* **161**: 255-270.

Itturriaga, R. and D. Siegel (1989). Microphotometric characterization of phytoplankton and detrital absorption properties in the Sargasso Sea. *Limnol. Oceanogr.* **34**(8): 1706-1726.

Iwanzik, W., M. Tevini, G. Dohnt, M. Voss, W. Weiss, P. Graber and G. Renger (1983). Action of UV-B on photosynthetic primary reactions in spinach chloroplasts. *Physiol. Plant.* **58**: 401-407.

Jansen, M., V. Gaba, B. Greenberg, A. Mattoo and M. Edelman (1993). UV-B driven degradation of the D1 reaction-center protein of photosystem II proceeds via plastosemiquinone. Photosynthetic Responses to the Environment. H. Yamamoto and C. Smith. Rockville, MD, American Soc. of Plant Physiologists**:** 142-149.

Jeffrey, S. and G. Humphrey (1975). New spectrophotometric equations for determining chlorophylls *a, b, c1* and *c2* in higher plants, algae, and natural phytoplankton. *Biochem. Physiol. Pflanzen* **167**: 191-194.

Jeffrey, S., S. Wright and M. Zapata (1999). Recent advances in HPLC pigment analysis of phytoplankton. *Mar. Freshwater. Res.* **50**: 879 - 896.

Jones, R. (1988). Vertical distribution and diel migration of flagellated phytoplankton in a small humic lake. *Hydrobiologia* **161**: 75-87.

Jordan, B. (1996). The effects of ultraviolet-B radiation on plants: A molecular perspective. Advances in Botanical Research, Academic Press Limited. **22:** 97-162.

Kaczamarska, I., T. Clair, J. Ehrman, S. MacDonald, D. Lean and K. Day (2000). The effect of ultraviolet B on phytoplankton populations in clear and brown temperate Canadian lakes. *Limnol. Oceanogr.* **45**(3): 651-663.

Kamiya, A. and S. Miyachi (1984). Effects of light quality on formation of 5-aminolevulinic acid, phycoerythrin and chlorophyll in *Cryptomonas* sp. cells collected from the subsurface chlorophyll layer. *Plant and Cell Physiol.* **25**(5): 831-839.

Kiefer, D. and B. Mitchell (1983). A simple, steady state description of phytoplankton growth based on absorption cross section and quantum efficiency. *Limnol. Oceanogr.* **28**(4): 770-776.

Kirk, J. (1994). Light and Photosynthesis in Aquatic Ecosystems, Cambridge University Press.

Klaveness, D. (1988). Ecology of the Cryptomonadida: A first review. Growth and Reproductive Strategies of Freshwater Phytoplankton. C. Sandgren. New York, Cambridge University Press**:** 105-133.

Kobayashi, T., E. Degenkolb, R. Bersohn, P. Rentzepis, R. MacColl and D. Berns (1979). Energy transfer among the chromophores in phycocyanins measured by picosecond kinetics. *Biochemistry*.

Kolber, Z., O. Prasil and P. Falkowski (1998). Measurements of variable chlorophyll fluorescence using fast repetition rate techniques: defining methodology and experimental protocols. *BBA* **1367**: 88-106.

Kolber, Z., J. Zehr and P. Falkowski (1988). Effects of growth irradiance and nitrogen limitation on photosynthetic energy conversion in PS II. *Plant Phys.* **88**: 923-929.

Kulandaivelu, G. and A. Noorundeen (1983). Comparative study of the action of ultraviolet-C and ultraviolet-B radiation on photosynthetic electron transport. *Physiol. Plant.* **58**: 389-394.

Laws, E. and T. Bannister (1980). Nutrient- and light-limited growth of *Thalassiosira fluviatilis* in continuous culture, with implications for phytoplankton growth in the ocean. *Limnol. Oceanogr.* **25**(3): 457-473.

Lee, C. and N. Hawley (1998). The response of suspended particulate material to upwelling and downwelling events in southern Lake Michigan. *J. Sed. Res.* **68**(5): 819-831.

Lee, E., A. Lewitus and R. Zimmer (1999). Chemoreception in a marine cryptophyte: Behavioral plasticity in response to amino acids and nitrate. *Limnol. Oceanogr.* **44**(6): 1571-1574.

Lesser, M., J. Cullen and P. Neale (1994). Carbon uptake in a marine diatom during acute exposure to ultraviolet B radiation: Relative importance of damage and repair. *J. Phycol.* **30**: 183-192.

Lewis, M. and J. Smith (1983). A small-volume short-incubation-time method for measurement of photosynthesis as a function of incident irradiance. *Mar. Ecol. Prog. Ser.* **13**: 99-102.

Lewitus, A. and D. Caron (1990). Relative effects of nitrogen or phosphorous depletion and light intensity an the pigmentation, chemical composition, and volume of *Pyrenomonas salina* (Cryptophyceae). *MEPS* **61**: 171-181.

Lewitus, A., D. Caron and K. Miller (1991). Effects of light and glycerol on the organization of the organization of the photosynthetic apparatus in the facultative heterotroph *Pyrenomonas salina* (Cryptophyceae). *J. Phycol.* **27**: 578-587.

Lewitus, A. and T. Kana (1995). Light respiration in six estuarine phytoplankton species: Contrasts under photoautotrophic and mixotrophic growth conditions. *J. Phycol.* **31**: 754-761.

Lichtlé, C. (1979). Effects of Nitrogen deficiency and light of high intensity in *Cryptomonas rufescens* (Cryptophyceae). *Protoplasma* **101**: 283-299.

Lichtlé, C., H. Jupin and J. Duval (1980). Energy transfers from Photosystem II to Photosystem I in *Cryptomonas rufescens* (Cryptophyceae). *BBA* **591**: 104-112.

Lloyd, D. and M. Cantor (1979). Subcellular structure and function in acetate algae. <u>Biochemistry and physiology of Protozoa, Second Edition</u>. Levandowsky and Hunter, Academic Press. **2:** 9-65.

Lohmann, M., G. Dohler, N. Huckenbeck and S. Verdini (1998). Effects of UV radiation of different wavebands on pigmentation, 15N-ammonium uptake, amino acid pools and adenylate contents of marine diatoms. *Marine Biology* **130**: 501-507.

Lou, J., D. Schwab, D. Beletsky and N. Hawley (2000). A model of sediment resuspension and transport dynamics in southern Lake Michigan. *JGR* **105**(C3): 6591-6610.

Lucas, I. (1970). Observations on the fine structure of the Cryptophyceae. I. The genus *Cryptomonas*. *J. Phycol.* **6**: 30-38.

MacColl, R. (1982). Yearly Review: Phycobilisomes and biliproteins. *Photochem. Photobio.* **35**: 899-904.

Maccoll, R. and D. Guard-Friar (1987). <u>Phycobiliproteins</u>. Boca Raton, FL, CRC Press.

Mackey, D., H. Higgins, M. Mackey and D. Holdsworth (1998). Algal class abundances in the western equatorial Pacific: Estimation from HPLC measurements of chloroplast pigments using CHEMTAX. *Deep-Sea Research* **45**: 1441-1468.

Mackey, M., D. Mackey, H. Higgins and S. Wright (1996). CHEMTAX - A program for estimating class abundances from chemical markers: application to HPLC measurements of phytoplankton. *Mar. Ecol. Prog. Ser.* **144**: 265-283.

Makarewicz, J., T. Lewis and P. Bertram (1994). Epilimnetic phytoplankton and zooplankton biomass and species composition in Lake Michigan, 1983 to 1992. Chicago, IL, US EPA.

Mallin, M. (1994). Phytoplankton ecology of North Carolina estuaries. *Estuaries* **17**(3): 561-574.

Margalef, R. (1978). Life-forms of phytoplankton as survival alternatives in an unstable environment. *Oceanologica Acta* **1**: 493-509.

Marshall, W. and J. Laybourn-Parry (2002). The balance between photosynthesis and grazing in Antarctic mixotrophic cryptophytes during summer. *Freshwater Biol.* **47**: 2060-2070.

McKerracher, L. and S. Gibbs (1982). Cell and nucleomorph division in the alga *Cryptomonas*. *Can. J. Bot.* **60**: 2440-2452.

Melis, A. (1991). Dynamics of photosynthetic membrane composition and function. *Biochim. Biophys. Acta* **1058**: 87-106.

Melis, A., J. Nemson and M. Harrison (1992). Damage to functional components and partial degradation of photosystem II reaction center proteins upon chloroplast exposure to ultraviolet-B radiation. *Biochim. Biophys. Acta* **1100**: 312-320.

Meybeck, M. (1982). Carbon, nitrogen, and phosphorous transport by world rivers. *American Journal of Science* **282**: 401-450.

Millie, D., G. Fahnenstiel, H. Carrick, S. Lohrenz and O. Schofield (2002). Phytoplankton pigments in coastal Lake Michigan: distributions during the spring isothermal period and relation with episodic sediment resuspension. *J . Phyc.* **38**: 639-648.

Mobley, C., L. Sundman and E. Boss (2002). Phase function effects on oceanic light fields. *Applied Optics* **41**(6): 1035-1050.

Moreira, D., H. Le Guyader and H. Philippe (2000). The origin of red algae and the evolution of chloroplasts. *Nature* **405**: 69.

Morgan, K. and J. Kalff (1975). The winter dark survival of an algal flagellate - *Cryptomonas erosa*. *Verh. Internat. Verein. Limnol.* **19**: 2734-2740.

Morgan, K. and J. Kalff (1979). Effect of light and temperature interactions on growth of *Cryptomonas erosa* (Cryptophyceae). *J. Phycol.* **15**: 127-134.

Mortimer, C. (1988). Discoveries and testable hypotheses arising from Coastal Zone Color Scanner imagery of southern Lake Michigan. *Limnol. Oceanogr.* **33**(2): 203-226.

Murata, N. (1969). Control of excitation transfer in photosynthesis I. Light induced change of chlorophyll *a* fluorescence in *Porphyridium cruentum*. *Biochim. Biophys. Acta* **172**: 242-251.

ÓhEocha, C. and M. Raftery (1959). Phycoerythrins and phycocyanins of cryptomonads. *Nature* **184**: 1049.

Ojala, A. (1993b). The influence of light quality on growth and phycobiliprotein/chlorophyll a fluorescence quotients of some species of freshwater algae in culture. *Phycologia* **32**(1): 22-28.

Ojala, A., S. Heaney, L. Arvola and F. Barbosa (1996). Growth of migrating and non-migrating cryptophytes in thermally and chemically stratified experimental columns. *Freshwater Biol.* **35**: 599-608.

Olli, K. (1999). Diel vertical migration of phytoplankton and heterotrophic flagellates in the Gulf of Riga. *J. Mar. Sys.* **23**: 145-163.

Oppenheimer, M. (1998). Global warming and the stability of the West Antarctic Ice Sheet. *Nature* **393**: 325-332.

O'Reilly, J., S. Maritorena, B. Mitchell, D. Siegel, K. Carder, S. Garver, M. Kahru and C. McClain (1998). Ocean color algorithms for SeaWiFS. *JGR* **103**(C11): 24937-24953.

O'Reilly, J., S. Maritorena, M. O'Brien, D. Siegel, D. Toole, D. Menzies, R. Smith, J. Mueller, B. Mitchell, M. Kahru, F. Chavez, P. Strutton, G. Cota, S. Hooker, C. McClain, K. Carder, F. Müller-Karger, L. Harding, A. Magnuson, D. Phinney, G. Moore, J. Aiken, K. Arrigo, R. Letelier and M. Culver (2000). SeaWiFS postlaunch technical report series, Volume 11, SeaWiFS postlaunch calibration and validation analyses, Part 3, NASA Technical Memorandum.

Ortner, P. and M. Dagg (1995). Nutrient-enhanced coastal ocean productivity in the Gulf of Mexico. *EOS* **76**: 97-109.

Osmond, C. (1994). What is photoinhibition? Some insights from comparisons of shade and sun plants. Photoinhibition of Photosynthesis from Molecular mechanisms to the Field. N. Baker and J. Bowyer. Oxford, BIOS Scientific Publ.**:** 1-19.

Paerl, H. (1998). Structure and function of anthropogenically altered microbial communities in coastal waters. *Current Opinion in Microbiology* **1**: 296-302.

Paerl, H., M. Mallin, C. Donahue, M. Go and B. Peierls (1995). Nitrogen loading sources and eutrophication of the Neuse River Estuary, NC: Direct and indirect roles of atmospheric deposition. Raleigh, UNC Water Resources Research Institute**:** 119.

Park, Y., W. Chow and J. Anderson (1995). Light inactivation of functional photosystem II in leaves of peas grown in moderate light depends on photon exposure. *Planta* **196**: 401-411.

Pegau, W., D. Gray and J. Zaneveld (1997). Absorption and attenuation of visible and near-infrared light in water: dependence on temperature and salinity. *Applied Optics* **36**(24): 6035-6046.

Petchey, O., P. McPherson, T. Casey and P. Morin (1999). Environmental warming alters food-web structure and ecosystem function. *Nature* **402**: 69-72.

Petersen, J., C. Chen and W. Kemp (1997). Scaling aquatic primary productivity: experiments under nutrient- and light-limited conditions. *Ecology* **78**: 2326-2338.

Pethick, J. (2001). Coastal management and sea-level rise. *Catena* **42**: 307-322.

Pinckney, J., D. Millie, K. Howe, H. Paerl and J. Hurley (1996). Flow scintillation counting of 14C-labeled microalgal photosynthetic pigments. *J. Plankton Res.* **18**: 1867-1880.

Pinckney, J., D. Millie, B. Vinyard and H. Paerl (1997). Environmental controls of phytoplankton bloom dynamics in the Neuse River Estuary, NC, USA. *Can. J. Fish. Aquat. Sci.* **54**: 2491-2501.

Pinckney, J., H. Paerl, M. Harrington and K. Howe (1998). Annual cycles of phytoplankton community-structure and bloom dynamics in the Neuse River Estuary, NC. *Marine Biology* **131**: 371-381.

Plante, A. and M. Arts (2000). Effects of chronic, low levels of UV radiation on carbon allocation in *Cryptomonas erosa* and competition between *C. erosa* and bacteria in continuous cultures. *JPR* **22**(7): 1277-1298.

Platt, T., C. Gallegos and W. Harrison (1980). Photoinhibition of photosynthesis in natural assemblages of marine phytoplankton. *J. Mar. Res.* **38**: 687-701.

Prézelin, B., G. Samuelsson and H. Matlick (1986). Photosystem II photoinhibition and altered kinetics of photosynthesis during nutrient-dependent high-light photoadaptation in Gonyaulax polyedra. *Marine Biology* **93**: 1-12.

Quian, S., M. Borsuk and C. Stow (2000). Seasonal and long-term nutrient trend decomposition along a spatial gradient in the Neuse River watershed. *Env Sci Tech* **34**(21): 4474-4482.

Renger, G., M. Volker, H. Eckert, R. Fromme, S. Hohm-Veit and P. Graber (1989). On the mechanism of photosystem II deterioration by UV-B irradiation. *Photochem. Photobio.* **49**(1): 97-105.

Rhiel, E., E. Mörschel and W. Wehrmeyer (1985). Correlation of pigment deprivation and ultrastructural organization of thylakoid membranes in *Cryptomonas maculata* following nutrient deficiency. *Protoplasma* **129**: 62-73.

Richardson, K., J. Beardall and J. Raven (1983). Adaptation of Unicellular Algae to Irradiance: An analysis of strategies. *New Phytol.* **93**: 157-191.

Richardson, T., J. Pinckney and H. Paerl (2001). Responses of estuarine phytoplankton communities to nitrogen form and mixing using microcosm bioassays. *Estuaries* **in press**.

Richter, M., W. Rühle and A. Wild (1990). on the mechanism of photosystem II photoinhibition I. A two-step degradation of D1-protein. *Photosynthesis Research* **24**: 229-235.

Rintamaki, E., R. Salo and E. Aro (1994). Rapid turnover of the D1 reaction-center protein of PS II as a protection mechanism against photoinhibition in a moss, Ceratodon purpureus (Hedw.) Brid. *Planta* **193**: 520-529.

Robbins, J. and J. Bales (1995). Simulation model of hydrodynamics and solute transport in the Neuse River Estuary, North Carolina. Raleigh, NC, USGS Open File Rep. No. 94-511. US Geological Survey.

Roemmich, D. and J. McGowan (1995). Climatic warming and the decline of zooplankton in the California current. *Science* **267**: 1324-1326.

Rudek, J., H. Paerl, M. Mallin and P. Bates (1991). Seasonal and hydrological control of phytoplankton nutrient limitation in the lower Neuse River Estuary, North Carolina. *Mar. Ecol. Prog. Ser.* **75**: 133-142.

Salonen, K. and S. Jokinen (1988). Flagellate grazing on bacteria in a small dystrophic lake. *Hydrobiologia* **161**: 203-209.

Samson, G. and D. Bruce (1995). Complementary changes in absorption cross sections of Photosystems I and II due to phosphorylation and Mg 2+ depletion in spinach thylakoids. *BBA* **1232**: 21-26.

Sanders, R., U. Berninger, E. Lim, P. Kemp and D. Caron (2000). Heterotrophic and mixotrophic nanoplankton predation on picoplankton in the Sargasso Sea on Georges Bank. *Mar. Ecol. Prog. Ser.* **192**: 103-118.

Schindler, D., K. Beaty, E. Fee, D. Cruikshank, E. Debruyn, D. Findlay, G. Linsey, J. Shearer, M. Stainton and M. Turner (1990). Effects of climatic warming on lakes of the central boreal forest. *Science* **250**: 967-970.

Schluter, L., F. Mohlenberg, H. Havskum and S. Larsen (2000). The use of phytoplankton pigments for identifying and quantifying phytoplankton groups in coastal areas: testing the influence of light and nutrients on pigment/chlorophyll a ratios. *Mar. Ecol. Prog. Ser.* **192**: 49-63.

Schreiber, U., H. Hormann, C. Neubauer and C. Klughammer (1995). Assessment of photosystem II photochemical quantum yield by chlorophyll fluorescence quenching analysis. *Aust. J. Plant Physiol.* **22**: 209-220.

Sciandra, A., L. Lazzara, H. Claustre and M. Babin (2000). Responses of growth rate, pigment composition and optical properties of *Cryptomonas* sp. to light and nitrogen stress. *MEPS* **201**: 107-120.

Sidler, W. (1994). Phycobilisome and phycobiliprotein structure. The Molecular Biology of Cyanobacteria. D. Bryant. Netherlands, Kluwer Academic Publisher**:** 139-216.

Smayda, T. (1989). Primary production and the global epidemic of phytoplankton blooms in the sea: A linkage? Novel Phytoplankton Blooms: Causes and Impacts of Recurrent Brown Tide and Other Unusual Blooms. E. Cosper, V. Bricelj and E. Carpenter, Springer-Verlag.

Smith, R., K. Baker, O. Holm-Hansen and R. Olson (1980). Photoinhibition of photosynthesis in natural waters. *Photochem. Photobio.* **31**: 585-592.

Smolander, U. and L. Arvola (1988). Seasonal variation in the diel vertical distribution of the migratory alga *Cryptomonas maesonii* (Cryptophyceae) in a small, highly humic lake. *Hydrobiologia* **161**: 89-98.

Sommer, U. (1988). Some size relationships in phytoflagellate motility. *Hydrobiologia* **161**: 125-131.

Spear-Bernstein, L. and K. Miller (1989). Unique location of the phycobiliprotein light-harvesting pigment in the Cryptophyceae. *J. Phycol.* **25**: 412-419.

Stephens, F. (1995). Variability of spectral absorption efficiency within living cells of *Pyrocystis lunula* (Dynophyta). *Marine Biology* **122**: 325-331.

Styring, S. and C. Jegerschold (1994). Light induced reactions impairing electron transfer through photosystem II. Photoinhibition of Photosynthesis. N. Baker and J. Bowyer. Oxford, UK, BIOS Scientific Publishers Limited**:** 55-74.

Sullivan, B., F. Prahl, L. Small and P. Covert (2001). Seasonality of phytoplankton production in the Columbia River: A natural or anthropogenic pattern? *Geochim. Cosmochim. Acta* **65**(7): 1125-1139.

Tamigneaux, E., E. Vazquez, M. Mingelbier, B. Kelein and L. Legendre (1995). Environmental control pf phytoplankton assemblages in nearshore marine waters, with special emphasis on phototrophic ultraplankton. *J. Plankton Res.* **17**(7): 1421-1447.

Tandeau de Marsac, N. (1977). Occurrence and nature of chromatic adaptation in Cyanobacteria. *J. Bacteriology* **130**(1): 82-91.

Telfer, A. and J. Barber (1994). Elucidating the molecular mechanisms of photoinhibition by studying isolated photosystem II reaction centres. Photoinhibition of Photosynthesis. N. Baker and J. Bowyer. Oxford, Bios Scientific Publishers**:** 25-49.

Thinh, L. (1983). Effect of irradiance on the physiology and ultrastructure of the marine cryptomonad, *Cryptomonas* strain Lis (Cryptophyceae). *Phycologia* **22**(1): 7-11.

Titus, J., R. Park, S. Leatherman, S. Weggel, M. Greene, P. Mausel, S. Brown, G. Gaunt, M. Trehan and G. Yohe (1991). Greenhouse effect and sea level rise: The cost of holding back the sea. *Coastal Management* **19**: 171-204.

Tuchman, N. (1996). The role of heterotrophy in algae. Algal Ecology. R. Stevenson, M. Bothwell and R. Lowe, Academic Press**:** 299-340.

Vernet, M., E. Brody, O. Holm-Hansen and B. Mitchell (1994). The response of Antarctic phytoplankton to ultraviolet radiation: absorption, photosynthesis, and taxonomic composition. *Ant. Res. Ser.* **62**: 143-158.

Vesk, M., D. Dwarte, S. Fowler and R. Hiller (1992). Freeze fracture immunocytochemistry of light-harvesting pigment complexes in a cryptophyte. *Protoplasma* **170**: 166-176.

Wangberg, S., J. Selmer and K. Gutavson (1998). Effects of UV-B radiation on carbon and nutrient dynamics in marine plankton communities. *Journal of Photochemistry and Photobiology B: Biology* **45**: 19-24.

Wastl, J. and U. Maier (2000). Transport of proteins into Cryptomonads complex plastids. *J. Biol. Chem.* **275**(30): 23194-23198.

Wastl, J., H. Sticht, U. Maier, P. Rösch and S. Hoffman (2000). Identification and characterization of a eukaryotically encoded rubredoxin in a cryptomonad alga. *FEBS Lett.* **471**: 191-196.

Watanabe, M. and M. Furuya (1978). Phototactic responses of cell population to repeated pulses of yellow light in a Phytoflagellate *Cryptomonas* sp. *Plant Phys.* **61**: 816-818.

Wedemayer, G., D. Wemmer and A. Glazer (1991). Phycobilins of cryptophycean algae: Structures of novel bilins with acryloyl substituents from phycoerythrin 566. *J. Biol. Chem.* **266**(8): 4731-4741.

Wheeler, P., B. North and G. Stephens (1974). Amino acid uptake by marine phytoplankters. *Limnol. Oceanogr.* **19**(2): 249.

Worrest, R., B. Thomson and H. Van Dyke (1981). Impact of UV-B radiation upon estuarine microcosms. *Photochem. Photobio.* **33**: 861-867.

Wright, S., D. Thomas, H. Marchant, H. Higgins, M. Mackey and D. Mackey (1996). Analysis of phytoplankton of the Australian sector of the Southern Ocean: comparisons of microscopy and size frequency data with interpretations of pigment HPLC data using the 'CHEMTAX' matrix factorisation program. *MEPS* **144**: 285-298.

Yin, Z. and G. Johnson (2000). Photosynthetic acclimation of higher plants to growth in fluctuating light environments. *Photosynthesis Research* **63**: 97-107.

Zaneveld, J. and J. Kitchen (1994). The scattering error correction of reflecting tube absorption meters. *SPIE* **2258**: 44-55.

Zimmerman, A. and E. Canuel (2000). A geochemical record of eutrophication and anoxia in Chesapeake Bay sediments: anthropogenic influence on organic matter composition. *Marine Chemistry* **69**: 117-137.

Curriculum Vita

Trisha I Bergmann

EDUCATION

2003 Ph.D. Biological Oceanography, Rutgers University, New Brunswick, New Jersey.
1996 B.S. Environmental Sciences, Marine and Coastal Studies, Cook College, Rutgers University, New Brunswick, New Jersey.

EMPLOYMENT

September 1997 – present, Graduate Assistant, Coastal Ocean Observation Lab, Institute of Marine and Coastal Sciences, Rutgers University, New Brunswick, New Jersey.
March 1994 – September 1997, Research Assistant, Marine Remote Sensing Lab, Institute of Marine and Coastal Sciences, Rutgers University, New Brunswick, New Jersey.

TEACHING EXPERIENCE

Spring 2001 - “Scientific Inquiry: Human Impacts on Marine Environments”
2000-2001 Teaching Assistant Project TA Liaison
Spring 2000 - Teaching Assistant “Oceanographic Methods and Data Analysis”

FIELD EXPERIENCE (Research expeditions longer than 3 days)

2001 R.V. Endeavor (10 days) Utilization of Bistatic CODAR system
2001 R.V. Walford (4 Weeks) Coastal predictive skill experiments focused on coastal upwelling
2000 R.V. Endeavor (10 days) Utilization of KSS laser lidar for assessing thermocline depth
2000 R.V. Walford (4 Weeks) Coastal predictive skill experiments focused on coastal upwelling
2000 R.V. Laurentian, Lake Michigan (2 Weeks) Hydrological optics of a coastal turbidity plume
*2000 R.V. Endeavor (7 days) Mooring deployment and calibration – *Chief Scientist
1999 R.V. Walford (4 Weeks) Coastal predictive skill experiments focused on coastal upwelling
1999 R.V. Laurentian, Lake Michigan (2 weeks) Hydrological optics of a coastal turbidity plume
1998 CPSE, NJ (3 weeks) Impact of upwelling on coastal optical properties
1998 R.V. Laurentian, Lake Michigan (1.5 weeks) Optics of a coastal turbidity plume
1997 CPSE, NJ (3 weeks) Impact of upwelling - coastal optical properties
1996 CPSE, NJ (3 weeks) Impact of upwelling - coastal optical properties
1995 CPSE, NJ (3 weeks) Impact of upwelling on biological dynamics
1994 Coastal Predictive Skill Experiments, NJ (3 weeks) Impact of upwelling on bottom hypoxia